# Final Progress Report

**Project Title:**

**High Temperature, Low Relative Humidity, Polymer-type Membranes Based on Disulfonated Poly(arylene ether) Block and Random Copolymers Optionally Incorporating Protonic Conducting Layered Water Insoluble Zirconium Fillers**

**Project Period: 01 May 2006 to 31 March 2010**

**Date of Report:** June 03, 2010

**Recipient: Virginia Tech**

**Award Number: DE-FG36-06G016038**

**Working Partners:** James E. McGrath and Donald G. Baird, Virginia Tech

**Cost-Sharing Partners:** None

**Contact:** James E. McGrath, 540-231-5976, jmcgrath@vt.edu

Donald G. Baird, 540-231-5998, dbaird@vt.edu

**DOE Managers:** Greg Kleen (Project Officer/Manager, gregory.kleen@go.doe.gov) and Shaun Onorato (Project Monitor, shaun.onorato@go.doe.gov)

## Executive Summary: Structure Property Relationship of Proton Exchange Membranes

Proton exchange membrane fuel cells (PEMFC) are well recognized to be environmentally attractive alternative automotive, stationary and portable power sources for the future. **Arguably, the most important criterion for PEMFC is the need to maintain proton conduction over a range of temperatures, under partially hydrated conditions.** State of the art PEMFC systems are based on perfluorosulfonic acid ionomer membranes such as Nafion. **Our research group has been engaged with the DOE to better understand how molecular structure of the polymeric membrane influences protonic conductivity as well as other important issues which currently limit the development of PEMFC for commercial applications.** Our laboratory has emphasized the synthesis and characterization of wholly aromatic 4,4'-biphenol based partially disulfonated poly(arylene ether sulfone) random copolymers as potential PEMs.[1-4] These copolymers have been defined by a shortened name, BPSH-xx where BP stands for biphenol, S is for sulfonated, and H denotes the proton form of the acid where xx represents the degree of disulfonation. In addition hydroquinone(HQSH) based disulfonated poly(arylene ether sulfone) random copolymers were also prepared and studied.[5] HQSH has the potential for being the more economical of the two. Both series of copolymers with varying degree of disulfonation were characterized and under fully hydrated conditions, they were comparable and even better than the commercially available Nafion. **Open circuit (OCV) voltage measurements done under DOE support at UTC showed that their stability at 100C and 25% RH, in pure H2/O2 was actually better than Nafion, regardless of the apparent drawbacks as shown by Fenton tests**. However, proton transport was limited at low hydration level for the random copolymer and was less attractive than Nafion.

**Thus the challenge lies in how to modify the chemistry and molecular structure of the copolymers to obtain significant protonic conductivity even at low or intermediate hydration levels.**

Even the disulfonated random ion containing copolymers partially phase separate phase separate to form nano scale hydrophilic and hydrophobic morphological domains due to the well known ionomer aggregation effect. Water confined in hydrophilic pores in concert with the sulfonic acid groups serve the critical function of proton (ion) conduction and water transport in these systems. The molecular structure of the water is very important to the transport behavior. There are at least three states of water that have been associated with water residing in hydrophilic phases of polymers.[6] The presence of these three states can be defined by thermal properties and relaxation behavior. *Non-freezing bound water* is strongly associated with the polymer and depresses its $T_g$, but the water shows no melting endotherm by differential scanning calorimetry (DSC). *Freezable bound water* is weakly bound to the polymer (or weakly bound to the non-freezing water), and displays broad melting behavior around 0 °C. *Free water* exhibits a sharp melting point at 0 °C. A strong relationship between the states of water and transport properties is well known to exist.

**A major challenge of the research was to characterize and develop concepts for establishing structure/property relationships between the functionality of the polymer backbone, the state of water, and the membrane transport.** Our vision is that this will guide the synthesis of copolymers with improved performance **particularly under partially hydrated conditions**.

**Objectives:** The main objective of the research continues to be to investigate the influence of chemical composition, chemical microstructure and morphology on various transport properties of proton

exchange membranes and to use this knowledge to design membranes with improved conductivity-humidity profiles.

**Approaches: Ion containing multi-block copolymers:**

The VT group has synthesized thermally stable multi-block copolymers with varying chemical structures and compositions which have been abbreviated as BisSF-BPSH, BPSH-BPS and BPSH-PI.[2, 7-13] **In contrast to the random copolymers, where the sulfonic acid groups are randomly distributed along the chain, the multi-block copolymers feature an ordered sequence of hydrophilic and hydrophobic segments.** If, like in Nafion, connectivity is established between the hydrophilic domains in these multiblock copolymers, they will not need as much water, and hence will show much better protonic conductivity than the random copolymers (with similar degree of sulfonation, or IEC) at partially hydrated conditions.

Among the transport properties, **proton, water and to a lesser extent methanol transport were evaluated.** The fundamental properties were correlated to the real time fuel cell performances. Special emphasis was given to **investigate the influence of morphology under partially hydrated conditions.** This knowledge, coupled with the state of water experiments, transport measurements, and chemical structure of the copolymers provide a fundamental picture of how the chemical nature of a phase separated copolymer influences its transport properties. The experimental procedures involved impedance spectroscopy, DSC, TGA, FTIR, DMA, PGSE NMR, NMR relaxation experiments and various electrochemical fuel cell performance experiments.

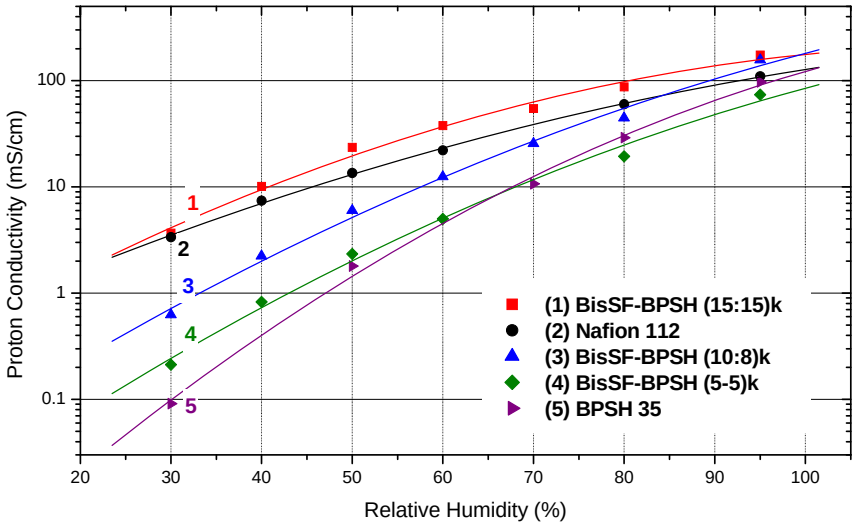


**Proton Conductivity under partially hydrated conditions for BisSF-BPSH multi-blocks.**

## Project Objectives

The goal of this research is to develop a material suitable for use as a polymer electrolyte membrane which by the year 2010 will meet all the performance requirements associated with fuel cell operation at high temperatures and low relative humidity, and will out-perform the present standard Nafion®. In particular, it is our objective to extend our previous research based on the use of thermally, oxidatively, and hydrolytically, ductile, high Tg ion containing polymers based on poly(arylene ethers) to the production of polymer electrolyte membranes which will meet all the performance requirements in addition to having an areal resistance of < 0.05 ohm-cm2 at a temperature of up to 120°C, relative humidity of 25 to 50%, and up to 2.5 atm total pressure. In many instances, our materials already out performs Nafion®, and it is expected that with some modification by either combining with conductive inorganic fillers and/or synthesizing as a block copolymer it will meet the performance criteria at high temperatures and low relative humidity. A key component in improving the performance of the membranes (and in particular proton conductivity) and meeting the cost requirements of $40/$m^2$ is our development of a film casting process, which shows promise for generation of void free thin films of uniform thickness with controlled polymer alignment and configuration.

## Background

Our research group has been engaged in the past few years in the synthesis of biphenol based partially disulfonated poly(arylene ether sulfone) random copolymers as potential PEMs. This series of polymers are named as BPSH-xx, where BP stands for biphenol, S stands for sulfonated, H stands for acidified and xx represents the degree of disulfonation. All of these sulfonated copolymers phase separate to form nano scale hydrophilic and hydrophobic morphological domains. The hydrophilic phase containing the sulfonic acid moieties causes the copolymer to absorb water. Water confined in hydrophilic pores in concert with the sulfonic acid groups serve the critical function of proton (ion) conduction and water transport in these systems. Both Nafion and BPSH show high proton conductivity at fully hydrated conditions. However proton transport is especially limited at low hydration level for the BPSH random copolymer. It has been observed that the diffusion coefficients of both water and protons change with the water content of the pore. This change in proton and water transport mechanisms with hydration level has been attributed to the solvation of the acid groups and the amount of bound and bulk-like water within a pore. At low hydration levels most of the water is tightly associated with sulfonic groups and has a low diffusion coefficient. This tends to encourage isolated domain morphology. Thus, although there may be significant concentrations of protons, the transport is limited by the discontinuous morphological structure.

Hence the challenge lies in how to modify the chemistry of the polymers to obtain significant protonic conductivity at low hydration levels. This may be possible if one can alter the chemical structure to synthesize nanophase separated ion containing block copolymers. Unlike the BPSH copolymers, where the sulfonic acid groups are randomly distributed along the chain, the multiblock copolymers will feature an ordered sequence of hydrophilic and hydrophobic segments. If, like in Nafion, connectivity is established between the hydrophilic domains in these multiblock copolymers, they will not need as much water, and hence will show much better protonic conductivity than the random copolymers (with similar degree of sulfonation, or IEC) at partially hydrated conditions.

## TASKS UNDERTAKEN DURING THE DURATION OF THE PROJECT

**Task 1:** Synthesize random copolymers based on poly(arylene ethers) of three different molecular weights and ion content of 35 mole % and prepare composites from these copolymers reinforced with various levels (2, 4, 6, 8 and 10 wt%) of protonic conductive zirconium phenyl phosphonate (zpp) layered structures and cast membranes(batch technique).

- (M1) By 4Q Year 1 identify compositions suitable for membrane generation and select materials for performance analysis.

**Task 2:** Assess electrical and mechanical properties, durability, survivability at low temperatures, and permeability of membranes produced in Task 1.

- (M2) By 3Q Year 2 demonstrate conductivity of 0.07 S/cm at 80% relative humidity at room temperature.
- (M3) By 3Q Year 3 demonstrate a conductivity > 0.1 S/cm at 50 % relative humidity at 120$^{o}$C.
- (M10) By 3Q Year 4 provided conductivity goal is met, develop and optimize system to reach the cost goal of \$40/m$^2$ and meet other performance goals.
- (M11) By 4Q Year 5 determine that the remainder of the technical targets (i.e. durability, survivability, cross-over, etc.) have been met for the cast films.

**Task 3:** Simultaneously prepare alternating hydrophilic-hydrophobic multiblock copolymers derived from a hydrophilic aromatic oligomer with reactive phenoxide endgroups, coupled with a perfluorinated or hydrocarbon functional hydrophobic material, to produce multiblocks that are also ductile and asses their ability to yield membranes

- (M4) By 4Q Year 1 identify compositions which yield membranes suitable for performance analysis.

**Task 4:** Assess electrical and mechanical properties, durability, survivability at low temperatures, and permeability of membranes produced in Task 3.

- (M5) By 3Q Year 2 demonstrate conductivity of 0.07 S/cm at 80% relative humidity at room temperature
- (M6) By 3Q Year 3 demonstrate a conductivity > 0.1 S/cm at 50 % relative humidity at 120$^{o}$C.
- (M12) By 3Q Year 4 provided conductivity goal is met develop and optimize system to reach the cost goal of \$40/m$^2$ and meet other performance goals.
- (M13) By 4Q Year 5 determine that the remainder of the technical targets (i.e. durability, survivability, cross-over, etc.) have been met for the cast films.

**Task 5:** Design a scheme based on an intensive experimental and modeling program which will relate coating thickness and uniformity as well as chain alignment and configuration, to the geometric, solution characteristics (e.g. polymer concentration, interfacial surface tension, and viscosity), heat and mass transfer, and the operating variables of the film casting process for the purpose of generating the optimum proton conductivity.

- (M7) By 4Q Year 1 develop a model and asses its ability to establish conditions which will yield films for a model polyarylsulfone system that are 2 to 3 inches in width, pinhole-free, and controllable with respect to their thickness and its uniformity which are 25-, 50-, and 75-microns (approximately 1, 2 and 3 mil) thick.
- (M8) By 4Q Year 2 Based on this fundamental study establish conditions for any experimental composition developed in this program to produce model films that are 2 to 3 inches in width, pinhole-free, and controllable with respect to their thickness. In particular, 25-, 50-, and 75-microns (approximately 1, 2 and 3 mil) thick.
- (M9) By 3Q Year 3 use model to establish conditions which will lead to thinnest films possible which is necessary to lower the cost of the membranes and reduce aerial resistance even more.
- (M14) By 4Q Year 4 scale film casting process to produce membranes of any desired width and thickness and test scale-up technique for producing films of widths of 4.0".

**Task 6:** Optimize the system composition (whether it be the composite or block copolymer system) in order to produce membranes by means of the film casting process as economically as possible and with properties which meet or exceed all the performance criteria.

- (M15) By 4Q Year 4 produce films as thin as 25 microns and up to 4.0 " wide from compositions which have met all the performance criteria using the batch casting process.
- (M16) By 4Q Year 5 show that films produced meet all performance criteria including conductivity, mechanical properties, survivability, durability, cross-over, etc.

**Task 7. Project Management and Reporting**

- After Year 2, delivery a membrane to the Topic 2 awardee for testing
- Participation in the annual DOE Hydrogen Program Review.
- Participation in the biannual DOE High Temperature, Low Relative Humidity Working Group Meetings.
- Project highlights will be requested bi-annually to be posted on the DOE High Temperature, Low Relative Humidity Membrane Working Group website.
- Participation in Tech Team Meetings as requested by DOE

## TASKS RESULTS FROM WORK COMPLETED DURING THE PROJECT

Below, we summarize the results for Tasks 1-4 that involve the synthesis and characterization of the polymer systems. The work to model and produce films from these systems, which encompasses Tasks 5 and 6 is discussed thereafter.

For Tasks 1-4, our work involved investigation, synthesis and characterization of three block copolymer systems. Each of these will be discussed separately in corresponding sections. Task 5 and 6 are discussed in a final section.

## Segmented Sulfonated Poly(arylene ether sulfone)-b-Polyimide Copolymers for Proton Exchange Membrane Fuel Cells

### Summary of Results

Segmented disulfonated poly(arylene ether sulfone)-b-polyimide copolymers based on hydrophilic and hydrophobic oligomers were synthesized and evaluated for use as proton exchange membranes (PEMs). Amine terminated sulfonated poly (arylene ether sulfone) hydrophilic oligomers and anhydride terminated naphthalene based polyimide hydrophobic oligomers were synthesized via step growth polymerization including high temperature one-pot imidization. Synthesis of the multiblock copolymers was achieved by an imidization coupling reaction of hydrophilic and hydrophobic oligomers oligomers in a m-cresol/NMP mixed solvent system, producing high molecular weight tough and ductile membranes. Proton conductivities and water uptake increased with increasing ion exchange capacities (IECs) of the copolymers as expected. The morphologies of the multiblock copolymers were investigated by tapping mode atomic force microscopy (TM-AFM) and their measurements revealed that the multiblock copolymers had well-defined nano-phase separated morphologies which were clearly a function of block lengths. Hydrolytic stability test at 80 °C water for 1000 h showed that multiblock copolymer membranes retained intrinsic viscosities of about 80% of the original values and maintained flexibility which was much improved over polyimide random copolymers. The synthesis and fundamental properties of the multiblock copolymers are reported here and the systematic fuel cell properties will be provided in a separate article.

### Introduction

The fuel cell is an energy conversion device which directly transforms the chemical energy of fuels such as hydrogen and methanol into electrical energy. The fuel cell has been gaining serious attention as a next-generation energy source owing to its advantages including high efficiency, high energy density, quiet operation, and environmental friendliness relative to conventional energy generators such as internal combustion engines. Among the various types of fuel cells, the proton exchange membrane fuel cell (PEMFC) is considered to be the most promising power source for portable and automotive applications. As its name implies, one of the core components of a PEMFC is the proton exchange membrane (PEM). Currently, the state-of-the-art PEMs are perfluorinated sulfonated ionomer membranes, such as Nafion (DuPont), Aciplex (Asahi Kasei), and Flemion (Asahi Glass). These membranes have good mechanical strength and high chemical stability along with high proton conductivity, especially under high relative humidities at moderate operation temperatures. However, at high operation temperatures (>80°C), which are essential for practical applications, mechanical, and electrochemical properties of the perfluorinated membranes are severely deteriorated by the

depressed hydrated a relaxations of the membranes. These disadvantages and others, such as cost, have limited perfluorinated membranes' applicability and triggered the quest for alternative membranes. Much effort has been devoted in the study of aromatic polymers, including sulfonated poly(arylene ether sulfone)s, poly(ether ether ketone)s, and polybenzimidazoles, to find cost-effective and high performance PEMs.9,10 Among them, 4,4-biphenol-based disulfonated poly(arylene ether sulfone) random copolymers (BPSH) are strong candidates as alternative membranes and have been extensively investigated in high temperature PEM applications. These random copolymers were synthesized via direct step-growth polycondensation by using disulfonated and nonsulfonated dihalide diphenyl sulfone and biphenol type monomers. Even though BPSH-type membranes demonstrated enhanced stability at high temperatures and performance comparable to Nafion, their proton conductivities under low relative humidity were inadequate. To increase the proton conductivity under partially hydrated conditions, the degree of disulfonation was increased. However, once the degree of disulfonation reaches 60 mol%, a percolated hydrophilic phase appears and results in excessive water swelling, forming a hydrogel that is impractical as a PEM. Recently, PEMs based on multiblock copolymers have been considered as a solution to overcome the drawbacks of a random copolymer system. PEMs based on segmented multiblock copolymers consist of ion conducting hydrophilic blocks and mechanically robust hydrophobic blocks. Once they are cast into membranes, they exhibit unique phase separated morphologies and each phase governs independent or distinct properties. The ionic groups of the hydrophilic blocks act as proton conducting sites while the nonionic hydrophobic component provides dimensional stability. In the case of direct methanol fuel cells (DMFCs), the hydrophobic component may serve as a barrier against methanol transport. The proton conductivities, water uptake, and mechanical properties of multiblock copolymer based PEMs can be tailored by carefully adjusting the relative lengths of their hydrophilic and hydrophobic blocks. One strong candidate for the hydrophobic blocks in multiblock copolymer-based PEMs may be polyimides because of their high performance properties. These properties include excellent thermal stability, high mechanical strength, good film-forming ability, low gas permeability, and superior chemical resistance. Not all polyimides are ideal for PEM applications. For example, conventional five-membered ring polyimides based on phthalic anhydride are easily degraded under acidic conditions because of the ease of hydrolysis of imido rings. Several scientists have shown that this problem can be partially addressed by using six-membered ring polyimides, which are found to be more hydrolytically stable under acidic conditions than five-membered ring polyimides, yet slow hydrolysis can still be problematic. In this article, we report the synthesis of a full series of multiblock copolymers produced by a coupling reaction between hydrophilic BPSH oligomers and hydrophobic polyimide oligomers as an extension of our earlier research. The BPSH oligomers were capped with primary amine groups and prepared with different block lengths ranging from 5 to 20 kg/mol. These functionalized BPSH telechelic oligomers were then combined with controlled molecular weight anhydride terminated naphthalene based polyimide oligomers of the same molecular weight range to produce high molecular weight multiblock copolymers. By the described synthetic route, a series of multiblock copolymers with different block lengths was synthesized and fundamental properties were characterized. This article also evaluates the effect of block lengths in terms of the morphologies and membrane properties, including atomic force

microscopy (AFM), impedance spectroscopy, and hydrolysis stability.

**EXPERIMENTAL**

*Materials*

N,N-Dimethylacetamide (DMAc), N-methyl-2pyrrolidinone (NMP), 3-methylphenol (m-cresol), and toluene were purchased from Aldrich and distilled from calcium hydride before use. Monomer grade 4,4-dichlorodiphenyl sulfone (DCDPS) and 4,4-biphenol (BP) were provided by Solvay Advanced Polymers and Eastman Chemical Company, respectively, and vacuum dried at 110 °C prior to use. 1,4,5,8-Naphthalenetetracarboxylic dianhydride (NDA) and fuming sulfuric acid ($SO_3$ content 30%), were used as received from Aldrich. Bis[4-(3-aminophenoxy)phenyl]sulfone (m-BAPS) was purchased from TCI and purified by recrystallization from ethanol. 3-Aminophenol (m-AP) was purchased from Aldrich and sublimed in vacuo before use. Potassium carbonate, benzoic acid, ethanol, 2-propanol (IPA), and isoquinoline were purchased from Aldrich and used without further purification.

*Synthesis of 3,3-Disulfonated-4,4dichlorodiphenylsulfone*

3,3-Disulfonated-4,4-dichlorodiphenylsulfone (SDCDPS) was prepared by the reaction of DCDPS and fuming sulfuric acid. The detailed synthesis of and purification of SDCDPS has been described in the literature.

*Synthesis of Controlled Molecular Weight Disulfonated Poly(arylene ether sulfone)s with Telechelic Amine Functionality*

Disulfonated poly(arylene ether sulfone) hydrophilic blocks (BPSH) with molecular weights ranging from 5 to 20 kg/mol were synthesized via nucleophilic aromatic substitution. Molecular weight control and telechelic amine functionality of BPSH hydrophilic blocks were achieved by using stoichiometrically adjusted amounts of monomers (BP, SDCDPS) and end-capping reagent (m-AP). A typical coupling reaction was performed as follows: 7.54 g (40.5 mmol) of BP, 21.61g (44.0 mmol) of SDCDPS, 0.77 g (7.1 mmol) of m-AP, and 7.05 g (51 mmol) of potassium carbonate were added to a three-necked 250 mL flask equipped with a condenser, a Dean Stark trap, a nitrogen inlet/outlet, and a mechanical stirrer. Distilled DMAc (70 mL) and toluene (35 mL) were added to the flask. The solution was allowed to reflux at 150 °C while the toluene azeotropically removed the water in the system. After 4h, the toluene was completely removed from the flask by slowly increasing the temperature to 180 °C. The reaction was allowed to proceed for another 96h. The resulting viscous solution was cooled to room temperature and diluted with DMAc to facilitate filtration. After filtration, the polymer solution was coagulated in isopropyl alcohol (IPA). The polymer was dried at 120 °C in vacuo for at least 24h.

*Synthesis of Controlled Molecular Weight Anhydride-Terminated Polyimides*

Naphthalene dianhydride-based polyimide hydrophobic blocks with molecular weights ranging from 5 to 20 kg/mol were synthesized via a one-pot high temperature imidization process.

Molecular weight control and end group functionality were achieved by stoichiometrically

adjusted amounts of the monomers. A typical coupling reaction was performed as follows: 4.96 g (18.5 mmol) of NDA, 7.05 g (16.3 mmol) of m-BAPS, and 2.26 g (18.5 mmol) of benzoic acid were dissolved in 108 mL of m-cresol in a three-necked 250-mL flask equipped with a condenser, a Dean Stark trap, a nitrogen inlet/outlet and a mechanical stirrer. The reaction mixture was heated at 80 8C for 4 h and then at 180 8C for 12 h. Then 2.39 g (18.5 mmol) of isoquinoline was added and the reaction was conducted at 180 8C for another 12 h. The resulting dark red polymer solution was precipitated in IPA. The polymer was filtered and purified in a Soxhlet extractor with methanol overnight. The polymer was dried at 120 8C in vacuo for at least 24 h.

*Synthesis of Hydrophilic-Hydrophobic Multiblock Copolymers*

A series of multiblock copolymers was synthesized via a modified one-pot high temperature imidization. The series consisted of 16 different copolymers with a systematic combination of hydrophilic and hydrophobic block lengths. A typical coupling reaction was performed as follows: 3.0 g (0.6 mmol) of hydrophilic oligomer (Mn = 5 kg/mol), 3.0 g (0.6 mmol) of hydrophobic oligomer (Mn = 5 kg/mol), 0.73 g (6 mmol) of benzoic acid, and 30 mL of NMP were added to a three-necked 100-mL flask equipped with a mechanical stirrer, and a nitrogen inlet/outlet. The reaction mixture was heated at 80 °C for 4 h to obtain a homogeneous solution. Approximately 15 mL of m-cresol was slowly added until the mixture became inhomogeneous. The solution homogeneity was recovered by adding additional NMP (~ 15 mL) to achieve a final solution concentration of ~ 10% (w/v) solid. A coupling reaction was conducted at 180 °C for 12 h and then 0.78 g (6 mmol) of isoquinoline was added. The reaction was allowed to proceed for another 12 h at 180 °C. The resulting dark red viscous polymer solution was precipitated in IPA. The polymer was filtered and purified in a Soxhlet extractor with methanol overnight. The polymer was dried at 120 8C in vacuo for at least 24 h.

*Characterization*

$^{1}$H NMR analyses were conducted on a Varian INOVA 400 MHz spectrometer with DMSO-d6 to confirm the chemical structures of oligomers and copolymers. $^{1}$H NMR spectroscopy was also used to determine copolymer compositions and molecular weights of the oligomers via end-group analyses. Intrinsic viscosities were determined using NMP containing 0.05 M LiBr at 25 8C using an Ubbelohde viscometer. Thermooxidative behavior of both the salt-and acid-form copolymers was measured on a TA Instruments TGA Q500. The samples were evaluated over the range of 80–800 °C at a heating rate of 10 °C/min in air. The ion exchange capacity (IEC) values of the acid-form copolymers were determined by titration with 0.01 M NaOH.

*Film Casting and Membrane Acidification*

Copolymer membranes in the potassium sulfonate salt form were prepared by solution casting. The copolymers were dissolved in NMP (10% w/v), filtered through 0.45 µm Teflon syringe

filters, and cast onto clean glass substrates. The solvent was evaporated under an infrared lamp for 48 h, resulting in transparent, tough, and flexible films. The films were further dried in vacuo at 120 8C for 24 h to remove residual solvent. The salt form films were acidified by boiling in 0.5 M sulfuric acid for 2 h, followed by boiling in deionized water for 2 h.

*Determination of Proton Conductivity and Water Uptake*

Proton conductivities were measured in liquid water at 30 °C. All conductivity measurements were made using a Solartron (1252A + 1287) impedance/gain-phase analyzer over the frequency range of 10 Hz–1 MHz. The conductivity of the membrane was determined from the geometry of the cell and resistance of the film which was taken at the frequency that produced the minimum imaginary response. To obtain water uptake values, membranes were dried in vacuo for 24 h at 100 °C, weighed, and then immersed in deionized water at room temperature for 24 h. The wet membranes were blotted dry and immediately reweighed. The water uptake of the membranes was calculated from the ratio of the increase in membrane weight divided by the dry membrane weight and expressed as a weight percent.

*Atomic Force Microscopy Characterization*

AFM images were obtained with a Digital Instruments MultiMode scanning probe microscope with a NanoScope IVa controller (Veeco Instruments, Santa Barbara, CA) in tapping mode. A silicon probe (Veeco) with an end radius of less than 10 nm and a force constant of 5 N/m was used to image samples. The ratio of amplitudes used in the feedback control was adjusted to 0.90–0.98 of the free-air amplitude. The samples were dried in vacuo at 60 8C for 3 h and then equilibrated at 30% relative humidity for at least 12 h before being imaged immediately at room temperature and a relative humidity of ~ 15–20%.

**RESULTS AND DISCUSSION**

*Synthesis of Hydrophilic and Hydrophobic Oligomers*

Amine-terminated sulfonated poly(arylene ether sulfone) hydrophilic oligomers (BPSH) were synthesized via polycondensation of SDCDPS, BP, and m-AP (Figure 1). The m-AP was used as an end-capping agent to produce amine telechelic functionality of the oligomers. The target number-average molecular weights of the BPSH oligomers were 5, 10, 15, and 20 kg/mol. Control of molecular weight was achieved by stoichiometric imbalance of monomers and end-capping agent. The number-average molecular weights of the BPSH oligomers were determined by $^{1}$H NMR spectra end group analysis. The peaks at 6.15 and 8.25 ppm were assigned to the protons on the m-AP moieties, which are located at the end of the oligomers, and the protons on the phenyl ring next to the sulfonated groups, respectively, (Figure 2). The integrals of both peaks were compared to calculate the number-average molecular weights of the hydrophilic oligomers. (Table 1). These match well with the target molecular weights. the structure, is less reactive with amines than five-membered ring anhydrides.

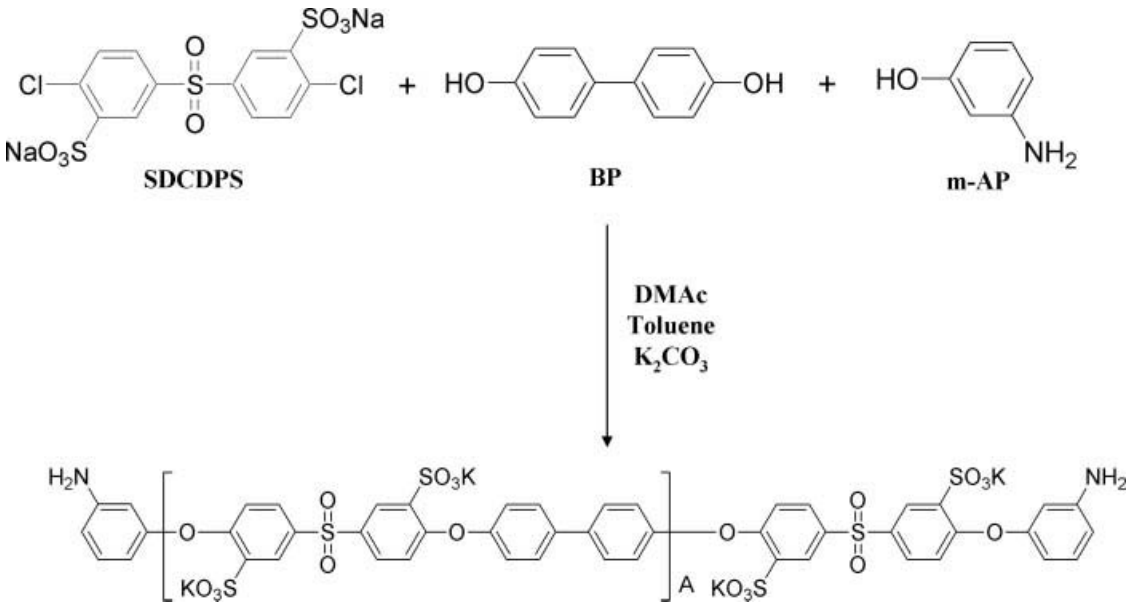


Figure 1. Synthesis of an amine-terminated disulfonated hydrophilic oligomer.

Naphthalene dianhydride-based polyimide hydrophobic oligomers (PI) were synthesized via a one-pot high-temperature imidization of NDA and m-BAPS (Figure 3). NDA is a six-membered ring anhydride, and because of lower strain in the structure, is less reactive with amines than five-membered ring anhydrides. To overcome the low reactivity of NDA, benzoic acid, and isoquinoline were used as catalysts. In addition, the imidization was carried out in m-cresol, which has been reported as the sole successful solvent for the synthesis of six-membered ring

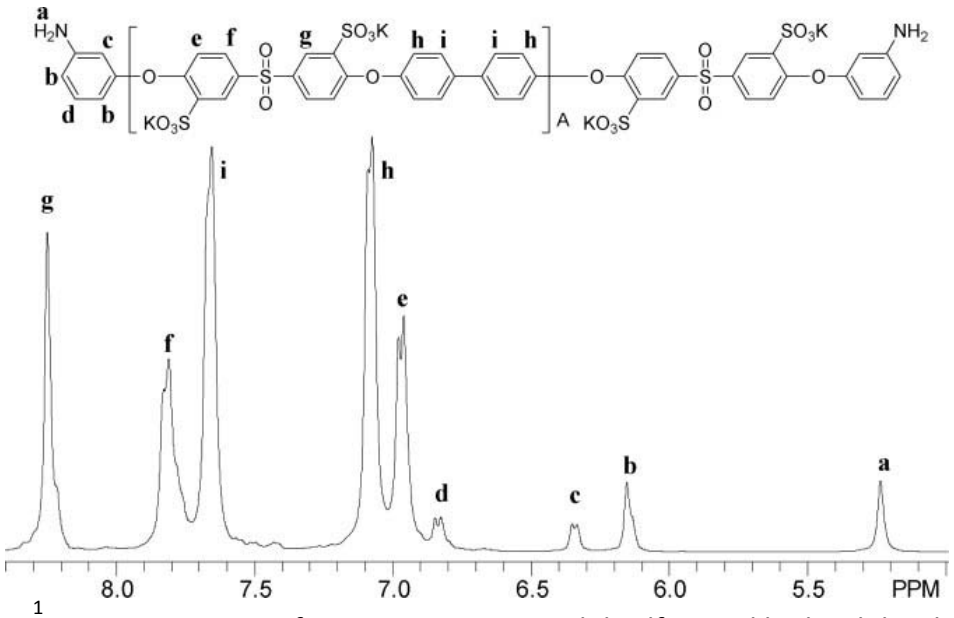


Figure 2. $^1$H-NMR spectrum of an amine-terminated disulfonated hydrophilic oligomer.

Table 1. Characterization of Hydrophilic and Hydrophobic Telechelic Oligomers

| | Hydrophilic Blocks | | Hydrophobic Blocks | |
|---|---|---|---|---|
| Target $M_n$ (g $mol_1$) | $M_n$ (g $mol_1$)[a] | IV (dL $g_1$)[b] | $M_n$ (g $mol_1$)[a] | IV (dL $g_1$)[b] |
| 5000 | 5500 | 0.18 | 5600 | 0.16 |
| 10,000 | 9800 | 0.28 | 10,200 | 0.22 |
| 15,000 | 14,500 | 0.30 | 17,200 | 0.34 |
| 20,000 | 20,100 | 0.47 | 23,800 | 0.41 |

[a] Determined by $^1$H NMR. [b] In NMP with 0.05 M LiBr at 25 8C.

polyimides. The molecular weight control and anhydride end group functionality of the oligomers were achieved by offsetting monomer stoichiometry. The number-average molecular weights of the PI oligomers were determined by $^1$H NMR spectra. The peaks ranging from 8.5 to 8.7 ppm and from 7.8 to 8.0 were assigned to the protons on the naphthalene moieties and the protons on the m-BAPS phenyl ring, respectively (Fig. 4). By comparing the integrals, number-average molecular weights were determined and are summarized in Table 1. A log–log plot between intrinsic viscosity and number-average molecular weight showed a linear relationship, confirming successful control of molecular weight for each hydrophilic and hydrophobic block series (Figs. 5 and 6).

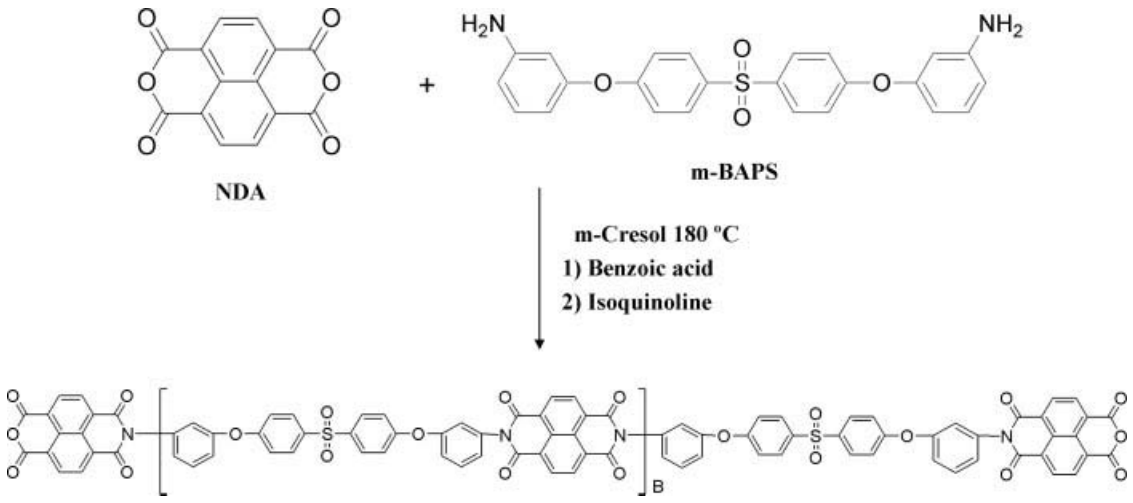


Figure 3. Synthesis of an anhydride-terminated polyimide hydrophobic oligomer.

*Synthesis of BPSH-PI Multiblock Copolymers*

A series of multiblock copolymers was synthesized by an imidization coupling reaction between amine moieties on the BPSH oligomers and anhydride moieties on the PI oligomers (Fig. 7). As described in the section on PI synthesis, a successful imidization of six-membered ring anhydrides needs to be conducted in m-cresol with catalysts. However, the coupling reaction between BPSH and PI oligomers in m-cresol was unsuccessful because of the insolubility of

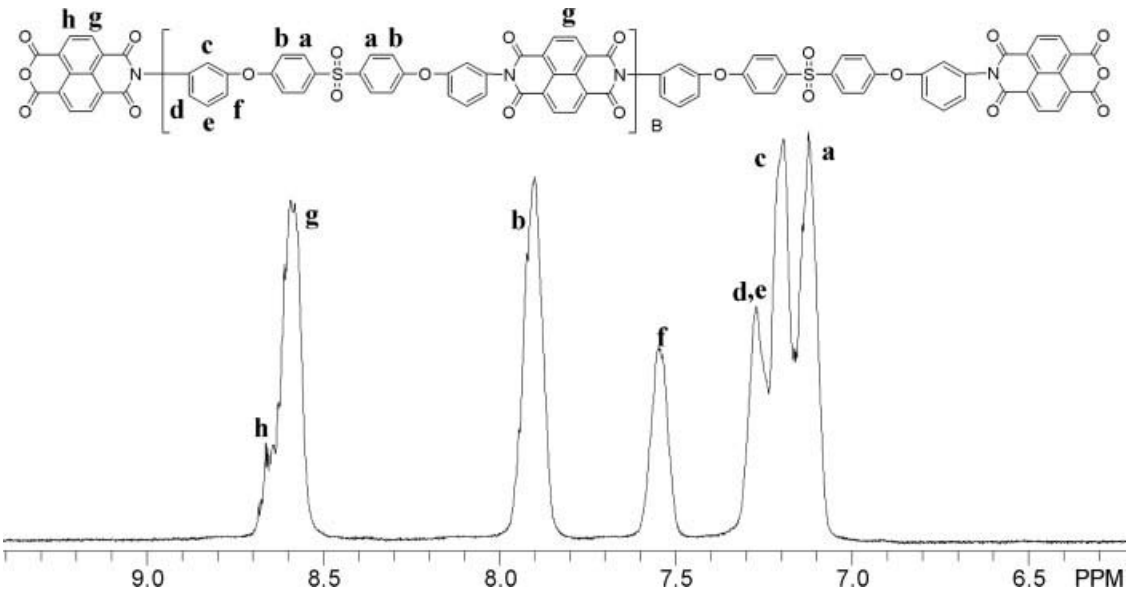


Figure 4. $^{1}$H NMR spectrum of an anhydride-terminated polyimide hydrophobic oligomer.

BPSH oligomers in m-cresol. Although many sulfonated compounds can be dissolved in m-cresol by converting the sulfonic acid groups into triethylammonium salts, this modification did not improve the solubility of the BPSH oligomers. For this reason, early attempts of the coupling reaction were performed in NMP, which dissolved both BPSH and PI oligomers. Unfortunately, the coupling reaction in the absence of m-cresol resulted in relatively low molecular weight multiblock copolymers. Their intrinsic viscosities ranged from 0.3 to 0.45 dL g$^{-1}$ and the copolymers did not produce tough ductile membranes (Table 2).

This low degree of coupling reaction was addressed by utilizing a mixed solvent system which consisted of m-cresol and NMP. By using a mixed solvent system, NMP provided good solubility of both oligomers, and this afforded homogeneous solutions wherein m-cresol facilitated the imidization coupling reaction. On the NMR spectrum of BPSH5-PI5 copolymer, the

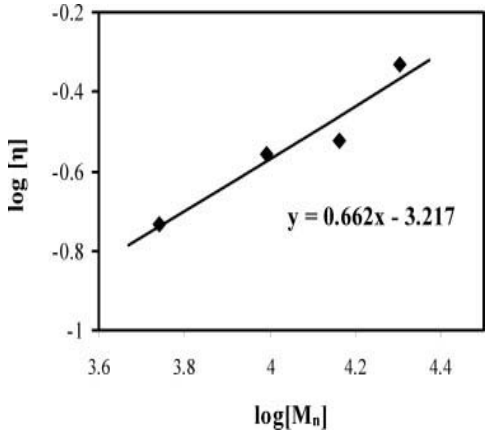


Figure5. Double logarithmic plot of [g] versus Mn of disulfonated poly(arylene ether sulfone) hydrophilic oligomers.

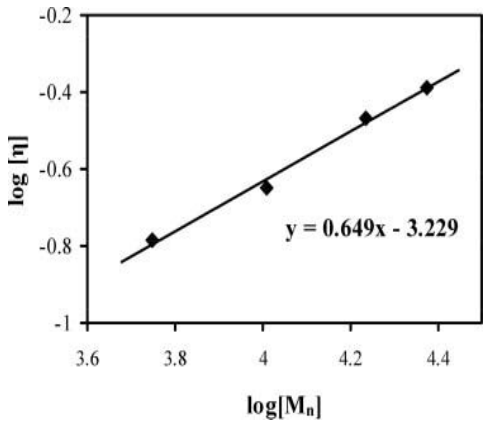


Figure 6. Double logarithmic plot of [g] versus Mn of disulfonated poly(arylene ether sulfone) hydrobic oligomers.

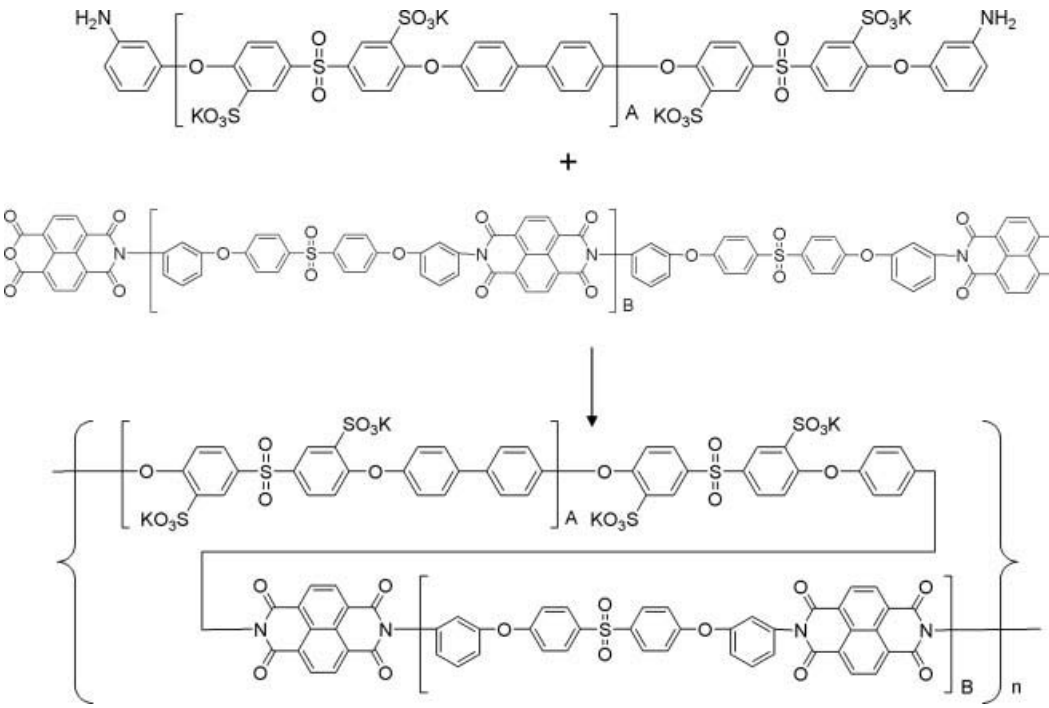

Figure 7. Synthesis of a segmented sulfonated poly(arylene ether sulfone)-b-polyimide copolymer.

disappearance of the end group peaks of the BPSH oligomer confirmed that the coupling reaction was successful (Figure 8). The BPSH-PI multiblock copolymers which were synthesized from the mixed solvent system showed higher intrinsic viscosities and produced tough, ductile membranes. A comparison of the membrane properties synthesized in different solvents is summarized in Table 2.

*Characterization of Membrane Properties of BPSH-PI Multiblock Copolymers*

The IEC values of the copolymers were determined by titrating the acid form membranes in aqueous sodium sulfate solution with standard sodium hydroxide solution (0.01 N). In all cases, the IEC values agreed with the theoretical values(Table 3). The proton conductivities of the membranes were measured under fully hydrated conditions in water at room temperature. The proton conductivities showed linear correlation with the IECs and increased up to 1.6 S/cm at an IEC of 1.9 meq/g. Conductivities of the samples with IECs higher than 1.9 meq/g could not be determined because ofthe poor mechanical strength of the hydrated membranes. The water uptake of the multiblock copolymers was investigated as a function of IEC (Figure 9). It also exhibited a linear relationship with IEC values up to 1.8 meq/g. However, once the IEC reached 1.8 meq/g, a drastic increase in water uptake was observed and the membranes became highly swollen hydrogels. This phenomenon can be explained by the development of a percolated morphology in the hydrophilic phase. A systematic explanation ofthe relationship between IECs, water uptake and proton conductivity will be provided in a separate article. Thermal and oxidative stabilities of the copolymers in their acid form were investigated by TGA. The

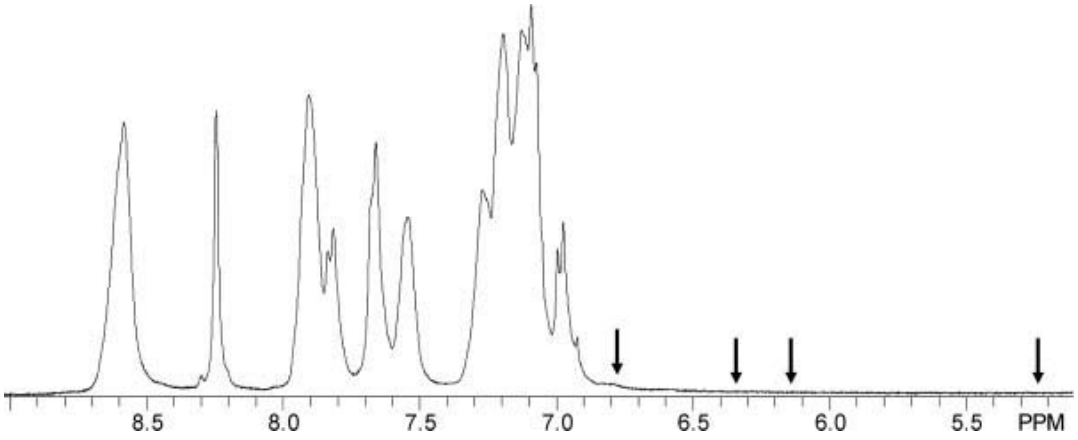


Figure 8. $^{1}$H NMR spectrum of a poly(arylene ether sulfone)-b-polyimide copolymer. Black arrows represent the disappearance of the amine end groups on the hydrophilic blocks after the coupling reaction with anhydride-terminated hydrophobic blocks.

Table 2. Comparison of Membrane Properties of BPSHx–PIy Copolymers Synthesized in Different Reaction Solvents

| | NMP | | | Mixed Solvent (NMP + m-Cresol) | | |
|---|---|---|---|---|---|---|
| Copolymers | IV (dL g_1)b | Water Uptake (%) | Conductivity (S/cm)c | IV Conductivity (dL/g)b | Water Uptake (%) | (S/cm)c |
| BPSH5–PI5 | 0.30 | 58 | 0.054 | 0.50 | 55 | 0.090 |
| BPSH10–PI10 | 0.35 | 100 | 0.060 | 0.63 | 70 | 0.100 |
| BPSH15–PI15 | 0.40 | – d | – d | 0.68 | 85 | 0.110 |
| BPSH20–PI20 | 0.44 | – d | – d | 1.20 | 56 | 0.100 a |

Acronym for copolymers (BPSHx–PIy): x =molecular weight of the hydrophilic block (BPSH) in units of kg/mol. y= molecular
weight of the hydrophobic block (polyimide) in units of kg/mol.
b: In NMP with 0.05 M LiBr at 25 8C.
c: Measured in deionized water at 30 8C.
d: Not available due to poor mechanical strength of hydrated film.

copolymer samples were preheated at 200 °C for 10 min in the TGA furnace to remove the moisture. The TGA was conducted from 100 to 800 °C at a heating rate of 10 °C/min under air (Fig. 10). All films displayed a two-step degradation profile. The initial weight loss was observed from 300 °C and was assigned to the decomposition of sulfonic acid groups on the BPSH block. The second decomposition, which ranged from 550 to 650 °C, was assigned to main-chain polymer degradation. As the hydrophilic component of the copolymer increased, the weight loss between 300 and 400 °C increased because of the increase of sulfonic acid content in the polymer.

Table 3. Properties of BPSH–PI Multiblock Copolymers in the Sulfonic Acid Form

| Copolymers | Calculated IEC (meq/g) | Experimental IEC (meq g1)a | Intrinsic Viscosity (dL g1)b | Water Uptake (%) | Conductivity (S cm1)c | Temperature at 5% Weight Loss (°C)d |
|---|---|---|---|---|---|---|
| BPSH5–PI5 | 1.63 | 1.65 | 0.50 | 55 | 0.090 | 367 |
| BPSH5–PI10 | 1.13 | 1.09 | 0.74 | 22 | 0.018 | 448 |
| BPSH5–PI15 | 0.80 | 0.78 | 0.71 | 15 | 0.010 | 484 |
| BPSH5–PI20 | 0.62 | 0.53 | 0.71 | 12 | 0.006 | 493 |
| BPSH10–PI5 | 2.10 | 1.98 | 0.61 | – e | – e | 340 |
| BPSH10–I10 | 1.59 | 1.57 | 0.63 | 70 | 0.100 | 346 |
| BPSH10–I15 | 1.20 | 1.17 | 0.72 | 40 | 0.073 | 351 |
| BPSH10–I20 | 0.96 | 0.86 | 0.92 | 24 | 0.030 | 507 |
| BPSH15–PI5 | 2.38 | 2.12 | 0.77 | – e | – e | 347 |
| BPSH15–I10 | 1.91 | 1.83 | 0.71 | 156 | 0.161 | 369 |
| BPSH15–I15 | 1.51 | 1.55 | 0.68 | 85 | 0.110 | 373 |
| BPSH15–I20 | 1.25 | 1.12 | 0.89 | 38 | 0.055 | 510 |
| BPSH20–PI5 | 2.58 | 2.20 | 0.75 | – e | – e | 317 |
| BPSH20–I10 | 2.17 | 2.02 | 0.92 | – e | – e | 333 |
| BPSH20–I15 | 1.78 | 1.71 | 0.83 | 97 | 0.092 | 345 |
| BPSH20–I20 | 1.51 | 1.20 | 1.20 | 56 | 0.100 | 365 |

[a] Determined by titration with NaOH. [b] In NMP with 0.05 M LiBr at 25 8C. [c] Measured in deionized water at 30 8C. [d] Conducted under air. [e] Not available due to poor mechanical strength of the hydrated film.

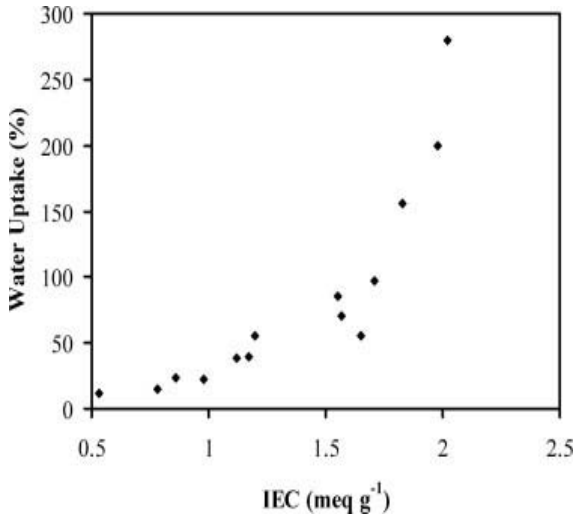


Figure 9. Influence of IEC on water uptake of BPSH-PI multiblock copolymers.

*Morphological Characterization of the Multiblock Copolymers*

Phase separated morphologies of the cast film surfaces were characterized by tapping mode atomic force microscopy (TM-AFM). It has been shown that water adsorbed on the surface of a sample increases adhesive forces between the tip and sample. This causes energy dissipation which results in a phase lag between the cantilever's oscillation and the initial oscillation imparted by the piezoelectric actuator. In these BPSH-PI films, the ionic groups on the BPSH adsorb water, resulting in an increased phase lag. Consequently, the ionic domains of the films appear darker in the TM-AFM phase images while the nonionic domains appear brighter. Contrast in the TM-AFM height images is based on height; lower features appear darker and higher features appear brighter.

TM-AFM images were obtained for the BPSH-PI copolymers. While phase separated morphologies were observed for multiblock copolymers with unequal block lengths, the sharpest and most uniform phase separated morphologies were observed for the copolymers with equal block lengths (Fig. 11). The brighter nonionic domains increased in size from small round domains [Fig. 11(a)] to cocontinuous lamellar structures [Fig. 11(c)] as block length increases. The darker ionic domains also formed longer channels with increasing block length. These morphologies were not limited to isolated regions within each membrane, but existed over longer scales across each membrane surface as evidenced by the uniform, long-range order displayed in the height and phase micrographs of BPSH15-PI15 [Figs. 11(d,e)].

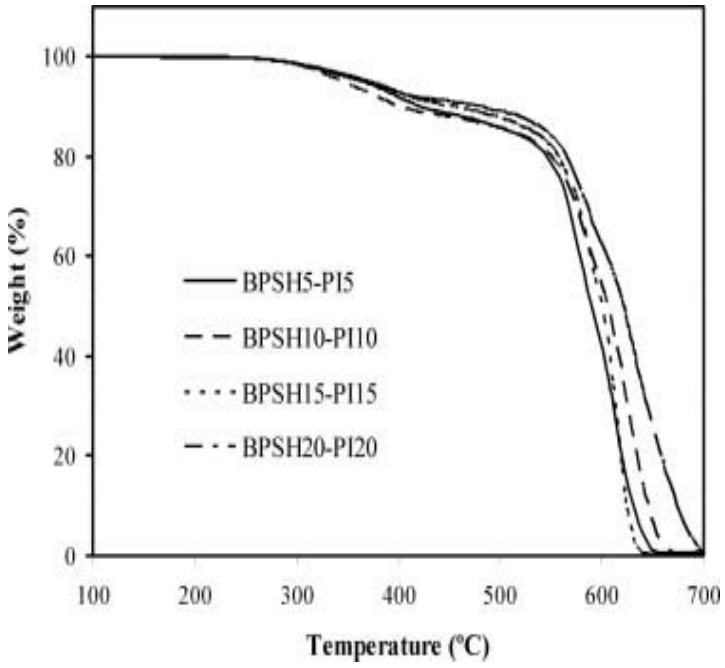


Figure 10. TGA Thermograms of BPSH-PI multiblock copolymers with different hydrophilic and hydrophobic block lengths.

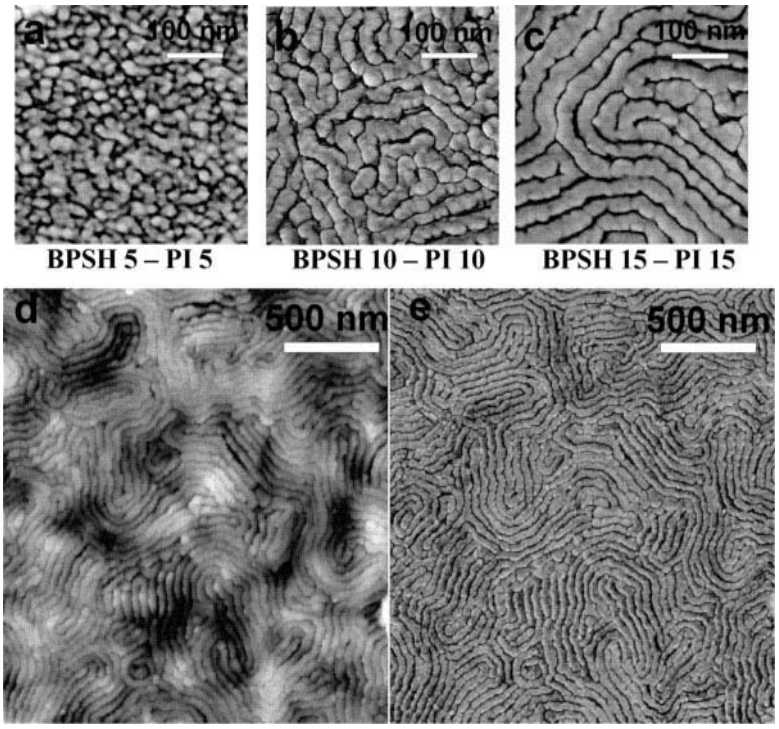


Figure 11. (a)–(c) Tapping mode AFM phase images of BPSH-PI multiblock copolymers with different block lengths, (d) height image, and (e) phase image of BPSH15PI15 demonstrating long-range order.

*Hydrolytic Stability Test*

Hydrolytic stability of a PEM is a crucial property for long-term fuel cell operation. Intense research on sulfonated polyimides revealed that five-membered ring polyimides were not suitable for PEM applications because of hydrolysis of the imido ring under acidic conditions. Although this poor hydrolytic stability has been improved by using a six-membered ring polyimide, their long-term stability under a harsh fuel cell environment is still suspect. The hydrolytic stabilities of two series of sulfonated naphthalene dianhydride-based random copolymers were previously reported by our laboratory. Those membranes became brittle in less than 100 h of submersion in 80 °C water. The intrinsic viscosities of the samples after the test were reduced to 10–20% of the original values, which is attributed to hydrolysis of the imide moieties within the polymer. Hydrolytic stabilities of the BPSH-PI copolymers were determined by monitoring changes in intrinsic viscosity and mechanical flexibility.

*Conclusions*

Novel multiblock copolymers based on hydrophilic and hydrophobic blocks were developed and characterized. The multiblock copolymers were synthesized from amine terminated sulfonated poly(arylene ether sulfone) as hydrophilic block and anhydride terminated polyimide as

hydrophobic block by imidization coupling reaction. In the coupling reaction, m-cresol and catalysts were required to produce high molecular weight multi-block copolymers. Transparent and ductile membranes were prepared from NMP by solvent casting. Their proton conductivities and water uptake values were influenced by IEC values. Morphological characterization by tapping-mode AFM showed clear nano-phase separation of hydrophilic and hydrophobic domains. Changes in block length affected the morphologies of the multiblock copolymers and the BPSH15-PI15 membrane showed long-range cocontinuous morphology of the hydrophilic and hydrophobic regimes. Hydrolytic stability testing of the multiblock copolymers in 80 8C water revealed that they maintained flexibility after 1000 h, which is much improved over earlier random copolymer systems.

# Development of Multiblock Copolymers with Novel Hydroquinone-Based Hydrophilic Blocks for Proton Exchange Membrane (PEM) Applications

**Summary of Results**

Hydrophilic-hydrophobic sequenced multiblock copolymers were synthesized and evaluated for use as proton exchange membranes (PEMs). The multiblock copolymers were prepared by a coupling reaction between fully disulfonated hydroquinone based hydrophilic oligomers (HQS100) and unsulfonated poly(arylene ether sulfone) hydrophobic oligomers (BPS0). The hydroquinone-based hydrophilic oligomers possess several advantages over previously utilized biphenol-based hydrophilic oligomers (BPS100), including higher hydrophilicity, enhanced nano-phase separation with hydrophobic segments, and lower cost. To maintain the hydrophilic-hydrophobic sequences in the system, the coupling reactions were conducted at low temperature (e.g., 105 °C) to avoid ether-ether exchange reactions. The coupling reaction was solvent sensitive due to a low reactivity of the hydroquinone-phenoxide end-group on the HQS100. All copolymers produced tough ductile films when cast from an NMP or DMF solution. Fundamental membrane parameters including water uptake, proton conductivity, and swelling ratio were investigated along with morphology characterizations by atomic force microscopy (AFM).

**INTRODUCTION**

Over the last decade, a substantial body of research has been devoted to developing novel proton exchange membranes (PEMs) which can replace the state-of-the-art Nafion®. Among a variety of candidates, wholly aromatic high temperature polymers have been considered to be the most promising materials. The major advantages for utilizing high temperature polymers for fuel cell applications include their excellent thermal and oxidative stability, as well as the fact that they are economical and easy to produce. The most

extensively studied materials are the so-called BPSH-type materials, which are statistical random copolymers based on disulfonated poly(arylene ether sulfone)s. BPSH-type copolymer systems utilize 3,3'-disulfonated-4,4'-dichlorodiphenylsulfone (SDCDPS) as the key monomer, which can facilitate precise control over the degree of sulfonation, and excellent stability of the sulfonic acid moieties. Although PEMs based on BPSH-type materials display improved properties over Nafion® under fully hydrated conditions with respect to conductivity, durability, and fuel cross-over, their proton conductivities under partially hydrated conditions have remained somewhat disappointing. This could be due to the fact that the proton conduction channels in sulfonated hydrocarbon-based materials are narrower than those of Nafion-type materials, which accounts for the significant reduction in conductivity under low humidity conditions. A number of strategies have been used to address this problem, including (1) the partial fluorination of the aromatic polymer backbone to form a sharp phase separation, (2) the incorporation of bulky pendent groups to increase free-volume, (3) the addition of hydrophilic nano-particles to help retain water, and (4) the addition of heteropolyacid (HPA). Although each of these approaches was somewhat beneficial in increasing proton conductivity under low RH conditions, none of these methods could overcome important fundamental limitations.

Recently, PEMs based on hydrophilic-hydrophobic sequenced multiblock copolymers have been considered as strong candidates for overcoming limited proton conduction under partially hydrated conditions. These multiblock copolymers utilize fully disulfonated biphenol-based poly(arylene ether sulfone) as the hydrophilic block (BPSH100), with various engineering materials used as the hydrophobic block. These multiblock copolymer-based PEMs exhibit nano-phase separated morphologies and well-connected ionic hydrophilic phases. As such, they can facilitate high proton conductivity even under low relative humidity conditions, while the well-connected hydrophobic phase can provide dimensional stability. A number of extensive structure-property studies revealed that property enhancements can be strongly influenced by the length of the hydrophilic and hydrophobic blocks. Generally, proton conductivity and water uptake increase with increasing hydrophilic and hydrophobic block length by forming long-range co-continuous lamellae morphologies. Even though the multiblock copolymers based on BPSH100 hydrophilic block were comparable or superior to Nafion with respect to proton conductivity under low humidity conditions, we were unable to achieve even higher conductivity by solely increasing IEC values. Increasing the volume fraction of hydrophilic segments in a system in order to improve IEC values produces a decrease in the hydrophobic segment volume fraction, resulting in poor mechanical properties and excess swelling behavior. In other words, a balancing act is hard to achieve for maintaining both high IEC and advantageous mechanical properties.

A possible solution to this dilemma is utilizing a more hydrophilic (e.g., higher IEC) block for the multiblock copolymer system. When a higher IEC hydrophilic oligomer is used to obtain an IEC multiblock copolymer, the amount of the higher IEC hydrophilic block should be less than that of lower IEC hydrophilic block to obtain the target IEC. Using the same logic, if the feed ratio of the hydrophilic and hydrophobic blocks is fixed, a higher IEC hydrophilic block system will incorporate more sulfonic acid moieties in the multiblock copolymers. As a result, one can increase the IEC values of the multiblock copolymers without scarifying the volume fraction of hydrophobic segments, which plays an important role in producing desirable mechanical

properties. In addition, higher IEC hydrophilic blocks can lead a sharper phase separation in the copolymer membrane due to the increased hydrophilic-hydrophobic contrast.

This paper, therefore, describes the synthesis and characterization of a novel multiblock copolymer system with hydroquinone-based hydrophilic oligomers. The fully disulfonated hydroquinone based poly(arylene ether sulfone) hydrophilic oligomer (HQSH100) has an IEC of 3.89 meq/g, which is approximately 20% higher than that of BPSH100. A series of multiblock copolymers with HQSH100 hydrophilic blocks was synthesized, and their fundamental membrane properties and morphology will be described.

## EXPERIMENTAL

### Materials

Monomer grade 4,4'-dichlorodiphenylsulfone (DCDPS), 4,4'-biphenol(BP) were provided by Solvay Advanced Polymers and Eastman Chemical, respectively, and were dried *in vacuo* at 110 °C prior to use. Hydroquinone (HQ) was purchased from Aldrich and was purified by sublimation under reduced pressure. The sulfonated comonomer 3,3'-disulfonated-4,4'-dichlorodiphenylsulfone (SDCDPS) was synthesized and purified according to previously reported procedures. The purity of SDCDPS was determined by UV-Vis spectroscopy. Hexafluorobenzene (HFB) and potassium carbonate were purchased from Aldrich and used without further purification. N-methyl-2-pyrrolidone (MNP), dimethyl sulfoxide (DMSO), N,N-dimetheylacetamide (DMAc), and toluene were received from Aldrich and were distilled at reduced pressure before use.

### Synthesis of Hydroquione-Based Hydrophilic Oligomers (HQS100) with Phenoxide Telechelic Functionality.

HQ-based fully disulfonated hydrophilic blocks of different molecular weights were synthesized via step growth polymerization. A sample oligomer synthesis with molecular weight of 3,000 g/mol is as follows: 66.6 mmol of HQ (7.3351 g), 56.3 mmol of SDCDPS (27.6649 g) and 79.9 mmol of potassium carbonate (20 mol% excess) were dissolved in 140 ml of distilled NMP and 70ml of toluene in a 3-necked flask equipped with a condenser, a Dean Stark trap, nitrogen inlet and mechanical stirrer. The reaction mixture was heated at 150ºC for 4 hours with refluxing toluene to dehydrate the system. The reaction temperature was then slowly increased to 185 ºC to remove the toluene and allowed to react for 48 hours. The reaction solution was cooled to room temperature and filtered to remove salts. For high molecular weight oligomers, dilution with NMP was necessary to ease the filtration. The oligomer was coagulated in acetone followed by filtration and drying *in vacuo* at 110 ºC for 24 h.

### Synthesis of Phenoxide Terminated Poly(arylene ether sulfone) Hydrophobic Oligomers (BPS0) and Their End-Capping with Hexafluorobenzene (HFB).

BP based unsulfonated hydrophobic blocks of different molecular weights were synthesized via step growth polymerization. A sample oligomer synthesis with molecular weight of 5,000 g/mol is as follows: 66.5 mmol of BP(13.0210 g), 61.4 mmol of DCDPS (12.0210 g) and

79.8 mmol of potassium carbonate (20 mol% excess) were dissolved in 120 ml of distilled DMAc and 60ml of toluene in a 3-necked flask equipped with a condenser, a Dean Stark trap, nitrogen inlet and mechanical stirrer. The reaction mixture was heated at 150ºC for 4 hours with refluxing toluene to dehydrate the system. The reaction temperature was slowly increased to 175 ºC to remove the toluene and allowed to react for 48 hours. The dried oligomer was obtained according to procedures used for HQS100 synthesis.

The isolated BPS0 oligomers were then end-capped with HFB via a nucleophilic aromatic substitution reaction. A sample end-capping reaction of the 5,000 g/mol oligomer is as follows: 5.0000 g (1.0 mmol) of BPS0 oligomer and 0.5528 g (4.0 mmol) of potassium carbonate were charged to a 3-necked 100-mL flask equipped with a condenser, a Dean Stark trap, a nitrogen inlet, and a mechanical stirrer. Distilled DMAc (50 mL) and cyclohexane (15 mL) were added to the flask. The solution was allowed to reflux at 100 °C to azeotropically remove the water in the system. After 4 h, the cyclohexane was removed from the system by distillation. The reaction temperature was decreased to 80 °C and the nitrogen purge was stopped to avoid the possible loss of low-temp boiling HFB (b.p.=80 °C). Afterwards, 1.1163 g (6.0 mmol) of HFB was added and the reaction was allowed to proceed for 12 h.

**Synthesis of Hydrophilic-Hydrophobic Multiblock Copolymers (HQSH-BPS).**

Multiblock copolymers with various lengths of hydrophilic and hydrophobic blocks were synthesized. A sample coupling reaction is as follows: Into a 100mL 3-necked flask equipped with a mechanical stirrer, nitrogen inlet and a Dean-Stark trap, 3.0000 g of hydrophilic oligomer (Mn = 3,000 g/mol 1.0 mmol), 0.5528 g of $K_2CO_3$ (4.0 mmol), 20 mL of cyclohexane and 40 mL of DMSO were added and dehydrated at 100 °C for 4 h. The cyclohexane was then removed by distillation and 5.0000 g of hydrophobic oligomer (Mn = 5,000 g/mol 0.1 mmol) was added. The coupling reaction was conducted at 105 °C for 24 h. The obtained brown polymer solution was coagulated in isopropyl alcohol. The resulting polymer was filtered and dried in a vacuum oven at temperatures up to 110 ºC.

**Characterization**

The chemical structures of the oligomers and copolymers were confirmed by H NMR analyses on a Varian INOVA 400 MHz spectrometer with DMSO-$d_6$. In addition, $^1$H NMR spectroscopy was utilized for end-group analyses of the oligomers to determine their $\overline{M_n}$. Intrinsic viscosities were determined in NMP containing 0.05 M LiBr at 25 ºC using an Ubbelohde viscometer. Ion exchange capacity (IEC) values were determined by titration with a 0.01 M NaOH solution.

**Film Casting and Membrane Acidification.**

The starting membranes were cast in their salt form by solution casting. The salt form copolymers were dissolved in NMP or DMF (7% w/v) and filtered with syringe filters (0.45 µm Teflon®). The filtered solutions were then cast onto clean glass substrates. The films were dried under an IR ramp at 60 ºC for 1 day and followed by drying *in vacuo* at 110 ºC for 24 h. The acid- form membranes were obtained by boiling in a 0.5 M sulfuric acid aqueous solution for 2

h, followed by boiling in deionized water for 2 h. The membranes were kept in deionized water at room temperature for 24 h for further characterization.

**Determination of Proton Conductivity and Water Uptake.**

Both fully and partially hydrated proton conductivities were evaluated in a water bath and a humidity-temperature controllable chamber, respectively. The conductivity of the membrane was determined from the geometry of the cell and resistance of the film, which was taken at a frequency that produced the minimum imaginary response. A Solartron (1252A +1287) impedance/gain-phase analyzer over the frequency range of 10 Hz - 1 MHz was used for the measurements. The membrane water uptake was determined by the weight difference between dry and wet membranes. The vacuum dried membranes were weighed ($W_{dry}$), and then immersed in deionized water at room temperature for 24 h. The wet membrane was blotted dry and immediately weighed again ($W_{wet}$). The water uptake of the membranes was calculated according to the following equation.

$$Water\,Uptake\ (\%) = \frac{W_{wet} - W_{dry}}{W_{dry}} \times 100$$

**Atomic force microscopy (AFM)**

Tapping mode AFM was performed using a Veeco Multimode Atomic Force Microscope. Samples were equilibrated at 30% relative humidity (RH) at room temperature for at least 24 h and sealed before imaging.

**RESULTS AND DISCUSSION**

**Synthesis of Controlled Molecular Weight Hydrophilic blocks (HQS100).**

Different number-average molecular weight hydrophilic oligomers were synthesized via the step growth polymerization of SDCDPS and HQ (Figure 1). We were able to precisely control molecular weight and end-group functionality via a stoichiometric imbalance of the monomers. All oligomers were designed to be terminated with phenoxide end-groups by using an excess amount of HQ. The target molecular weights for hydrophilic blocks ranged from 3,000 to 15,000 g/mol. Earlier, the synthesis was attempted in DMAc at 175 ºC for 96 h. However, the poor solubility of HQS100 in DMAc resulted in premature precipitation within just a few hours. As a result, it was impossible to control both molecular weight and end-group functionality. It has been suggested that the insolubility of the oligomers may stem from the formation of crystallites from the HQ moieties on the main chain backbone. To maintain homogeneous conditions during synthesis, DMSO was also used as the reaction solvent. Although it provided both good solubility and rapid reaction kinetics (i.e., the reaction can be completed in 48 h at 180 ºC), the resulting product was not pure enough to be used for the coupling reaction due to unidentified side reactions. On the one hand, although undesirable side reactions could be avoided when the reactions were conducted at fairy low temperatures (e.g., 135 ºC), the reaction time was significantly prolonged (e.g., ~200 h). On the other hand, when we conducted the reaction in NMP at 195 ºC for 48 h, we were able to avoid any side reactions. Thus, we used the latter reaction conditions for preparing the HQS100 oligomers used in this research.

End-group analyses of selected peaks via $^{1}H$ NMR spectra were used to determine the number-average molecular weight of the oligomers (Figure 2). On the NMR spectrum of the HQS100, two small peaks, **e** and **f,** at 6.75 and 6.83 ppm, respectively, were assigned to the protons on the HQ moieties, located at the end of the chain. Calculating the integration ratios between one of these peaks and one of the other main peaks (**a**, **b**, **c**, and **d**) was used to determine the number-average molecular weight of the oligomers. Table 1 lists the characterization data for the HQS100 hydrophilic telechelic oligomers used in this study.

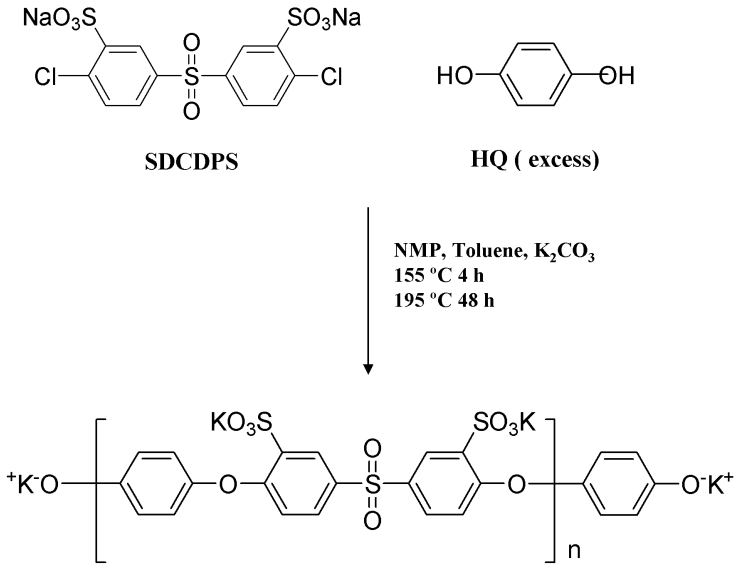


**Figure 1.** Synthesis of a phenoxide-terminated fully disulfonated poly(arylene ether sulfone) hydrophilic oligomer based on hydroquinone (HQS100)

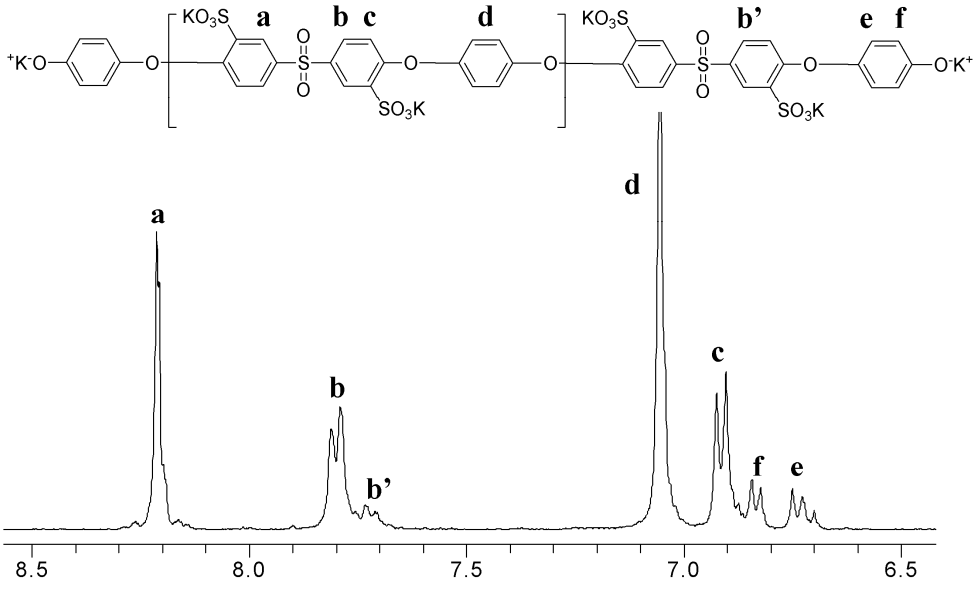

**Figure 2.** $^{1}$H NMR spectrum of HQS100 with a molecular weight of 3,000g/mol

**Table 1.** Characterization of HQS100 Hydrophilic Telechelic Oligomers

| Target $M_n$ (g mol$^{-1}$) | $M_n$ (g mol$^{-1}$)[a] | IV (dL g$^{-1}$)[b] |
|---|---|---|
| 3,000 | 3,200 | 0.12 |
| 5,000 | 4,700 | 0.14 |
| 6,000 | 5,500 | 0.16 |
| 9,000 | 9,100 | 0.22 |
| 10,000 | 10,700 | 0.23 |
| 12,000 | 12,900 | 0.24 |
| 15,000 | 14,800 | 0.29 |

[a] Determined by $^{1}$H NMR.
[b] In NMP with 0.05 M LiBr at 25 ºC.

**Synthesis of Controlled Molecular Weight Hydrophobic Blocks (BPS0) and Their End-Capping with Hexafluorobenzene (HFB)**

Unsulfonated poly(arylene ether sulfone) oligomers based on biphenol (BPS0) with varying molecular weights were synthesized as hydrophobic blocks (Figure 3). Control of molecular weight and end-group functionality was achieved by upsetting the feed ratios of the monomers. $^{1}$H NMR spectroscopy of the BPS0 hydrophobic oligomers showed that the oligomers possessed phenoxide end-group functionality as intended, and we were able to determine number-average molecular weight via end-group analyses (Figure 4). Molecular weight and intrinsic viscosity data for the BPS0 are summarized in Table 2. When log-log plots were made between number average molecular weight and intrinsic viscosity, linear relationships for both the hydrophilic and hydrophobic oligomers were identified, thereby confirming successful molecular weight control (Figure 5).

The synthesized hydrophilic and hydrophobic oligomers possessed the same phenoxide end-groups, making them unsuitable for the coupling reaction needed to produce multiblock copolymers since they are not reactive with each other (i.e., both end-groups are nucleophiles). Thus, it was necessary to modify the end-group functionality of either hydrophilic or hydrophobic block to facilitate the coupling reaction. For this research, we chose to modify the BPS0 hydrophilic blocks, which were end-capped with hexafluorobenzene (HFB) (Figure 6). In so doing, we could convert the nucleophilic BPS0 oligomers into elecrophilic, fluorine-terminated BPS0 oligomers, which would facilitate a coupling reaction with the HQS100 oligomers. As shown in Figure 7, the end-group peaks for the terminal BP moieties completely disappeared and a new peak appeared at 7.65 ppm. This peak corresponds to the same protons on the terminal BP moieties but were attached to HFB. Although NMR spectra comparisons before and after end-capping reaction confirmed that all the phenoxide end-groups had reacted with HFB, the formation of high molecular weight BPS0 oligomers via an inter-oligomer coupling reaction was still possible due to the multifunctionality of the HFB. To prevent this from occurring, a large excess of HFB was used. Specifically, the molar ratio between the BPS0 and HFB was 1:6.

In addition, intrinsic viscosity studies of the BPS0 oligomers before and after end-capping showed that there was little, if any, inter-oligomer coupling, as evidenced by the less than 0.02 dL/g increase with the end-capped oligomers. This implies that the end-capping reaction was successful without any significant inter-oligomer coupling, and that high molecular weight BPS0 oligomers had formed.

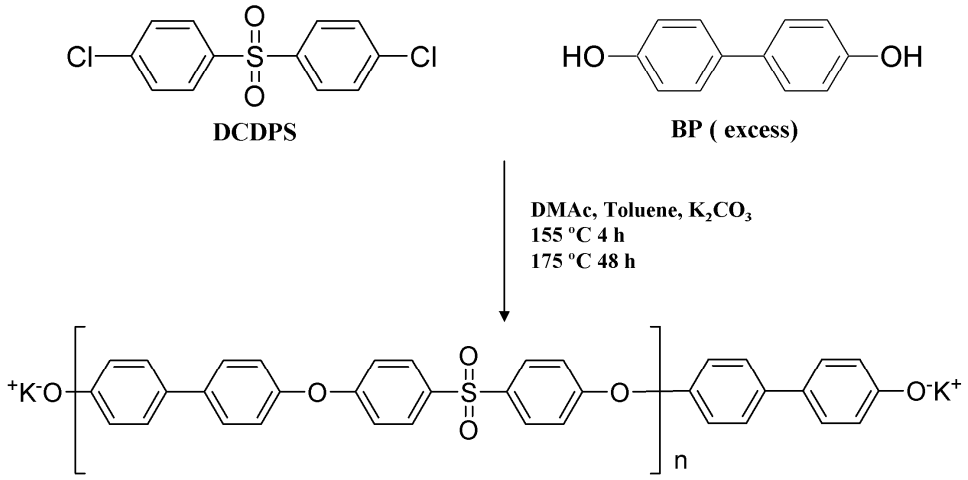


**Figure 3.** Synthesis of a phenoxide-terminated undisulfonated poly(arylene ether sulfone) hydrophobic oligomer based on biphenol (BPS0)

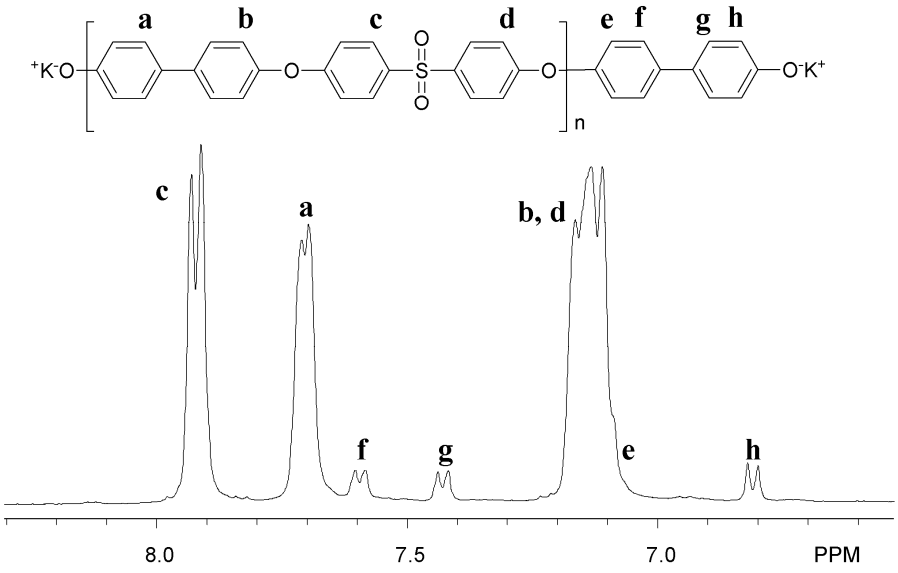


**Figure 4.** $^{1}$H NMR spectrum of BPS0 with a molecular weight of 3,000g/mol

**Table 2.** Characterization of BPS0 Hydrophobic Telechelic Oligomers

| Target $M_n$ (g mol$^{-1}$) | $M_n$ (g mol$^{-1}$)[a] | IV (dL g$^{-1}$)[b] |
|---|---|---|
| 3,000 | 3,200 | 0.19 |
| 5,000 | 5,200 | 0.26 |
| 10,000 | 10,400 | 0.35 |
| 15,000 | 14,700 | 0.46 |
| 20,000 | 20,800 | 0.51 |
| 25,000 | 24,400 | 0.54 |

[a] Determined by $^1$H NMR.
[b] In NMP with 0.05 M LiBr at 25ºC.

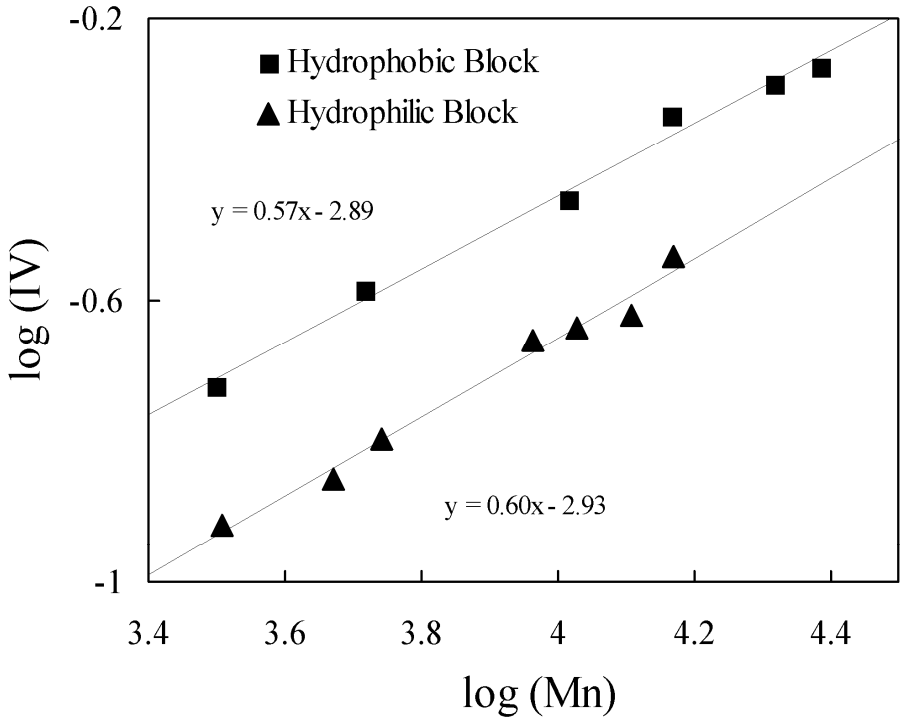


**Figure 5.** Double logarithmic plot of [η] versus $M_n$ of hydrophilic (HQS100) and hydrophobic (BPS0) oligomers.

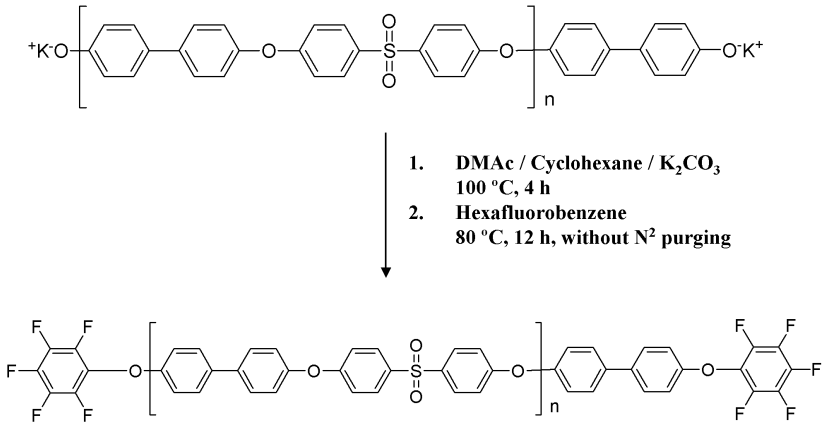


**Figure 6.** End-Capping of the phenoxide terminated hydrophobic oligomer (BPS0) with HFB. This procedure transforms the nucleophilic telechelic oligomer into an electrophilic telechelic oligomer.

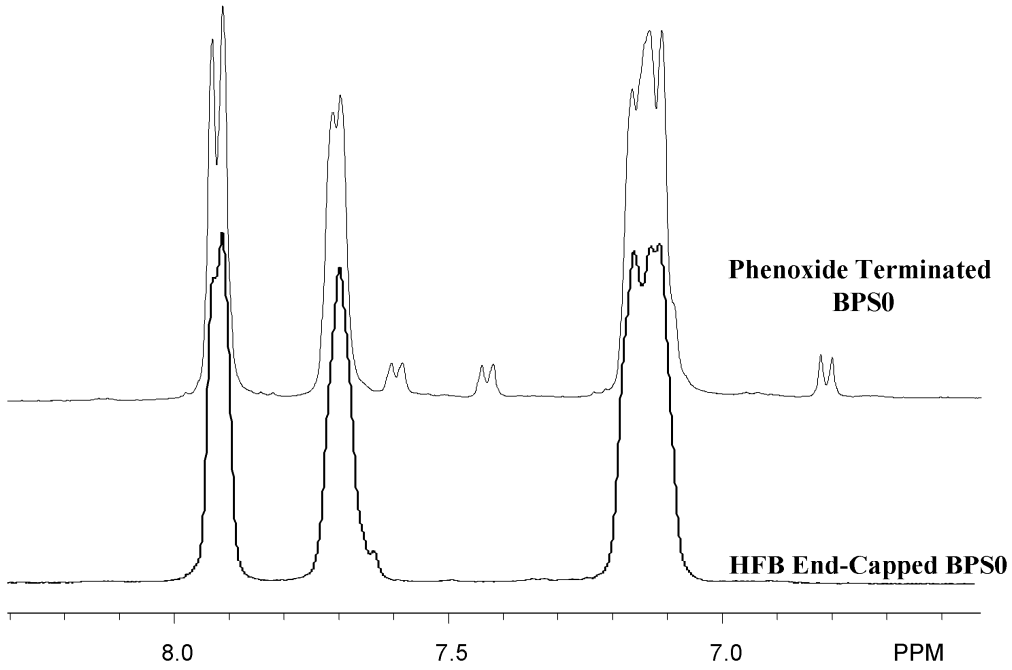


**Figure 7.** BPS0 hydrophobic oligomer $^1$H NMR spectra comparison before and after the end-capping reaction with HFB.

**Synthesis of Multiblock Copolymers by a Coupling Reaction of Hydrophilic and Hydrophobic Oligomers.**

Multiblock copolymers of varying hydrophilic and hydrophobic block length were synthesized via a coupling reaction (Figure 8). This reaction is a simple nucleophilic aromatic substitution reaction between the phenoxide and the fluorine end groups on the HQS100 and the BPS0 oligomers, respectively. Although expected to be fairly straightforward, this coupling reaction turned out to be solvent sensitive. Specifically, when the coupling reactions were conducted in NMP, the resulting intrinsic viscosity and IEC values for the multiblock copolymers were always lower than expected. Similar problems were observed with either DMAc or DMF. However, the low reactivity between the hydrophilic and hydrophobic oligomers was significantly enhanced when DMSO was used. As shown on the $^{1}$H NMR spectrum in Figure 9, the end-group peaks associated with the hydrophilic oligomer disappeared, confirming that the coupling reaction was successful. One possible explanation for the solvent sensitivity of the coupling reaction is that the reactivity of the phenoxide group on the HQ moieties could have been influenced by the polarity of the solvents. In other words, DMSO might have solvated the potassium ion more effectively than the other solvents with a higher dielectric constant, thereby increasing the reactivity of the phenoxide anion toward the fluorine electrophile of the BPS0 oligomers. Although the use of DMSO helped us to avoid solvent sensitivity, we did encounter another problem—namely the poor solubility of the BPS0 oligomers in DMSO, which became even more apparent when high molecular weight BPS0 oligomers were used (e.g., > 10,000 g/mol). This difficulty was addressed by reducing the oligomer concentration during the coupling reaction to 3-4 (w/v) %. All multiblock copolymers used in this study were synthesized through a coupling reaction in DMSO.

We also studied another strategy to overcome a low degree of coupling. Since poor reactivity seems to stem from the low reactivity of the HQ phenoxide moieties, we tried to avoid using HQ-phenoxide end-group on the hydrophilic oligomer for the coupling reaction. First, we end-capped phenoxide terminated HQS100 oligomers with HFB in DMSO. Since DMSO facilitates both good solubility and high reactivity, end-capping the HQS100 oligomers was successful with no complications. The HFB end-capped HQS100 can then typically be reacted with phenoxide terminated BPS0 oligomers in NMP or DMAc. In this case, the nucleophile is the BP phenoxide moiety which is strong enough to attack the fluorine end-groups on the HQS100 in either NMP or DMAc. By adopting this strategy, the coupling reaction can be successfully conducted without reducing oligomer concentrations. As mentioned earlier, the main reason for employing highly reactive HFB for the coupling reaction is to prevent hydrophilic-hydrophobic sequence randomization via transetherification by reducing the coupling reaction temperature. To confirm that the synthesized multiblock copolymers maintained the sequences, their $^{13}$C NMR spectra were compared with that of a random copolymer that had been synthesized from the same monomers (Figure 10). As expected, the multiblock copolymer showed sharp singlet or doublet peaks while the random copolymer exhibited complicated mutiplet peaks, thereby confirming that the multiblock copolymer possessed well-defined sequences in the system.

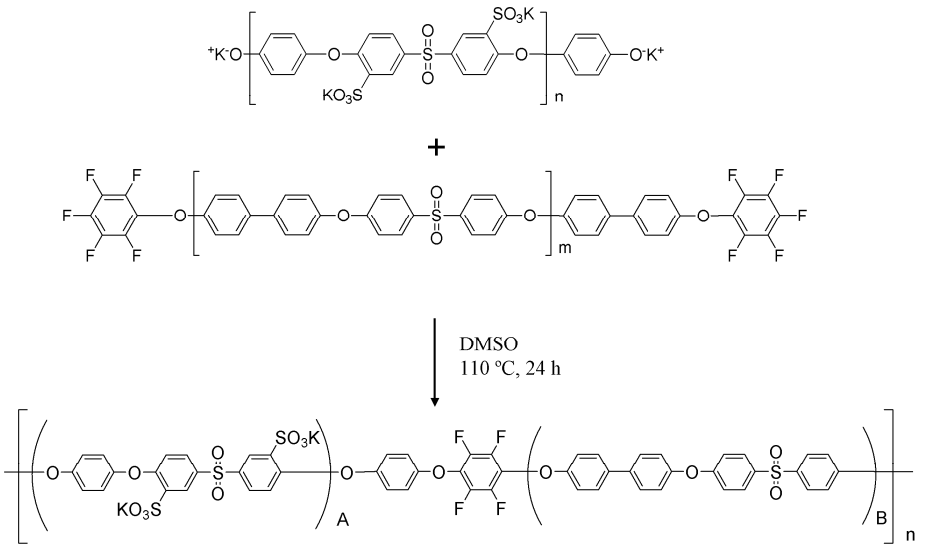


**Figure 8.** Synthesis of segmented sulfonated multiblock copolymers via a coupling reaction.

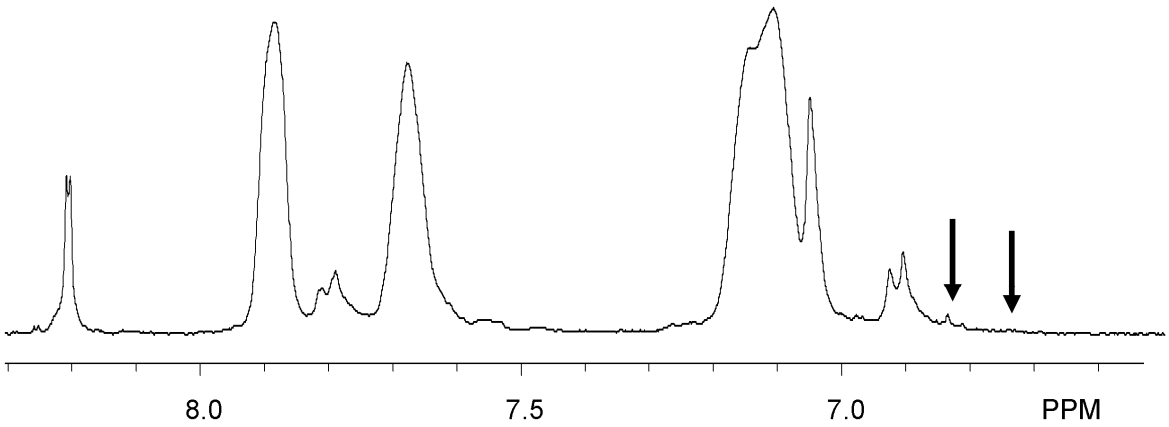


**Figure 9.** $^{1}$H NMR spectrum of HQSH3-BPS5. Black arrows indicate the disappearance of the end groups on the hydrophilic blocks after the coupling reaction with fluorine-terminated hydrophobic blocks.

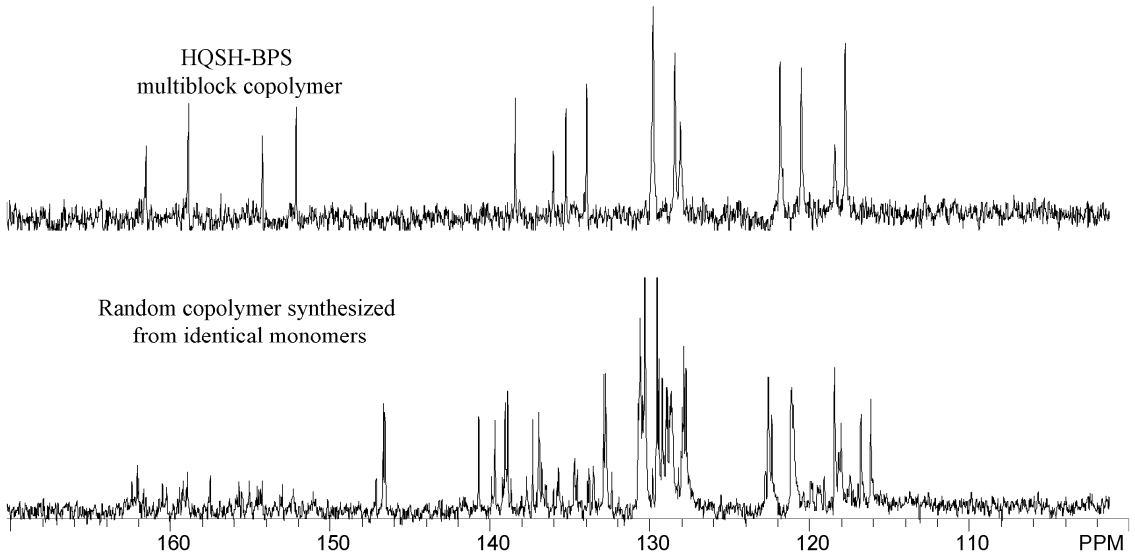


**Figure 10.** $^{13}C$ NMR spectra comparison of HQSH3-BPS5 multiblock copolymer and a random copolymer synthesized from the identical monomers.

**Characterization of Membrane Properties of HQSH-BPS Multiblock Copolymers**

A series of multiblock copolymers with varying hydrophilic and hydrophobic block lengths was synthesized, and subsequently examined to determine their potential fuel cell applications. Their fundamental membrane properties are summarized in Table 3. The copolymers are categorized into three groups. The first group includes Nafion 112 and BPSH35, which were used as controls. The second and third groups include the multiblock copolymers with different block lengths. Although varying length of hydrophilic and hydrophobic oligomers were used for the multiblock copolymer synthesis, target IEC values were set to approximately 1.4 and 1.9 meq/g for the second and the third group, respectively. To obtain the target IEC value of 1.4 meq/g for the second group, the composition ratio between hydrophilic and hydrophobic blocks was set to 3:5. For the third group, a composition ratio of 1:1 was used to attain the target IEC of 1.9. All polymerization feed ratios were calculated based on a 1:1 molar ratio between hydrophilic and hydrophobic oligomers to attain high molecular weight. The acronym developed for these multiblock copolymers is HQSHx-BPSy, where the HQSH and BPS refer to the use of HQSH100 and BPS0 oligomers, while x and y denote the molecular weight in Kg/mol unit of the oligomers, respectively.

All multiblock copolymers displayed high intrinsic viscosities ranging from 0.51 to 0.99 dL/g, and could form tough, ductile membranes from solvent casing. IEC values, which were determined by titration, were close to target values, indicating a high degree of coupling. It should be noted that original design of this study involved the preparation of 1.4 meq/g multiblock copolymers in order to compare their properties with a similar IEC random copolymer (e.g., BPSH35). We predicted that the HQSH-BPS multiblock copolymer with a sequenced architecture would outperform the BPSH35 random copolymer. Our results,

however, were unexpected. The multiblock copolymers displayed much lower water uptake and proton conductivity, with IEC values ranging from 1.2 to 1.4 meq/g, water uptake of 20%, and a proton conductivity of 0.04 S/Cm. These results were significantly lower compared with those of random copolymers with similar IEC values. We were able to explain these results using subsequent AFM characterization.

Figure 11 (a) shows an AFM phase image of the HQSH12-BPS20. The bright and dark regions in the images correspond to hard hydrophobic and soft hydrophilic segments, respectively. As shown in the picture, the dark hydrophilic segments are completely isolated by the hydrophobic segments. This type of morphology would suggest low water uptake and proton conductivity. After additional AFM studies, it turned out that all the copolymers with target IEC values of 1.4 meq/g possessed similarly isolated hydrophilic segments. This unexpected morphology can be explained as follows. Although the multiblock copolymers have adequate sulfonic acid moieties to achieve a high proton conductivity, their hydrophilic segment volume fractions were not sufficient to form well-connected channels. This observation suggests one critical consideration for designing hydrophilic-hydrophobic multiblock copolymers. In developing high proton conductive PEMs from hydrophilic-hydrophobic multiblock copolymers, the volume fraction of the hydrophilic segments should be considered as well as IEC values.

For this reason, in order to increase proton conductivity, we increased the hydrophilic fraction to induce the formation of well-connected hydrophilic regions. Thus, the third group of multiblock copolymers was designed with higher hydrophilic volume fractions by coupling equal block length hydrophilic and hydrophobic oligomers. The resulting multiblock copolymers showed significantly enhanced proton conductivities ranging from 0.13 to 0.21 S/Cm. Water uptake values also significantly increased up to 183% with the HQSH5-BPS5 system. This significant improvement can be ascribed to the formation of well-connected hydrophilic regions, which was confirmed by AFM (Figure 11 (b)). As evidenced in this image, the HQSH10-BPS10 displays high connectivity in the hydrophilic segment of the membrane. Thus, by utilizing the well-connected hydrophilic regime for proton conduction, enhanced proton conductivity was realized.

**Table 3.** Properties of HQSH–BPS Multiblock Copolymers in the Sulfonic Acid Form

| Copolymers | Calculated IEC (meq $g^{-1}$) | Experimental IEC (meq $g^{-1}$)[a] | Intrinsic Viscosity (dL $g^{-1}$)[b] | Water Uptake (%) | Conductivity (S $cm^{-1}$)[c] |
|---|---|---|---|---|---|
| **Nafion 112** | - | 0.90 | - | 25 | 0.090 |
| **BPSH 35** | 1.53 | 1.50 | 0.70 | 36 | 0.070 |
| **HQSH 3 – BPS 5** | 1.44 | 1.32 | 0.56 | 27 | 0.04 |
| **HQSH 6 – BPS 10** | 1.31 | 1.21 | 0.60 | 18 | 0.03 |
| **HQSH 9 – BPS 15** | 1.45 | 1.20 | 0.68 | 13 | 0.03 |

| | | | | | |
|---|---|---|---|---|---|
| **HQSH 12 – BPS 20** | 1.45 | 1.37 | 0.68 | 17 | 0.04 |
| **HQSH 3 – BPS 3** | 1.89 | 1.79 | 0.52 | 112 | 0.13 |
| **HQSH 5 – BPS 5** | 1.79 | 1.88 | 0.51 | 183 | 0.17 |
| **HQSH 10 – BPS 10** | 1.91 | 1.78 | 0.98 | 156 | 0.21 |
| **HQSH 15 – BPS 15** | 1.90 | 1.67 | 0.99 | 145 | 0.16 |

[a] Determined by titration with NaOH.
[b] In NMP with 0.05 M LiBr at 25 ºC.
[c] Measured in deionized water at 30 ºC.

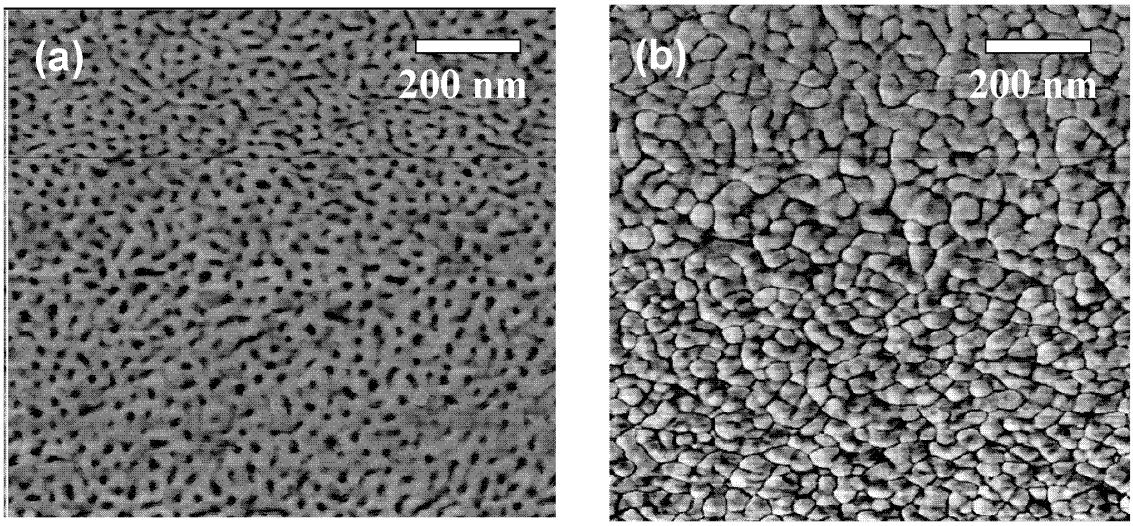


**Figure 11.** AFM phase images of HQSH-BPS multiblock copolymers. (a) HQSH12-BPS20, and (b) HQSH10-BPS10

**Conclusions**

Segmented sulfonated multiblock copolymers with varying block lengths were synthesized via a coupling reaction between phenoxide terminated hydrophilic oligomers (HQS100) and HFB end-capped hydrophobic oligomers (BPS0). The coupling reaction was conducted under mild reaction conditions (< 110°C) to prevent an ether-ether exchange reaction, which could result in randomized hydrophilic-hydrophobic sequences. The coupling reactions were solvent sensitive due to the low reactivity of the phenoxide groups on hydroquinone moieties. All the copolymers produced tough, ductile membranes when cast from NMP or DMF.

Several fundamental membrane parameters were investigated, including water uptake and proton conductivity. Characterization studies revealed that the volume fraction of the hydrophilic segments was critical for forming continuous hydrophilic channels, as well as improving IEC values. Using HQSH-BPS multiblock copolymers with high IEC values, we were able to achieve high proton conductivity up to 0.21 S/Cm at 30 ºC in liquid water via the formation of a nano-phase separated morphology. The results confirm that the multiblock copolymers described herein are potential candidates for use as PEM materials.

# Synthesis and Characterization of Multiblock Copolymers Based on Hydrophilic Disulfonated Poly(arylene ether sulfone) and Hydrophobic Partially Fluorinated Poly(arylene ether ketone) for Fuel Cell Applications

**Summary of Results**

Novel sulfonated fluorinated multiblock copolymers were synthesized and characterized for proton exchange membrane (PEM) fuel cell applications. The multiblock copolymers were synthesized via a coupling reaction between fully disulfonated poly(arylene ether sulfone) with phenoxide end-groups and hexafluorobenzene (HFB) end-capped partially fluorinated poly(arylene ether ketone) as hydrophilic and hydrophobic blocks, respectively. The coupling reactions between the hydrophilic and hydrophobic oligomers were conducted at relatively low temperatures to prevent a possible trans-etherification, which can randomize the hydrophilic-hydrophobic sequences. Tough ductile membranes were prepared by solution casting and their membrane properties were evaluated. With similar ion exchange capacities (IECs), proton conductivity and water uptake were strongly influenced by the hydrophilic and hydrophobic block lengths. Conductivity and water uptake increased with increasing block length by developing nanophase separated morphologies. Atomic force microscopy (AFM) and transmission electron microscopy (TEM) experiments revealed that the connectivity of the hydrophilic segments was enhanced by increasing the block length. The systematic synthesis and characterization of the copolymers are reported.

## INTRODUCTION

Commercial proton exchange membrane (PEM) materials have typically consisted of perfluorinated sulfonic acid containing ionomers (PFSAs), which can be synthesized from a copolymerization of tetrafluoroethylene (TFE) and a perfluorinated vinyl ether comonomer with a sulfonyl fluoride moiety in its side chain. Due to the perfluorinated backbone, these membranes demonstrate good chemical stability and mechanical strength along with high proton conductivity. Although PFSAs have performed well at moderate operation temperatures, their mechanical and electrochemical properties severely deteriorate at higher temperatures (>80 °C), which unfortunately can be essential for many practical applications. Another drawback of these materials is high fuel permeability especially in direct methanol fuel cell (DMFC) applications.

A significant effort has been devoted to the study of sulfonated aromatic copolymers as alternatives to PFSAs. Aromatic backbone-based PEMs have several favorable characteristics over PFSAs including excellent thermal and oxidative stability, high acid and hydrolytic resistance, and lower production costs. The most frequently utilized aromatic high temperature copolymers for PEM applications are poly(arylene ether sulfone)s, poly(arylene ether ketone)s, and poly(phenylene)s. Although PEM performance in several aspects can be significantly improved by utilizing these high performance materials, there are still a number of drawbacks that must be addressed. One of the main challenges is enhancing low proton conductivity under partially hydrated conditions. It has been widely accepted that many of the aromatic

backbone-based PEMs form narrower and less well-connected ion channels in comparison to PFSAs under low relative humidity (RH) conditions.

In order to overcome low proton conductivity under partially hydrated conditions, the use of PEMs based on hydrophilic-hydrophobic multiblock copolymers has recently been proposed due to their ability to form nanophase separated morphologies. PEMs based on hydrophilic-hydrophobic sequenced multiblock copolymers can form well-connected hydrophilic ionic channels, which can facilitate proton transport under low humidity conditions. In addition, well-connected nonionic hydrophobic domains can provide dimensional stability. In the case of DMFCs, their hydrophobic domain may also serve as a barrier against methanol permeability.

Recently, various types of hydrophilic-hydrophobic multiblock copolymers based on disulfonated poly(arylene ether sulfone)s have been developed by McGrath group . These multiblock copolymers have displayed significantly enhanced transport properties and improved performance, but their synthesis is more difficult than random copolymer. Specifically, careful oligomer preparation with proper end-group chemistry is essential for a successful coupling reaction. To address these issues, a convenient methodology to synthesize multiblock copolymer systems was recently developed by the group. This method utilizes highly reactive perfluorinated small molecules such as decafluorobiphenyl (DFBP) and hexafluorobenzene (HFB) as the linkage groups for the hydrophilic and hydrophobic oligomers. The use of highly reactive DFBP or HFB facilitates the coupling reactions at low temperatures and prevents a possible trans-etherification, which can randomize the hydrophilic-hydrophobic sequences.

This study, therefore, addresses the synthesis and characterization of novel multiblock copolymers based on fully disulfonated poly(arylene ether sulfone) (BPSH100) and partially fluorinated poly( arylene ether ketone) (6FK) as the hydrophilic and hydrophobic block, respectively. The fluorination of the hydrophobic segment is expected to promote nanophase separation with the hydrophilic segment, resulting in improved proton transport properties. The coupling reaction between the hydrophilic and hydrophobic blocks was achieved using HFB as the linkage group under mild reaction conditions (e.g. <110 °C). Using the synthetic procedures described below, ten multiblock copolymers with different IECs and block lengths were developed. Various membrane parameters, such as proton conductivity (under fully and partially hydrated conditions), water uptake, swelling behavior, and morphology will be described with respect to their impact on PEM performance.

## EXPERIMENTAL

### Materials

4,4’-Biphenol (BP) and 4,4’-dichlorodiphenyl sulfone (DCDPS) were provided by Eastman Chemical Company and Solvay Advanced Polymers, respectively, and were dried *in vacuo* at 110 °C for 24 h prior to use. The disulfonated monomer, 3,3’-disulfonated-4,4’-dichlorodiphenyl sulfone (SDCDPS), was synthesized and purified as reported earlier. The purity of SDCDPS was determined via UV-Vis spectroscopy measurements. 4,4’-Hexafluoroisopropylidenediphenol (6F-BPA) (Ciba) and 4,4’-difluorobenzophenone (Aldrich) were recrystallized from toluene and ethanol, respectively, and dried *in vacuo* prior to use. N,N-

dimethylacetamide (DMAc) was received from Aldrich and vacuum distilled before use. Potassium carbonate ($K_2CO_3$), hexafluorobenzene (HFB), 2-propanol (IPA), acetone, and toluene were purchased from Aldrich and used without further purification.

**Synthesis of Hydrophilic and Hydrophobic Oligomers with Phenoxide Telechelic Functionality**

Fully disulfonated poly(arylene ether sulfone) hydrophilic oligomers (BPS100) and partially fluorinated poly(arylene ether ketone) hydrophobic oligomers (6FK) were synthesized with different number-average molecular weights ($\overline{M_n}$). The oligomers were designed to be terminated with phenoxide end-groups by stoichiometrically off-setting the feed ratios of the monomers. A sample synthesis of 5,000 g/mol BPS100 hydrophilic oligomer is as follows: 8.9720 g (48.2 mmol) of BP, 21.0280 g (42.8 mmol) of SDCDPS and 7.9911 g (57.8 mmol) of $K_2CO_3$ were charged to a three-necked 250-mL flask equipped with a condenser, a Dean Stark trap, a nitrogen inlet, and a mechanical stirrer. Then distilled DMAc (120 mL) and toluene (60 mL) were added to the flask and the reaction was heated at 145 °C with stirring. The solution was allowed to reflux at 145 °C while the toluene azeotropically removed the moisture in the system. After 4 h, the toluene was removed from the reaction by stripping off the Dean Stark trap and the reaction temperature was slowly increased to 180 ºC. The reaction was kept at this temperature with nitrogen purging for another 96 h. The reaction solution was cooled to room temperature and filtered to remove salts. The oligomer was coagulated in IPA by pouring the filtered solution. The oligomer was vacuum dried at 110 °C for 24 h. A sample synthesis of 5,000 g/mol 6FK hydrophobic oligomer is as follows: 11.0665 g (50.7 mmol) of 4,4'-difluorobenzophenone, 18.9335 g (56.3 mmol) and 9.3392 g (67.6 mmol) of potassium carbonate were reacted in DMAc at 180 ºC for 36 h. The detailed synthesis and purification procedures for the hydrophobic oligomers are similar to the BPS100 hydrophilic block synthesis.

**End-capping of the Hydrophobic Oligomers with Hexafluorobenzene (HFB)**

End-capping of the phenoxide terminated 6FK oligomers with HFB was conducted via a nucleophilic aromatic substitution reaction. A typical end-capping reaction of 5,000 g/mol 6FK oligomer is as follows: 5.0000 g (1.0 mmol) of 6FK oligomer and 0.5528 g (4.0 mmol) of potassium carbonate were charged to a three-necked 100-mL flask equipped with a condenser, a Dean Stark trap, a nitrogen inlet, and a mechanical stirrer. Distilled DMAc (50 mL) and cyclohexane (15 mL) were added to the flask. The solution was allowed to reflux at 100 °C to azeotropically remove the moisture in the system. After 4 h, the cyclohexane was removed from the system. The reaction temperature was lowered to 80 °C and the nitrogen purge was stopped. Then 1.1163 g (6.0 mmol) of HFB was added and the reaction was allowed to proceed for 12 h. The solution was then cooled and filtered. The filtered solution was coagulated in methanol and filtered. The reacted oligomer was dried at 110 °C *in vacuo* for 24 h.

**Synthesis of Multiblock Copolymers**

The multiblock copolymers were synthesized by coupling HFB end-capped 6FK hydrophobic oligomers and phenoxide terminated BPS100 hydrophilic oligomers. A typical coupling reaction was conducted as follows: 5.0000 g (1.0 mmol) of BPS100 ($\overline{M_n}$ = 5,000

g/mol), 0.5528 g (4.0 mmol) of potassium carbonate, 100 mL of DMAc, and 30 mL of cyclohexane were added to a three-necked 250 mL flask equipped with a condenser, a Dean Stark trap, a nitrogen inlet, and a mechanical stirrer. The reaction mixture was heated at 100 ºC for 4 h to dehydrate the system with refluxing cyclohexane. After removing the cyclohexane, 5.0000 g (1.0 mmol) of vacuum dried HFB end-capped 6FK hydrophobic oligomer ($\overline{M_n}$ = 5,000 g/mol) was added. The coupling reaction was conducted at 105~110 ºC for 24 h. The reaction solution was filtered and precipitated in IPA. The copolymer was purified in a Soxhlet extractor with methanol for 24 h and with chloroform for another 24 h to remove the unreacted hydrophilic and hydrophobic oligomers, respectively. The copolymer was dried at 120 °C *in vacuo* for 24 h.

**Characterization**

The chemical structures of the oligomers and copolymers were confirmed by $^1$H NMR analyses on a Varian INOVA 400 MHz spectrometer with DMSO-$d_6$. In addition, $^1$H NMR spectroscopy was utilized for end-group analyses of the oligomers to determine their $\overline{M_n}$. Intrinsic viscosities were determined in NMP containing 0.05 M LiBr at 25 ºC using an Ubbelohde viscometer. The ion exchange capacity (IEC) values were determined by titration using a 0.01 M NaOH solution.

**Film Casting and Membrane Acidification.**

Initial membranes were cast in their salt form by solution casting. The salt form copolymers were dissolved in DMAc (7% w/v) and filtered with syringe filters ( 0.45 µm Teflon® ). The filtered solutions were then cast onto clean glass substrates. The films were dried under an IR lamp at 60 ºC for 1 day, followed by drying *in vacuo* at 110 ºC for 24 h. The acid form membranes were obtained by boiling in 0.5 M sulfuric acid aqueous solution for 2 h, followed by boiling in deionized water for 2 h. The membranes were kept in deionized water at room temperature for 24 h for further characterization.

**Determination of Proton Conductivity and Water Uptake.**

Fully and partially hydrated proton conductivities were evaluated in a water bath and a humidity-temperature controlled chamber, respectively. The conductivity of the membrane was determined from the geometry of the cell and resistance of the film, which was obtained at the frequency that produced the minimum imaginary response. A Solartron (1252A +1287) impedance/gain-phase analyzer over the frequency range of 10 Hz - 1 MHz was used for the measurements. The membrane water uptake was determined by the weight difference between dry and wet membranes. The vacuum dried membranes were weighed ($W_{dry}$), and then immersed in deionized water at room temperature for 24 h. The wet membrane was blotted dry and immediately weighed again ($W_{wet}$). The water uptake of the membranes was calculated according to the following equation.

$$Water\,Uptake\ (\%) = \frac{W_{wet} - W_{dry}}{W_{dry}} \times 100$$

The hydration number (λ), which can be defined as the number of water molecules absorbed per sulfonic acid unit, was determined from the water uptake and the ion content of the dry membrane, according to the following equation.

$$\lambda = \frac{(W_{wet} - W_{dry}) / MW_{H_2O}}{IEC \times W_{dry}} \times 1000$$

where $MW_{H2O}$ is the molecular weight of water (18.01 g/mol).

**Atomic Force Microscopy (AFM)**

Tapping mode AFM was performed using a Veeco Multimode Atomic Force Microscope. Samples were equilibrated at 30% relative humidity (RH) at room temperature for at least 24 h and sealed before imaging.

**Transmission Electron Microscopy (TEM)**

Electron density contrast between hydrophilic and hydrophobic segments within the membrane samples was enhanced by quantitatively exchanging the acidic protons on the sulfonic acid moieties with cesium ion. Acidified membranes were immersed in DI water and were titrated with aqueous CsOH solution until the solution became neutral. The cesium stained membranes were then embedded in epoxy and ultramicrotomed into 50–70 nm thin sections with a diamond knife. Transmission electron micrographs were obtained using a Philips EM 420 transmission electron microscope (TEM) operating at an accelerating voltage of 100 kV.

**Determination of Swelling Ratio**

The swelling ratios of the membranes were explored both in-plane and through-plane. The ratios were determined from the dimensional changes from wet to dry state. Membranes were stored in water for 24 h and wet dimensions were measured. The dried dimensions were obtained by drying the wet membrane at 80 $^{o}$C in a convection oven for 2 h.

**RESULTS AND DISCUSSION**

**Controlled Molecular Weight Hydrophilic and Hydrophobic Oligomer Synthesis**

Hydrophilic and hydrophobic telechelic oligomers with controlled molecular weight were synthesized via step-growth polymerization (Fig. 1, 2). The hydrophilic oligomers were fully disulfonated poly(arylene ether sulfone)s (BPS100) and the hydrophobic oligomers were partially fluorinated poly(arylene ether ketone)s (6FK). Controlling the molecular weight and end-group functionality of the oligomers was achieved by offsetting the stoichiometry of the monomers. Because phenoxide terminated hydrophilic and hydrophobic blocks were desired, a calculated excess amount of BP and 6F-BPA was used for the hydrophilic and hydrophobic block synthesis, respectively. Different molecular weight oligomers were prepared ranging from 3 to 20 kg/mol. Determining the molecular weight of the oligomers was conducted by comparing the integrals of the end-groups and the other main peaks on $^{1}$H NMR spectra. For the BPS100 hydrophilic block, the phenoxide end-group peaks were located at 6.80 , 7.40, 7.05 and 6.80 ppm (Fig. 3). These correspond to the protons on the BP moieties, which bear the phenoxide

moieties. Conversely, the peaks at 7.1 and 7.65 were assigned to the protons on the BP moieties, which bear ether linkages with SDCDPS. The number-average molecular weights of oligomers were determined by calculating the ratios of the end group BP and the main chain BP. Using a similar calculation, the number-average molecular weights of the hydrophobic oligomers were determined. On the $^{1}H$ NMP spectrum of 6FK oligomer (Fig.4), the two small peaks at 6.73 and 7.03 ppm were assigned to the terminal 6F-BPA moieties, while 6F-BPA moieties in the middle of the chain were assigned to the peaks at 7.20 and 7.48 ppm. The target and actual molecular weights of the oligomers are summarized in Table 1, along with their determined intrinsic viscosities. When a log-log plot between intrinsic viscosity and number-average molecular weight was generated, it showed a linear relationship, thereby confirming that we had been able to successfully control the molecular weight for both the hydrophilic and hydrophobic block series (Fig. 5).

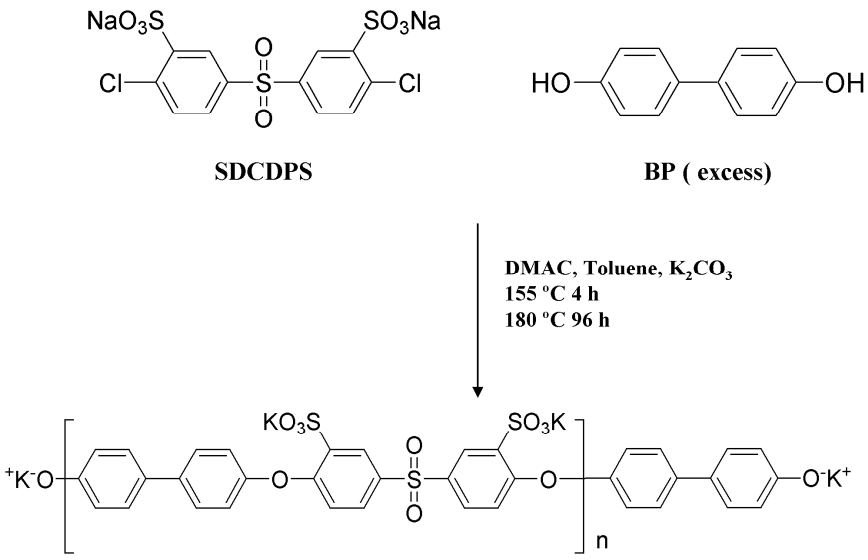


**Figure 1.** Synthesis of a phenoxide terminated, fully disulfonated poly(arylene ether sulfone) (BPS100) hydrophilic oligomer.

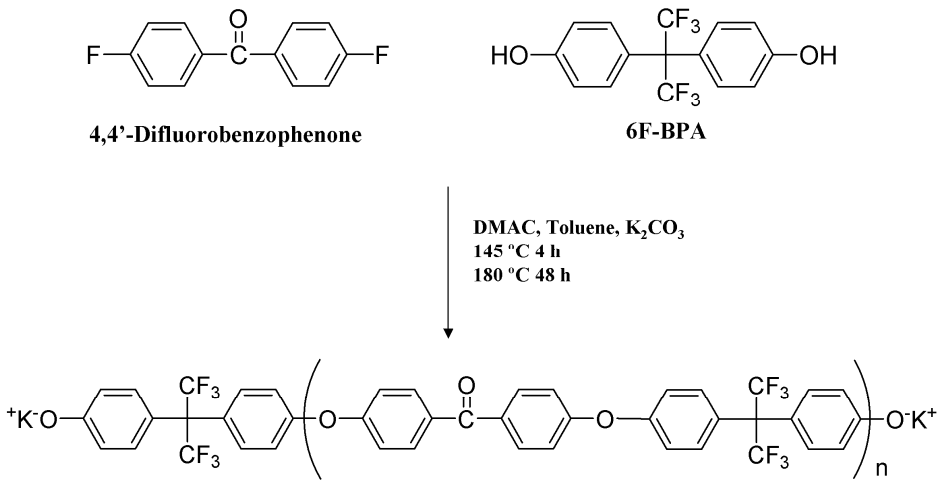


**Figure 2.** Synthesis of a partially fluorinated poly(arylene ether ketone) (6FK) hydrophobic oligomer with phenoxide telechelic functionality.

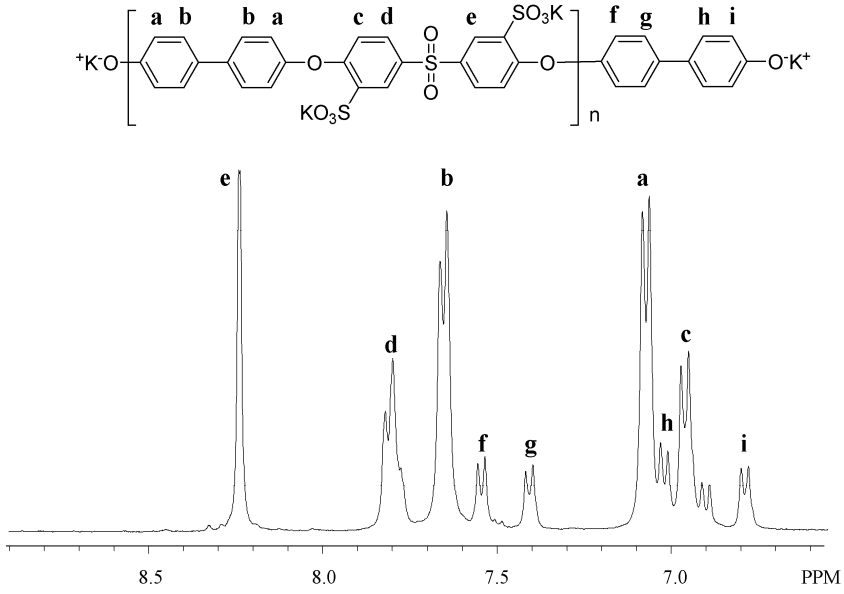


**Figure 3.** $^{1}$H NMR spectrum of phenoxide terminated BPS100 hydrophilic oligomer.

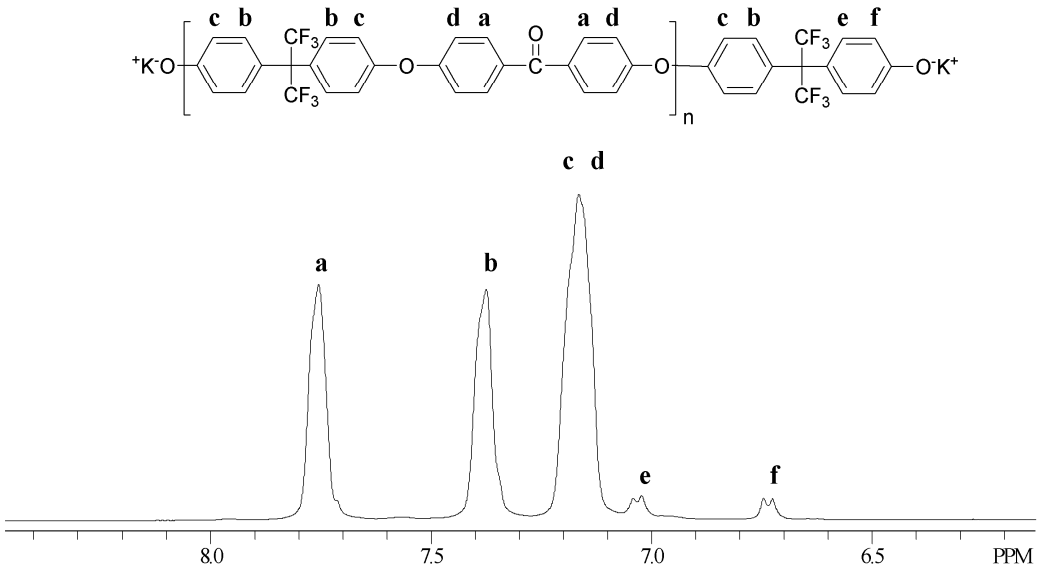


**Figure 4.** $^{1}$H NMR spectrum of phenoxide terminated 6FK hydrophobic oligomer.

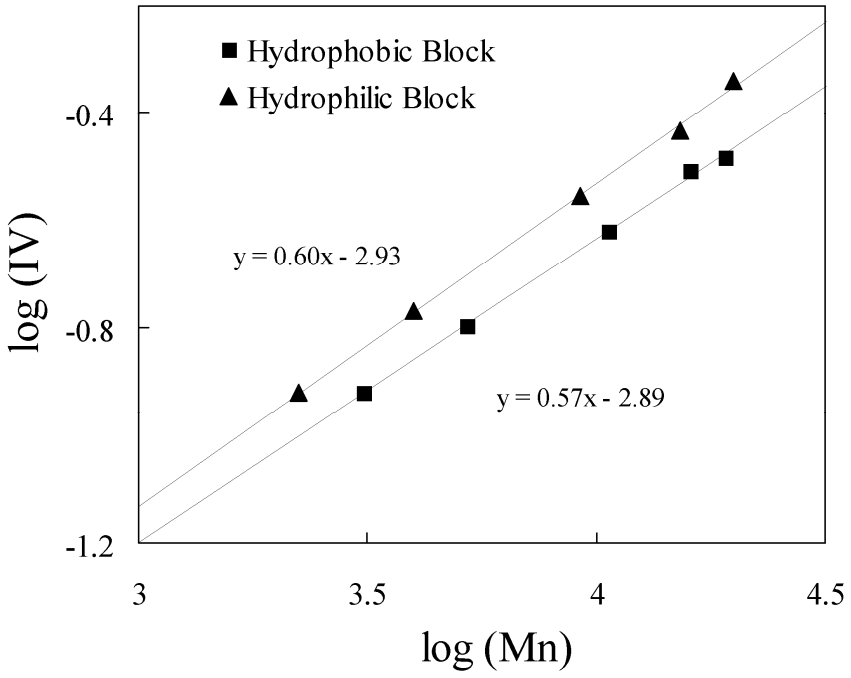


**Figure 5.** Double logarithmic plot of [η] versus $M_n$ of hydrophilic (BPS100) and hydrophobic (6FK) oligomers.

**Table 1.** Characterization of Hydrophilic and Hydrophobic Telechelic Oligomers

| Target $M_n$ (g mol$^{-1}$) | Hydrophilic Blocks | | Hydrophobic Blocks | |
|---|---|---|---|---|
| | $M_n$ (g mol$^{-1}$)[a] | IV (dL g$^{-1}$)[b] | $M_n$ (g mol$^{-1}$)[a] | IV (dL g$^{-1}$)[b] |
| 3,000 | 3,200 | 0.12 | 3,100 | 0.12 |
| 5,000 | 4,800 | 0.17 | 5,200 | 0.16 |
| 10,000 | 9,200 | 0.28 | 10,600 | 0.24 |
| 15,000 | 15,300 | 0.37 | 15,900 | 0.31 |
| 20,000 | 20,000 | 0.46 | 19,200 | 0.33 |

[a] Determined by $^1$H NMR.
[b] In NMP with 0.05 M LiBr at 25 ºC.

**End-capping of the Hydrophobic Oligomers**

Phenoxide terminated 6FK hydrophobic oligomers were end-capped with hexafluorobenzene (HFB) to facilitate a coupling reaction with the phenoxide terminated BPS100 hydrophilic blocks (Fig.6). Due to the high volatility of HFB, the reaction was conducted around the boiling point of HFB without a nitrogen purge to achieve both high reaction kinetic and minimal loss of HFB. The highly reactive nature of HFB allowed the completion of the reaction at low temperature, which was confirmed by $^1$H NMR spectra (Fig.7). As seen from the NMR spectrum of the end-capped oligomer, the phenoxide end-group peaks completely disappeared at 6.73 and 7.03. New peaks were found at 7.23 and 7.33, which can be assigned to the protons on 6F-BPA moieties connected with HFB. Because HFB is not a unifunctional but rather a multifunctional molecule, it was possible that the HFB was acting as a chain-extender between the hydrophobic oligomers via inter-oligomer coupling to form high molecular weight polymers. To eliminate this possibility, excess amounts of HFB toward the phenoxide end-groups were used. Since the equivalent amount of HFB needed to end-cap a single 6FK oligomer is 2, the theoretical molar ratio between HFB and 6FK oligomer is 2:1. However, in order to avoid an inter-oligomer coupling reaction, the actual molar ratio used was 6:1. Once the end-capping reaction had completed, we determined the intrinsic viscosities of the end-capped oligomers and compared them to their original values (Table 2). Although minor incremental increases were observed with the end-capped oligomers, this was likely due to the chain length extension by the HFB, rather than inter-oligomer coupling.

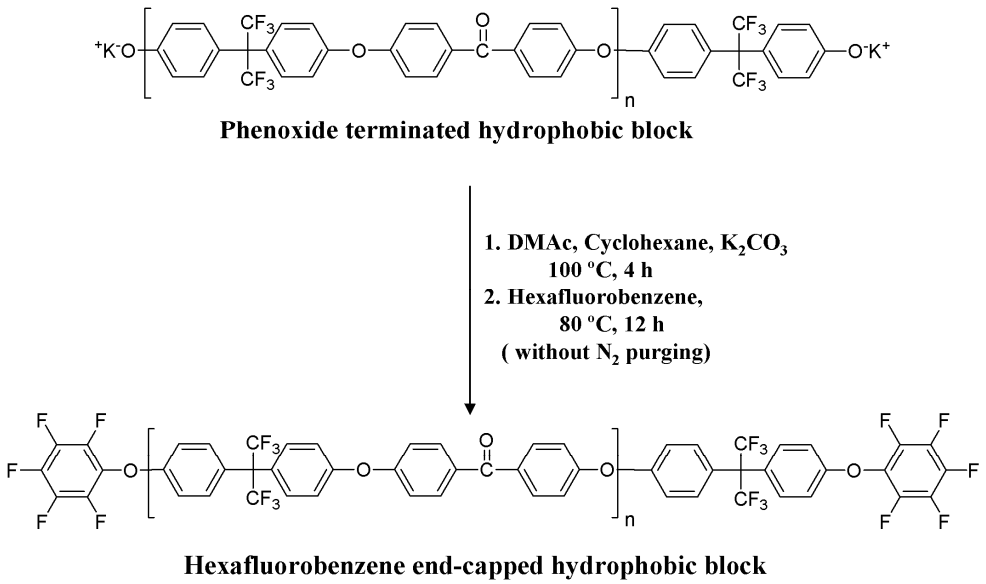


**Figure 6.** End-capping of a phenoxide terminated 6FK hydrophobic oligomer with HFB.

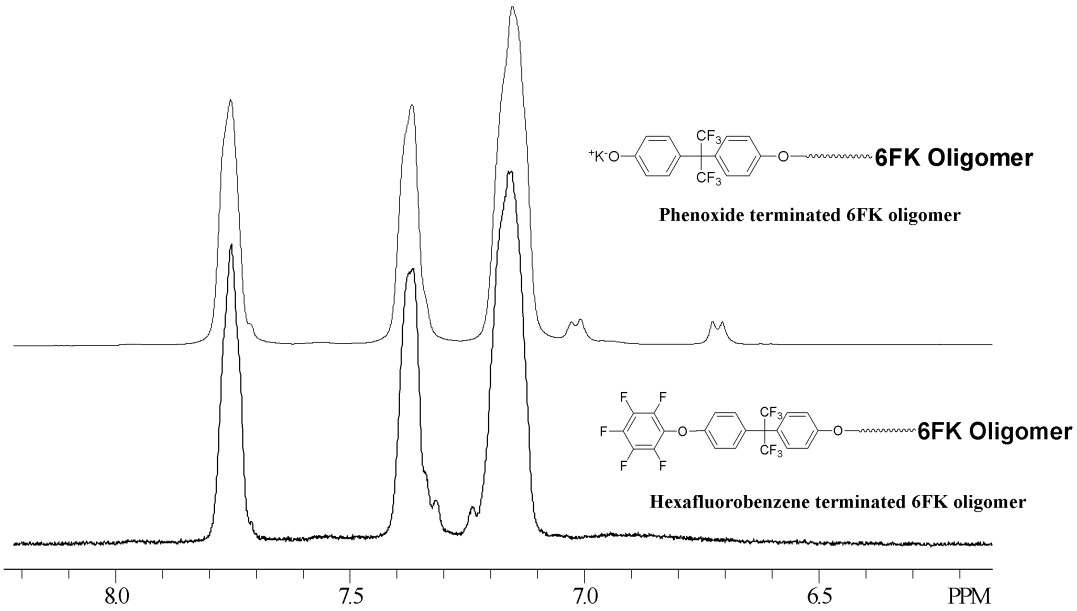


**Figure 7.** $^{1}$H NMR spectra of 6FK and HFB end-capped 6FK hydrophobic oligomers.

**Table 2.** Intrinsic Viscosities of 6FK Hydrophobic Blocks before and after End-Capping

| $M_n$[a] (g mol$^{-1}$) | Initial IV (dL g$^{-1}$)[b] | IV after end-capping (dL g$^{-1}$)[b] |
|---|---|---|
| 5,200 | 0.16 | 0.17 |
| 10,600 | 0.24 | 0.28 |
| 15,900 | 0.31 | 0.36 |
| 19,200 | 0.33 | 0.34 |

[a] Determined by $^1$H NMR.
[b] In NMP with 0.05 M LiBr at 25 ºC.

**Synthesis of BPSH-6FK Multiblock Copolymers**

Multiblock copolymers with various block lengths were synthesized by coupling the phenoxide terminated BPS100 and the HFB end-capped 6FK oligomers (Fig.8). Hereafter, an acronym for the multiblock copolymer—namely BPSHx-6FKy—will be used, where the BPSH and 6FK imply the hydrophilic and hydrophobic oligomers while the x and y denote the number-average molecular weights of the reacted oligomers in Kg/mol unit. The coupling reaction was conducted at 105 ºC, which was low enough to prevent possible trans-etherification. Since low temperature boiling HFB was already attached to the 6FK hydrophobic oligomers, it was not necessary to conduct the coupling reaction at 80 ºC. The completion of the coupling reaction was confirmed by comparing the $^1$H NMR spectra of the oligomers with that of the copolymers. As shown on the $^1$H NMR spectrum of the copolymer, the phenoxide end group peaks on the BPS100 oligomers at 6.80, 7.40, 7.05 and 6.80 ppm completely disappeared. This means that all the phenoxide end-groups reacted with the HFB on the 6FK hydrophobic oligomers to form multiblock copolymers (Fig. 9).

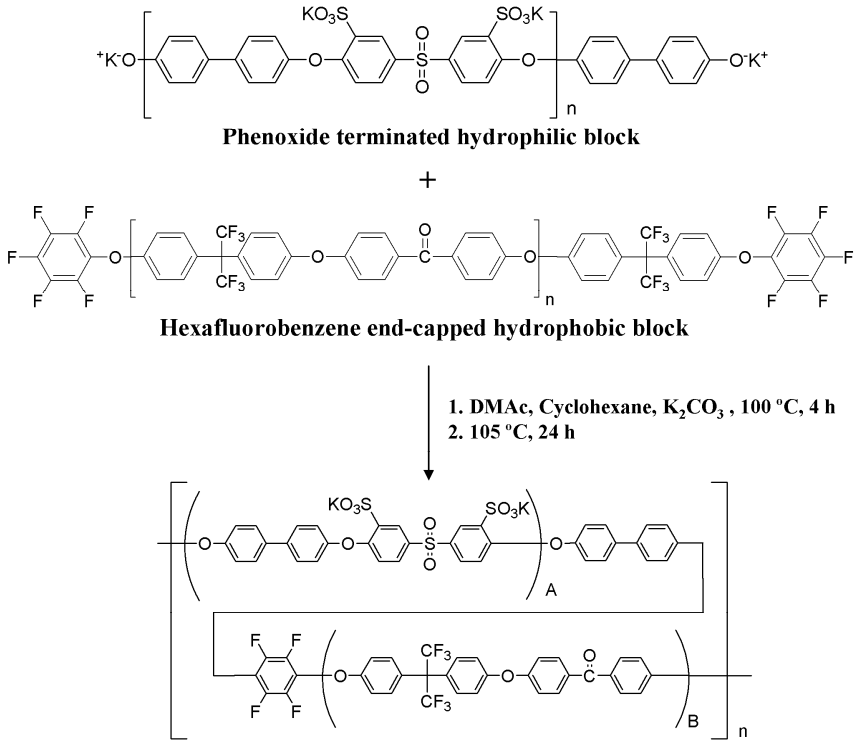


**Figure 8.** Synthesis of segmented sulfonated multiblock copolymers (BPSH-6FK) with HFB linkage group.

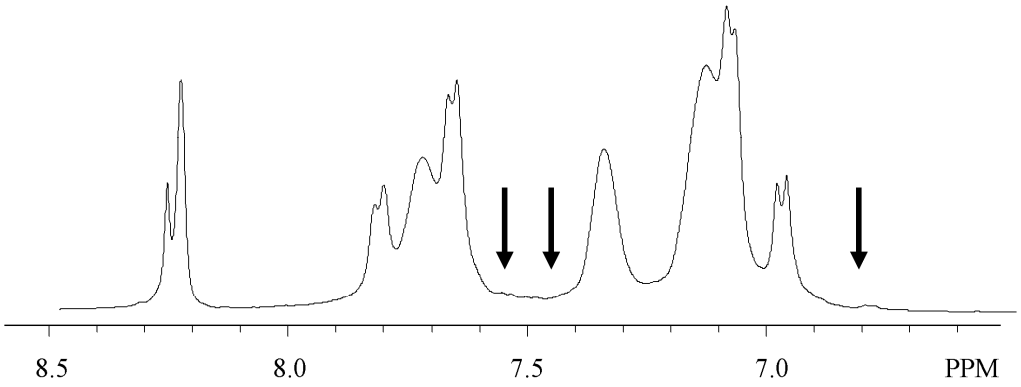


**Figure 9.** $^{1}$H NMR spectrum of BPSH3-6FK3. Black arrows indicate the disappearance of the end groups on the hydrophilic blocks after the coupling reaction with fluorine-terminated hydrophobic blocks.

**Characterization of Membrane Properties of BPSH-BPS Multiblock Copolymers**

Ten BPSH-6FK multiblock copolymers with different block lengths were systematically synthesized and their fundamental membrane properties were evaluated, which is summarized in Table 3, along with values for the control PEM materials, Nafion 112 and BPSH35. The multiblock copolymers were categorized into three subgroups according to their IEC values. The low IEC copolymers displayed longer hydrophobic block lengths compared to the hydrophilic blocks, with IEC values ranging from 1.01-1.33 meq/g. The medium IEC copolymers displayed equal hydrophilic and hydrophobic block lengths, with IEC values of around 1.5 meq/g. And the copolymers with high IEC values displayed longer hydrophilic block lengths compared to the hydrophobic blocks. In each subgroup, different block length copolymers with similar IEC values were prepared to evaluate the effect of hydrophobic-hydrophobic block length on membrane properties.

**Table 3.** Properties of BPSH–6FK Multiblock Copolymers in the Sulfonic Acid Form

| Copolymers | Calculated IEC (meq $g^{-1}$) | Experimental IEC (meq $g^{-1}$)[a] | Intrinsic Viscosity (dL $g^{-1}$)[b] | Water Uptake (%) | Conductivity (S $cm^{-1}$)[c] | Hydration Number (λ) |
|---|---|---|---|---|---|---|
| **Nafion 112** | - | 0.90 | - | 25 | 0.090 | 15.0 |
| **BPSH 35** | 1.53 | 1.50 | 0.70 | 36 | 0.070 | 13.3 |
| **BPSH 5 – 6FK 10** | 1.03 | 1.01 | 0.62 | 23 | 0.04 | 13 |
| **BPSH 10 – 6FK 15** | 1.21 | 1.32 | 0.80 | 20 | 0.07 | 8 |
| **BPSH 15 – 6FK 20** | 1.47 | 1.33 | 0.65 | 45 | 0.10 | 19 |
| **BPSH 3 – 6FK 3** | 1.68 | 1.51 | 0.78 | 31 | 0.08 | 12 |
| **BPSH 5 – 6FK 5** | 1.59 | 1.53 | 0.62 | 69 | 0.10 | 25 |
| **BPSH 10 – 6FK 10** | 1.54 | 1.48 | 0.88 | 81 | 0.11 | 30 |
| **BPSH 15 – 6FK 15** | 1.62 | 1.34 | 0.70 | 100 | 0.12 | 41 |
| **BPSH 10 – 6FK 5** | 2.11 | 1.86 | 0.94 | 300 | 0.06 | 90 |
| **BPSH 15 – 6FK 10** | 1.96 | 1.70 | 0.60 | 170 | 0.08 | 55 |
| **BPSH 20 – 6FK 15** | 1.84 | 1.70 | 0.72 | 178 | 0.09 | 58 |

[a] Determined by titration with NaOH.
[b] In NMP with 0.05 M LiBr at 25 ºC.
[c] Measured in deionized water at 30 ºC.

The IEC values for all the copolymers were determined by titration and subsequently compared with their theoretical values. The similar IEC vs. theoretical values we obtained confirmed the successful coupling reaction between the hydrophilic and hydrophobic oligomers. The intrinsic viscosity of the copolymers ranged from 0.6 to 0.94 dL/g, which was sufficiently high to obtain tough ductile membranes. As expected, the water uptake results for

the multiblock copolymers were shown to be strongly dependent on their IEC values, which is associated with increased ionic moieties in the system. In addition to the impact of IEC, the water uptake behavior of the multiblock copolymers was also strongly influenced by hydrophilic and hydrophobic block lengths. Specifically, the water uptake values for the multiblock copolymers with similar IECs increased with increasing block length. For example, the BPSH3-6FK3, BPSH5-6FK5, and BPSH10-6FK10 copolymers displayed very similar IEC values of around 1.5 meq/g. If water uptake is exclusively dependent on IEC, then the water uptake values for these copolymers should have been very similar. However, our results showed that water uptake was strongly influenced by the hydrophilic and hydrophobic block lengths, which increased from 31% for the BPSH3- 6FK3, to 81% for the BPSH10- 6FK10. It should be noted that while the BPSH15- 6FK15 displayed somewhat lower IEC (1.34 meq/g) than other equal length block copolymers, its water uptake was even higher than that of the BPSH10-6FK10.

A similar trend was observed with respect to proton conductivity measurements for the equal block length multiblock copolymers. The lowest conductivity measurement was 0.08 S/Cm for the shortest block length copolymer (BPSH3-6FK3), and then increased with increasing block length. The longest block length copolymer (BPSH 15-6FK 15) displayed the highest conductivity of 0.12 S/Cm. Based on our results, we propose that the observed increases in both water uptake and conductivity were influenced by morphological changes in the multiblock copolymer. Because the ionic compositions were similar, any change in properties with increasing block length would inevitably result from the expected increase in phase separation between the hydrophobic and hydrophilic phases in these multiblock copolymers.

Figure 10 shows the relationship between temperature and the proton conductivity of the fully hydrated multiblock copolymers. As clearly demonstrated, proton conductivity increased with increasing temperature, reaching 185 mS/Cm at 80 ºC for the BPSH10-6FK10. Moreover, the conductivity-temperature slope for each of the copolymers is similar, implying that the copolymers have a similar conduction mechanism. Compared with Nafion 112, the multiblock copolymers displayed a slightly lower temperature dependence on proton conductivity.

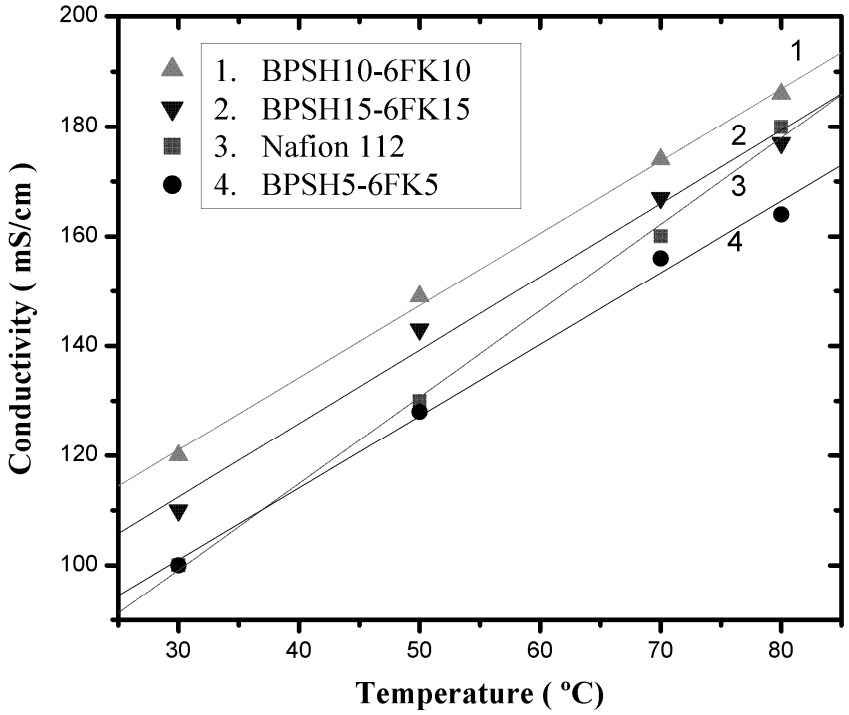


**Figure 10.** Proton conductivities of BPSH-6FK and Nafion112 in terms of temperature

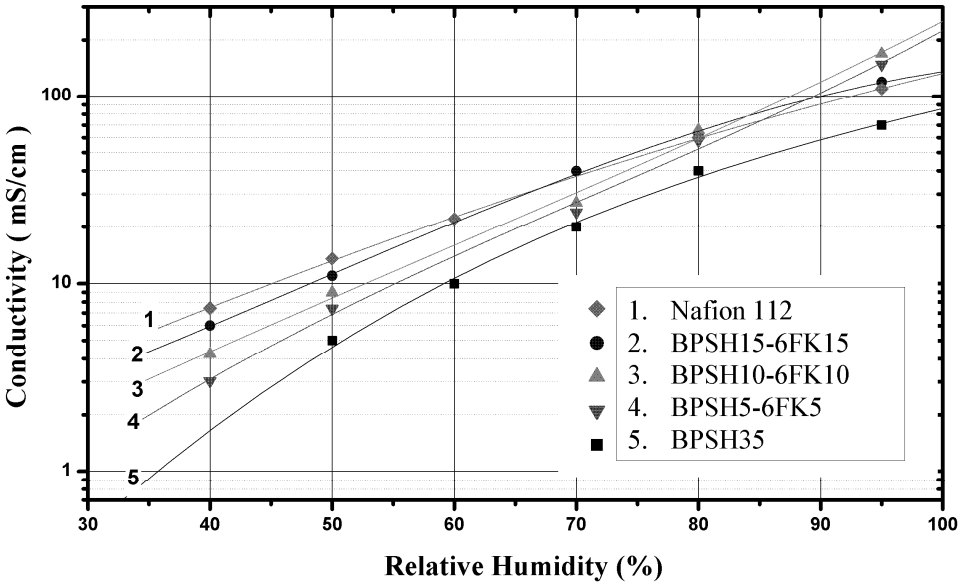


**Figure 11.** Proton conductivities of BPSH-6FK and Nafion112 under partially hydrated conditions at 80 ºC

Proton conductivity as a function of relative humidity (RH) at 80 ºC was studied (Fig. 11). As shown in the figure, the proton conductivity of the BPSH35 random copolymer dropped rapidly at lower RH values. Although BPSH35 demonstrated acceptable proton conductivity

under fully hydrated conditions on account of sufficient water content, its proton conductivity under partially hydrated conditions decreased significantly due to the scattered hydrophilic domains in the random copolymer. In short, the absence of the hydrophilic domain connectivity and insufficient water content in the membrane was unable to maintain high proton conduction under partially hydrated conditions.

Conversely, the performance of the multiblock copolymers under partially hydrated conditions was shown to be superior to the random copolymer, and also improved with increasing block lengths. For example, the conductivity of the BPSH15–6FK15 under partially hydrated conditions was comparable to that of Nafion 112. This performance improvement seems to be related to the formation of well-connected hydrophilic channels at higher block lengths. By forming continuous hydrophilic channels in the membranes, proton transport behavior can be significantly enhanced, especially under partially hydrated conditions.

Figure 12 shows AFM phase images of the BPSH-6FK multiblock copolymers with different block lengths. The bright and dark regions in the images correspond to hard hydrophobic and soft hydrophilic segments, respectively. Although no distinct phase-separation was observed for the BPSH5-6FK5 system (Figure 12 (a)), enhancements in connectivity of hydrophilic domain were found in longer block lengths multiblock systems (Figure 12 (b), (c)). A similar trend was also observed by investigating bulk morphologies of the samples. In the TEM images with different block lengths, the connectivity in each segment was significantly enhanced with increasing the block length. (Figure 13 (a), (b), and (c)). The darker cesium stained hydrophilic domains became visible with a medium block length of 10k-10K while a shorter block length ( e.g., 5k-5k) copolymer did not show no distinct phase separation. This implies that the shortest block length for the hydrophilic-hydrophobic nanophase separation lies between 5k and 10k of the block length. Further increase in the block length resulted in higher degree of phase separation showing a clear lamellar morphology (Figure 13 (c)). Thus, by utilizing the well-connected hydrophilic regime for proton conduction, improved proton conductivity under partially hydrated conditions was achieved.

Another phenomenon that can be related to morphological changes in the copolymer is swelling ratio. Table 4 shows the swelling ratios of the BPSH-6FK multiblock copolymers in comparison with the BPSH35 and Nafion controls. The x,y represent the in-plane swelling and z represents the through-plane swelling ratios. All the multiblock copolymers showed anisotropic swelling behaviors, while the BPSH 35 random copolymer and Nafion (NRE211) exhibited isotropic behaviors. Although the in-plane swelling ratios of the multiblock copolymers were very similar with no significant dependency on block length, the through-plane swelling ratios were strongly influenced by block length. Specifically, the swelling ratios increased from 15% to 66% with increasing block length from 5 Kg/mol to 15 Kg/mol. The increase in water uptake and through-plane swelling with increasing block length suggests the formation of ordered hydrophilic domains within the membranes. In addition, the lower in-plane swelling ratios for the higher block length copolymers could be beneficial for reducing mechanical fatigue during swelling-deswelling cycling operation under low RH conditions.

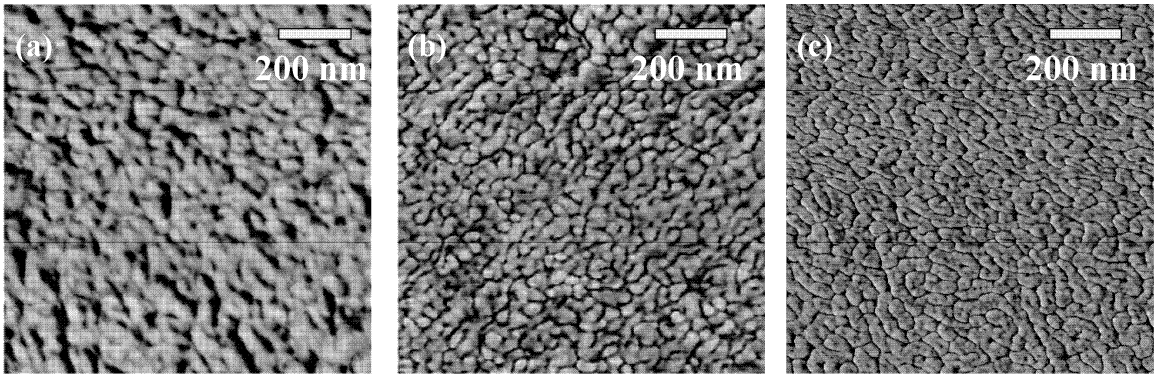


**Figure 12.** AFM phase images of BPSH-6FK multiblock copolymers. (a) BPSH5-6FK5, (b) BPSH10-6FK10, and (c) BPSH10-6FK15.

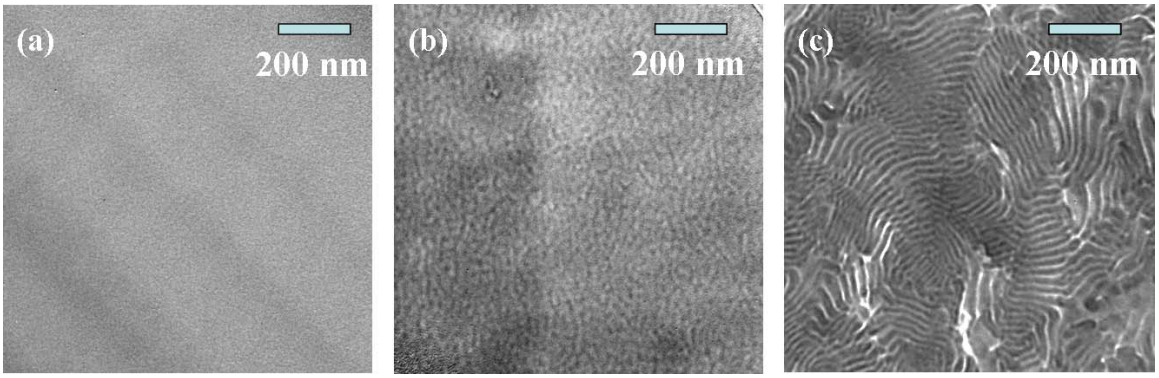


**Figure 13.** TEM phase images of BPSH-6FK multiblock copolymers. (a) BPSH5-6FK5, (b) BPSH10-6FK10, and (c) BPSH15-6FK15.

**Table 4.** Swelling Behavior of BPSH–6FK Multiblock Copolymers

| Copolymers | X direction[a] (%) | Y direction[a] (%) | Z direction[b] (%) | Volume (%) |
|---|---|---|---|---|
| **Nafion 211** | 15 | 16 | 18 | 57 |
| **BPSH 35** | 15 | 16 | 16 | 55 |
| **BPSH 3 – 6FK 3** | 9 | 9 | 15 | 37 |
| **BPSH 5 – 6FK 5** | 12 | 15 | 26 | 62 |
| **BPSH 10 – 6FK 10** | 10 | 10 | 37 | 66 |
| **BPSH 15 – 6FK 15** | 7 | 9 | 66 | 94 |

In-plane (length) swelling ratio
[b] Through-plane (thickness) swelling ratio

**CONCLUSIONS**

Multiblock copolymers with hydrophilic-hydrophobic sequences were developed as potential materials for proton exchange membranes. For systematic synthesis of the multiblock copolymers, various block lengths fully disulfonated poly(arylene ether sulfone) and partially fluorinated poly(arylene ether ketone) were prepared as hydrophilic and hydrophobic oligomers, respectively, and coupled to produce the multiblock copolymers. To minimize a possible sequence randomization during the coupling reaction, the highly reactive perfluorinated small molecule, hexaflurobenzene (HFB), was utilized as a linkage group. Due to its high reactivity, the coupling reaction could be performed at 105 ºC. The copolymers produced tough ductile membranes via DMAc solution casting. Resulting proton conductivity and water uptake measurements revealed that changes in hydrophilic and hydrophobic block length influenced membrane properties at similar IEC values by forming nanophase separated morphologies. The multiblock copolymer membranes showed highly anisotropic swelling behaviors in comparison to the random copolymers, which were isotropic.

# Development of Film Casting Technology for Manufacturing Fuel Cell Membranes

**SUMMARY OF RESULTS:**

DOE expressed an interesting in reducing film thickness from 25~75 μm to 5~15 μm. This quarter we tried to cast films continuously with thickness down to 10 μm. The film casting turned out to be quite successful but the release of thin film from substrate was very difficult. Further efforts will be made to overcome the difficulty in releasing the films so that they are void free and uniform in thickness.

Continuous films were cast successfully with a series of 6F random copolymer samples, that is, 6F0, 6F10, 6F20, 6F30, 6F35, 6F40 and 6F50 copolymers. All of the films appeared to be void-free and uniform in thickness (about 25 μm). The test of film properties and morphology is underway. The results will be helpful in understanding the structure-property relation of 6F copolymer films as well as block copolymers containing similar sequences.

Last quarter we succeeded in casting BisSF-BPSH block copolymer films with expected conductivity through modification of casting and drying conditions. However, a number of issues remained to be addressed. This quarter we obtained two new BisSF-BPSH block copolymer samples and used them for casting films successfully. By improving the purity of the polymer samples and using low concentration (7%), we were able to filter the solutions with a 5 micron filter before film casting. The films obtained looked much better than what we generated last quarter. The films are void-free and uniform in thickness (25 μm). The test of film properties and morphology is underway. We will gain a better understanding concerning the structure-processing-property relationship for this type of copolymers.

Theoretical work also started for studying the self-assembling and microphase separation of block copolymers used as fuel cell membranes. It has been realized that there are similarities between self-assembling of block copolymers and the crystallization process of semi-crystalline polymers. For this reason, a variety of experimental techniques that have been used to observe the crystallization process, such as dilatometry, X-ray diffraction, rheology, etc., may also be used for monitoring the ordering process of block copolymers. In particular, we will try to use rheological methods to study the ordering kinetics in block copolymers based on the large viscoelastic contrast between the disordered and ordered phases of block copolymers.

**CONTINUOUS CASTING OF 6F SERIES RANDOM COPOLYMER FILMS**

A series of 6F random copolymer samples was provided by McGrath's group (prepared by Dr. Zhang). They are 6F0, 6F10, 6F20, 6F30, 6F35, 6F40 and 6F50 (see Fig.1 and Table 1 for molecular structure and parameters). The continuous films were cast successfully with all these samples (see Fig.2). The solvent was DMAc and all solutions were filtered with 0.45 μm filter before use in film casting. The film thickness was about 25 to 30 μm. In Table 2 are presented the detailed film casting and drying conditions. The test of film properties and morphology is underway. The results are believed helpful in understanding the structure-property relation of 6F copolymer films as well as block copolymers containing similar sequences.

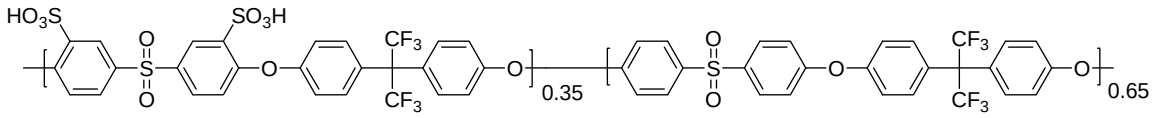


**Figure 1 Chemical structure of 6F copolymers (6F35 is shown).**

**Table 1.** Molecular structure and parameters of the 6F series copolymers for film casting.

| Name | Disulfonation Degree (%) | | IEC (meq/g) | | Mw (Dal) | Mn (Dal) | IV (dL/g) |
|---|---|---|---|---|---|---|---|
| | Theory | $H^1$ NMR | Theory | $H^1$ NMR | | | |
| 6F00 | 0 | 0 | 0 | 0 | 91K | 60K | 0.58 |
| 6F10 | 10 | 10.0 | 0.35 | 0.35 | 79K | 41K | 0.57 |
| 6F20 | 20 | 19.1 | 0.69 | 0.66 | 104K | 55K | 0.59 |
| 6F30 | 30 | 29.4 | 1.00 | 0.98 | 59K | 35K | 0.54 |
| 6F35 | 35 | 33.5 | 1.15 | 1.10 | 60K | 38K | 0.45 |
| 6F40 | 40 | 39.7 | 1.30 | 1.29 | 73K | 47K | 0.52 |
| 6F50 | 50 | 49.4 | 1.59 | 1.57 | 57K | 38K | 0.46 |

*Molecular weight and intrinsic viscosity were measured using GPC with NMP containing 0.05% LiBr as eluent.

**Table 2.** Conditions for casting 6F series copolymer films.

| | |
|---|---|
| Polymer | 6F-X Random Copolymer<br>X=0, 10, 20, 30, 35, 40, 50 |
| Solvent and concentration | DMAc, 30% (w/v) |
| Filter material, pore size | PTFE, 0.45 μm |
| Target dry film thickness | 25-30 μm |
| Speed of coating roll (Va) | 9.9 RPM, 316 cm/min |
| Speed of transporting roll (Vb) | 5.62 RPM, 179 cm/min |
| Wipe ratio ($\alpha$ = Va/Vb) | 1.76 (normally 1.5 ~ 2.0) |
| Gap (from Lubrication Model) | 0.004” |
| Heating plate temperature | 50°C |
| Material/width of belt | Stainless steel/6” |

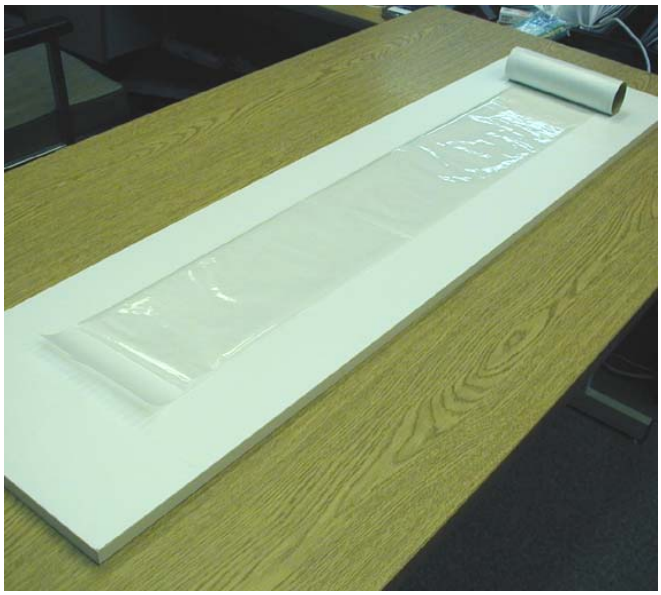

**Figure 2. 6F35 random copolymer film, one of seven 6F series copolymer films cast this quarter. The films appear to be void-free and uniform in thickness (25 μm).**

**CONTINUOUS CASTING OF THIN MEMBRANES**

DOE expressed an interest in reducing film thickness from 25~75 μm to 5~15 μm. In comparison, thinner membranes would:

- Promote back-diffusion of water from cathode to anode (alleviating dry-out and flooding)
- Have higher proton conductance (and performance for the fuel cells)
- Use less polymer material (lower the cost of PEM)
- Reduce the time for film drying (and thus the length of the production line)

We. tried to cast films continuously with thickness down to 10 μm. In Table 3 is presented the conditions used in the casting.

**Table 3.** Conditions for casting thin membranes.

| | |
|---|---|
| Polymer | 6F40 Random Copolymer |
| Solvent and concentration | DMAc, 30% (w/v) |
| Filter material, pore size | PTFE, 0.45 μm |
| Target dry film thickness | 5-15 μm |
| Speed of coating roll (Va) | 8.6 RPM, 274 cm/min |
| Speed of transporting roll (Vb) | 5.62 RPM, 179 cm/min |
| Wipe ratio ($\alpha$ = Va/Vb) | 1.5 (normally 1.5 ~ 2.0) |
| Gap (from Lubrication Model) | 0.002” |
| Heating plate temperature | 50°C |
| Material/width of belt | Stainless steel/6” |

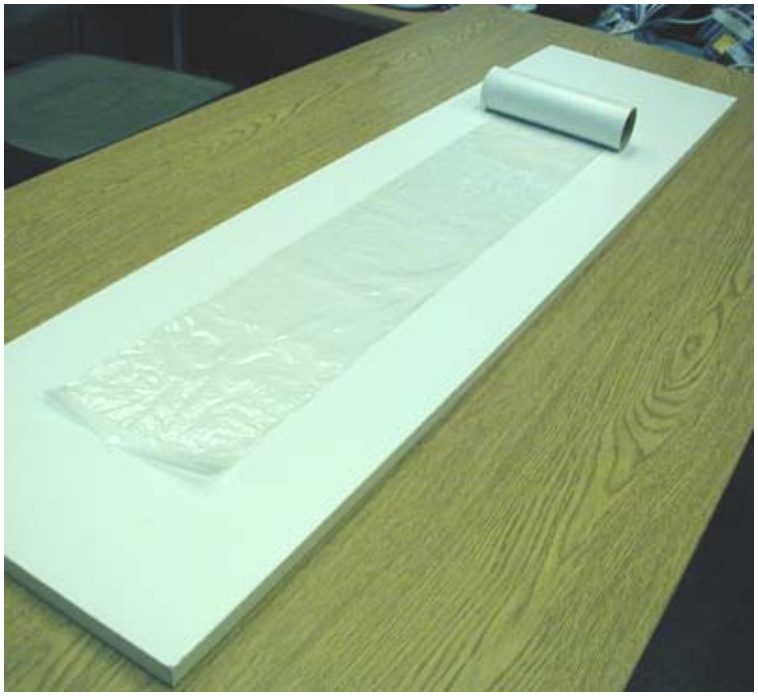

**Figure 3.** BisSF-BPSH (22k-14k) block copolymer films. The film appears to be void-free and uniform in thickness (10 μm).

The film casting turned out to be quite successful but the release of the thin film (10 μm) from substrate was very difficult. There were defects/voids formed in this process. In Fig.3 is presented the picture of the film after drying. In Table 4 are presented the dimensions (thickness) of the films. Note that the part with voids/defects had been cut out before taking the picture and thickness measurement. Table 4 also lists 6F40 films with thickness of 30 and 20 μm. These films were much easier to peel off the substrate compared to 10 μm thick film. As shown in the table, all these films have fairly uniform thickness. Further efforts will be made to overcome the difficulty of film releasing.

**Table 4 Dimensions of 6F40 copolymer films with normal and thin film thickness.**

| *Distance from end (inch)* | Thickness of Film-1 (μm) | | Thickness of Film-2 (μm) | | Thickness of Film-3 (μm) | |
|---|---|---|---|---|---|---|
| | L | R | L | R | L | R |
| *0* | 31 | 32 | 20 | 20 | 10 | 9 |
| *5* | 31 | 31 | 22 | 24 | 14 | 12 |
| *10* | 26 | 28 | 23 | 25 | 11 | 9 |
| *15* | 31 | 30 | 20 | 21 | 13 | 10 |
| *20* | 32 | 32 | 17 | 17 | 12 | 12 |
| *25* | 32 | 32 | 19 | 20 | 9 | 9 |
| *Average* | 30.5 | 30.8 | 20.2 | 21.2 | 11.5 | 10.2 |
| *Std Dev.* | 2.26 | 1.60 | 2.14 | 2.93 | 1.87 | 1.47 |

## CONTINUOUS CASTING OF BISSF-BPSH BLOCK COPOLYMER FILMS

We succeeded in casting BisSF-BPSH block copolymer films with expected conductivity through modification of casting and drying conditions. However, a number of issues remained to be addressed. For example, it was found very difficult to filter the solutions which was critical to ensure quality of the films. Due to this problem, the films generated last time had a number of visible defects despite their high proton conductivity. This quarter we obtained two new BisSF-BPSH block copolymer samples from McGrath's group (made by Mr. Xiang). They are BisSF-BPSH with block MWs of 22k-14k (#1) and 26k-16k (#2) (see Fig.4). The target IEC is 1.3 and 1.5, respectively. The casting solution was prepared by dissolving the polymer in NMP at concentration of 7% (w/v). This concentration is a little bit lower than what we used last time (8-10%), which may help the filtration process. We also improved the purification of polymer samples during synthesis. We were able to filter the solutions with a 5 micron filter before film casting. In Table 5 is presented detailed film casting and drying conditions (basically the same as the last run).

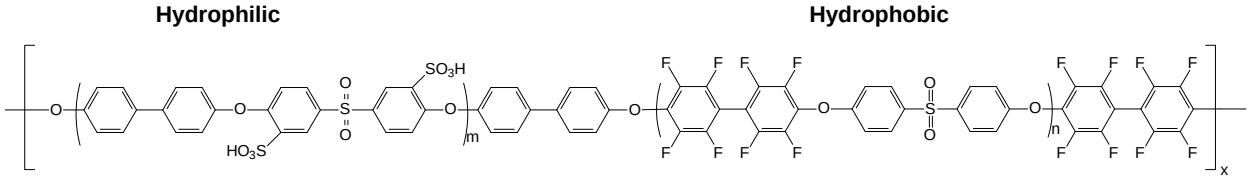


**Figure 4 Chemical structure of BisSF-BPSH block copolymers.**

**Table 5.** Conditions for casting BisSF-BPSH block copolymer films.

| | |
|---|---|
| BisSF-BPSH Copolymer | (1) 22k-14k, IEC=1.3<br>(2) 26k-16k, IEC=1.5 |
| Solvent and concentration | NMP, 7 % (w/v) |
| Filter material, pore size | PTFE, 5 μm |
| Target dry film thickness | 25-30 μm |
| Speed of coating roll (Va) | 11.2 RPM, 357 cm/min |
| Speed of transporting roll (Vb) | 5.62 RPM, 179 cm/min |
| Wipe ratio ($\alpha$ = Va/Vb) | 2.0 (normally 1.5 ~ 2.0) |
| Gap (from Lubrication Model) | 0.013" |
| Heating plate temperature | 30°C Overnight, then 50°C |
| Material/width of belt | Stainless steel/6" |

In Fig.5 is presented the picture of the film (22k-14k) after drying. The produced films were void-free and uniform in thickness (25 μm) and were superior to initial results.

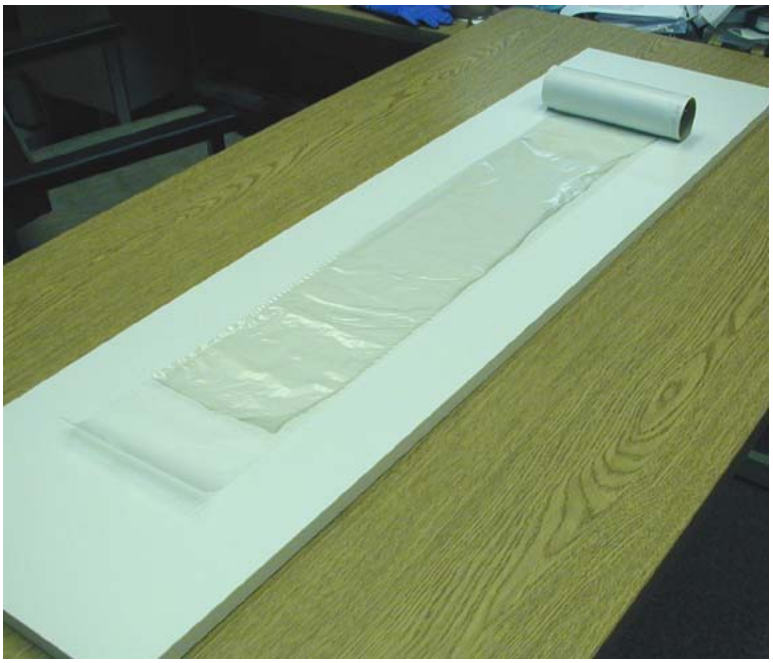

**Figure 5.** BisSF-BPSH (22k-14k) block copolymer films. The produced film was void-free and uniform in thickness (25 μm).

**RHEOLOGICAL STUDY ON THE KINETICS OF PHASE TRANSFORMATION OF BLOCK COPOLYMERS**

Fuel cell proton exchange membranes are also a copolymer system that consists of a sulfonated component for proton conduction and a non-sulfonated component for mechanical integrity. Recently microphase separation of block copolymer systems in the field of production of proton exchange membranes for fuel cells has received growing interest. The proton conductivity of sulfonated copolymers is related to extensive nano-scale phase separation, which leads to more co-continuous connectivity of the sulfonated ionic domains. In contrary to spinodal decomposition such as a demixing process in alloys or binary liquids caused by an abrupt change in temperature below the stability line, the kinetics of phase transformation of block copolymers have rich and interesting phenomena because of the softness of interactions and long relaxation times. Because the phase transformation of block copolymers has many current and potential applications, it is of practical importance to understand its kinetics and to design a processing method for obtaining suitable structures for optimum performances of proton exchange membranes.

A variety of different experimental techniques that have been used to observe the crystallization process, i.e., dilatometry, X-ray diffraction, rheology, etc. can be also used for monitoring the ordering process of block copolymers because of its similarities with the crystallization process of semicrystalline material. Dilatometry has been considered to be the most effective method, which enables the detection of the discontinuous change in specific volume and isothermal compressibility of the materials around the critical point. However, earlier studies disclosed that dilatometry was not an appropriate method because the change of the density and compressibility of diblock copolymers at the order-disorder transition (ODT) are very small. In contrast, rheology and small angle X-ray Scattering (SAXS) are very responsive to the structure evolution and viscoelastic properties during the ordering process.

Therefore, most of the experimental studies on the ODT in block copolymers involved rheology and SAXS techniques.

The success of the rheological study for the detection of the ordering kinetics in block copolymers is based on the large viscoelastic contrast between the disordered and ordered phases. The storage (G′) and loss (G′′) moduli of block copolymers jump up considerably during the structure evolution from the disordered to the ordered phase. The evolution shape of G′ and G′′ can be used to analyze the kinetics of structure ordering. In Figure 6 is presented some typical evolutions of G′ and G′′ for a symmetric styrene-isoprene (SI) diblock copolymer. Both G′ and G′′ show a sigmoidal shape with apparent plateaus before and after the upward change. The plateaus of G′ and G′′ before the change are the viscoelastic properties of the disordered phase at the quenched temperature, while the plateaus after the change describe the properties of the final ordered state. During the course of ordering, the block copolymer is considered as a composite material consisting of the disordered and ordered phases. The proportion of the two phases also changes, inducing the observed changes in the mechanical properties.

Floudas et al. employed the simplest 'series' and 'parallel' mechanical models, which provide the limits for the mechanical response of a two-phase system as a function of the properties of the constituent components and the composition, in order to investigate the time-dependence of the volume fractions of the constituent phases, and finally to analyze the ordering kinetics based on a nucleation and growth mechanism. The 'series' model allows the modulus of the two-phase system to be expressed as a linear combination of their compliances:

$$\frac{1}{G(t)} = \frac{1-\phi(t)}{G_0} + \frac{\phi(t)}{G_\infty} \qquad \text{(Eq. 1)}$$

and the 'parallel' model as a linear combination of the moduli of the constituent phases:

$$G(t) = (1-\phi(t))G_0 + \phi(t)G_\infty \qquad \text{(Eq. 2)}$$

where $G(t)$ $(=\sqrt{G'^2(t) + G''^2(t)})$ is the absolute value of the complex modulus, ϕ(t) is the fraction of the ordered phase, and $G_0$ and $G_\infty$ are the moduli of the completely disordered and ordered phases at the initial and final stages, respectively. The time-dependences of ϕ obtained from the two models are analyzed by fitting the Avrami equation

$$\phi(t) = 1 - \exp(-zt^n) \qquad \text{(Eq. 3)}$$

where n is the Avrami exponent, which is a combined function of the growth dimensionality and the time-dependence of the nucleation process, and presents quantitative information on the nature of the nucleation and growth process. In Eq. 3, the rate constant, z, gives quantitative information on the course of crystallization, and usually, the half-time,

$$t_{1/2} = \left(\frac{\ln 2}{z}\right)^{1/n} \qquad \text{(Eq. 4)}$$

is used to describe the ordering time. These Avrami parameters can be determined from a plot of log(-log(1- ϕ)) versus log t on which the Avrami exponent, n, and the rate constant, z, are the slope and intercept, respectively. In Figure 6 is also given the evolution of the viscoelastic properties during phase transformation of the symmetric SI diblock copolymer and the equivalent volume fractions of the ordered phase obtained using the two extreme 'series' and 'parallel' models. Based on this analysis method, the Avrami exponent was found to be about 3 for shallow quenches, indicating that the ordering process proceeds by heterogeneous nucleation and growth of three-dimensional objects. The kinetics curves at higher cooling had higher value of n (about 4), suggesting spinodal decomposition as a possible mechanism of phase transformation.

(A)

(B)

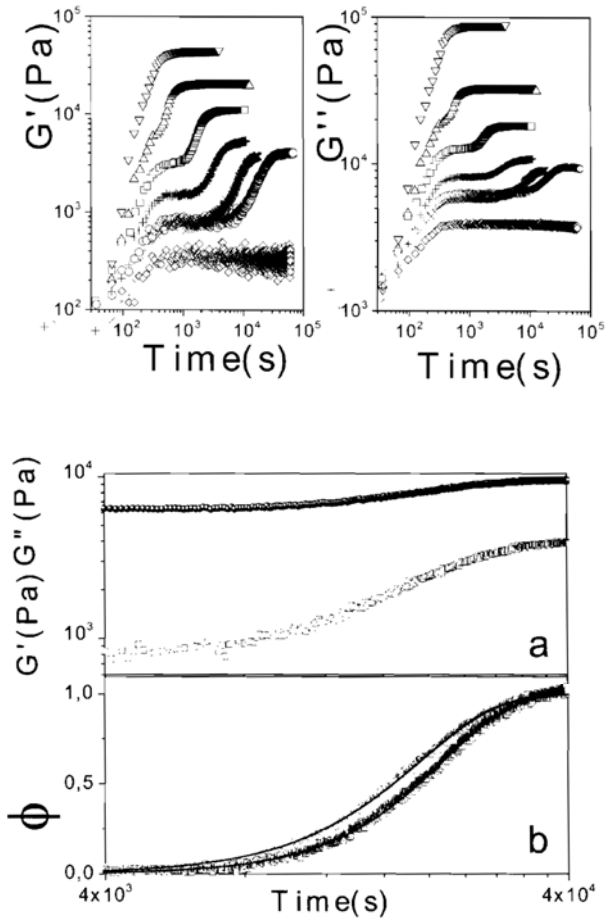


**Figure 6.** (A) Time evolution of G´ and G´´ for a symmetric poly(styrene-b-isoprene) diblock copolymer following quenches from the disordered state to different final temperatures in the ordered phase: rhombus: 359, circles: 358, X: 356.5, +: 356, squares: 355, triangles: 353, and inverted triangles: 347.6 K. (B) a. Time evolution of G´ and G´´ at 356.5 K following a quench from 363 K and b. time-dependence of the volume fraction of ϕ of the ordered phase calculated using the 'parallel' (squares) and 'series' (circles) models. Solid lines are fits to the Avrami equation.

## Study of the phase transformation and kinetics of solution-cast block copolymer films during drying process using rheological property (*G′* and *G″*) measurement and modeling of film drying

Fuel cell proton exchange membranes are also a copolymer system that consists of sulfonated component for proton conduction and a non-sulfonated component for physical integrity. Recently microphase separation of block copolymer systems in the field of production of proton exchange membranes for fuel cells has gained growing interest. The performance of sulfonated copolymers is related to extensive nano-scale phase separation, which leads to more co-continuous connectivity of the sulfonated ionic domains. Because the phase transformation of block copolymers has many current and potential applications, it is of practical importance to understand its kinetics and to design a processing method for obtaining suitable structures for optimum performances of proton exchange membranes.

A model for predicting film drying conditions such as drying temperature and mass transfer coefficient based on a lumped parameter analysis has been developed. The model was constructed by setting up mass and energy balances at the film-air interface on the assumption of negligible solvent diffusion inside the film. The mass and energy balances are as follows:

**Mass balance**

$$R_{mass,i} = \rho_i b_c \frac{d\phi_i}{dt} = k\,(C_i^{sat} - C_i^{\infty}) \qquad \textbf{(Eq. 1)}$$

**Energy balance**

$$(\rho_f H_f C_{pf} + \sum_{i=1}^{k} \rho_i z_i H_c C_{pi})\,\frac{dT}{dt} = h(T - T^{\infty}) - \sum_{i=1}^{k} R_{mass,i}\,(\Delta H_{vap})_i \qquad \textbf{(Eq. 2)}$$

where $R_{mass,i}$ is the evaporation rate of component $i$, $\varphi_i$ is the volume fraction of component $i$, $\rho_i$ is the density of pure component $i$, $H$ is the thickness, $C_i^{sat}$ is the saturated solvent concentration of component $i$, $C_i^{\infty}$ is the solvent concentration of component $i$ in the bulk air, $k$ is the mass transfer coefficient, $h$ is the heat transfer coefficient, $T$ is the temperature of coated film, $T^{\infty}$ is the temperature of convective air, $\Delta H_{vap}$ is the heat of vaporization, and $C_p$ is the heat capacity. Subscripts $f$ and $C$ mean the substrate and coated film, respectively. It was reported that the prediction of this model agreed well with the experimental results only at the constant drying rate period before solvent diffusion became the rate-controlling step of the drying process, as expected. Evidently, negligence of solvent diffusion will result in somewhat inaccurate predictions on the total drying time and dryer length. However, it is believed that this model is adequate to extend film drying modeling to the prediction of the final properties of copolymer membrane films because most of the morphology formation is completed in the constant drying rate period. This model allows one to predict the rate of solvent removal for a set of processing conditions. It does not tell us what morphology will form and the degree to which it is formed. This requires information pertaining to the rate of phase separation as a function of temperature and polymer concentration. Hence, we made an initial attempt at devising a scheme for obtaining this information, which is described below.

Rheology and small angle X-ray Scattering (SAXS) are known to be very responsive to the structure evolution and viscoelastic properties during the ordering process. So, most of the experimental studies on the order-disorder transition in block copolymers involved rheology and SAXS techniques. However, when the phase change kinetics involve processes which occur in the matter of minutes, then SAXS cannot be used to follow the kinetics but only the final structure, and rheology may be our only option. The success of using rheology for the detection of the ordering kinetics in block copolymers is based on the large viscoelastic contrast between the disordered and ordered phases. The storage ($G'$) and loss ($G''$) moduli of block copolymers jump up considerably during the structure evolution from the disordered to the ordered phase. The evolving shape of $G'$ and $G''$ can be used to analyze the kinetics of structure ordering. Some typical evolutions of $G'$ and $G''$ for a symmetric styrene-isoprene (SI) diblock copolymer, in which the sample was quenched from just above the order-disorder temperature(ODT) are presented in Figure 4. Both $G'$ and $G''$ show a sigmoidal shape with apparent plateaus before and after the upward change. The plateaus of $G'$ and $G''$ before the change are the viscoelastic properties of the disordered phase at the quenched temperature, while the plateaus after the change describe the properties of the final ordered state. During the course of ordering, the block copolymer is considered as a composite material consisted of the disordered and ordered phases. The proportion of the two phases also changes, inducing the observed changes in the mechanical properties. Floudas et al. employed the simplest 'series' and 'parallel' mechanical models, which provide the limits for the mechanical response of a two-phase system as a function of the properties of the constituent components and the composition, in order to investigate the time-dependence of the volume fractions of the constituent phases, and finally to analyze the ordering kinetics based on a nucleation and growth mechanism. The 'series' model allows the modulus of the two-phase system to be expressed as a linear combination of their compliances:

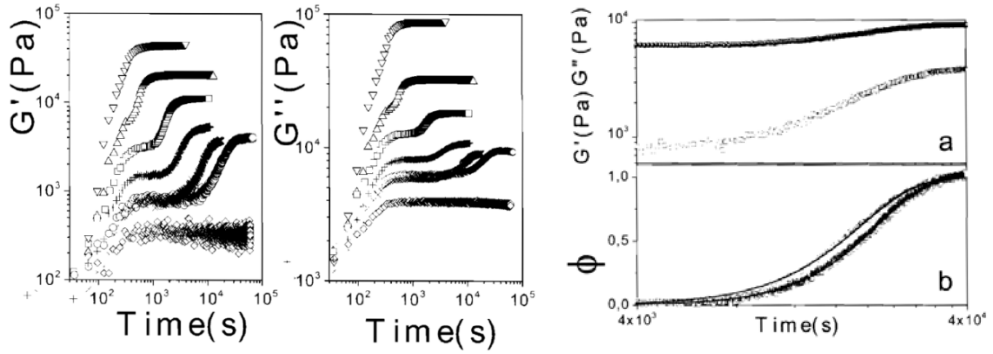


**Figure 4.** (1) Time evolution of $G'$ and $G''$ for a symmetric poly(styrene-b-isoprene) diblock copolymer following quenches from the disordered state to different final temperatures in the ordered phase: rhombus: 359, circles: 358, x: 356.5, +: 356, squares: 355, triangles: 353, and inverted triangles: 347.6 K. (2) a. Time evolution of $G'$ and $G''$ at 356.5 K following a quench from 363 K and b. time-dependence of the volume fraction of $\varphi$ of the ordered phase

calculated using the 'parallel' (squares) and 'series' (circles) models. Solid lines are fits to the Avrami equation.

$$\frac{1}{G(t)} = \frac{1-\phi(t)}{G_0} + \frac{\phi(t)}{G_\infty} \quad \text{(Eq. 3)}$$

and the 'parallel' model as a linear combination of the moduli of the constituent phases:

$$G(t) = (1-\phi(t))G_0 + \phi(t)G_\infty \quad \text{(Eq. 4)}$$

where $G(t)$ $(=\sqrt{G'^2(t) + G''^2(t)})$ is the absolute value of the complex modulus, *φ(t)* is the fraction of the ordered phase, and $G_0$ and $G_\infty$ are the moduli of the completely disordered and ordered phases at the initial and final stages, respectively. The time-dependences of *φ* obtained from the two models are analyzed by fitting the Avrami equation:

$$\phi(t) = 1 - \exp(-zt^n) \quad \text{(Eq. 5)}$$

where *n* is the Avrami exponent, which is a combined function of the growth dimensionality and the time-dependence of the nucleation process, and presents qualitative information on the nature of the nucleation and growth process. In Eq. 3, the rate constant, *z*, gives quantitative information on the course of crystallization, and usually, the half-time,

$$t_{1/2} = \left(\frac{\ln 2}{z}\right)^{1/n} \quad \text{(Eq. 6)}$$

is used to describe the ordering time. These Avrami parameters can be determined from a plot of *log(-log(1- φ))* versus *log t* on which the Avrami exponent, *n*, and the rate constant, *z*, are the slope and intercept, respectively.

In Figure 4 is also given the evolution of the viscoelastic properties during phase transformation of the symmetric SI diblock copolymer and the equivalent volume fractions of the ordered phase obtained using the two extreme 'series' and 'parallel' models. Based on this analysis method, the Avrami exponent was found to be about 3 for shallow quenches, indicating that the ordering process proceeds by heterogeneous nucleation and growth of three-dimensional objects. The kinetics curves at higher cooling had higher value of *n* (about 4), suggesting spinodal decomposition as a possible mechanism of phase transformation.

Although a reasonable method for tracking the phase conversion for block copolymer melts has been initiated, it has not been employed for polymer solutions. We designed and machined new rheometer plates in order to minimize the solvent evaporation during rheological measurements (Figure 5). We initiated measurements for a a block copolymer system and have been able to observe the evolution of G' and G" with time and connect that to

the change in volume fraction of an ordered phase. However, we realized that the quantitative determination of the phase change kinetics is much more involved and out of the scope of this project. Furthermore, the small quantities of block copolymer (~10 g) generated by the chemist is not enough to carry out the study of phase change kinetics in detail.

For this reason we are adapting an approach which will only allow us to approximate the phase separation kinetics. We will use transmission electron microscopy (TEM) to assess the structure of films generated under different drying conditions(batch drying device). The structures will then be analyzed to estimate the Avrami exponent and the rate constant that will give the desired structure. The Avrami equation (Eq. 5) coupled with the mass transfer equations (Eqs. 1 and 2) should allow us to approximate the drying conditions for the desired morphology. It is not an exact method, but it will allow us to get close to the conditions which will lead to a membrane for a given copolymer composition with optimum performance (proton conductivity at low relative humidity).

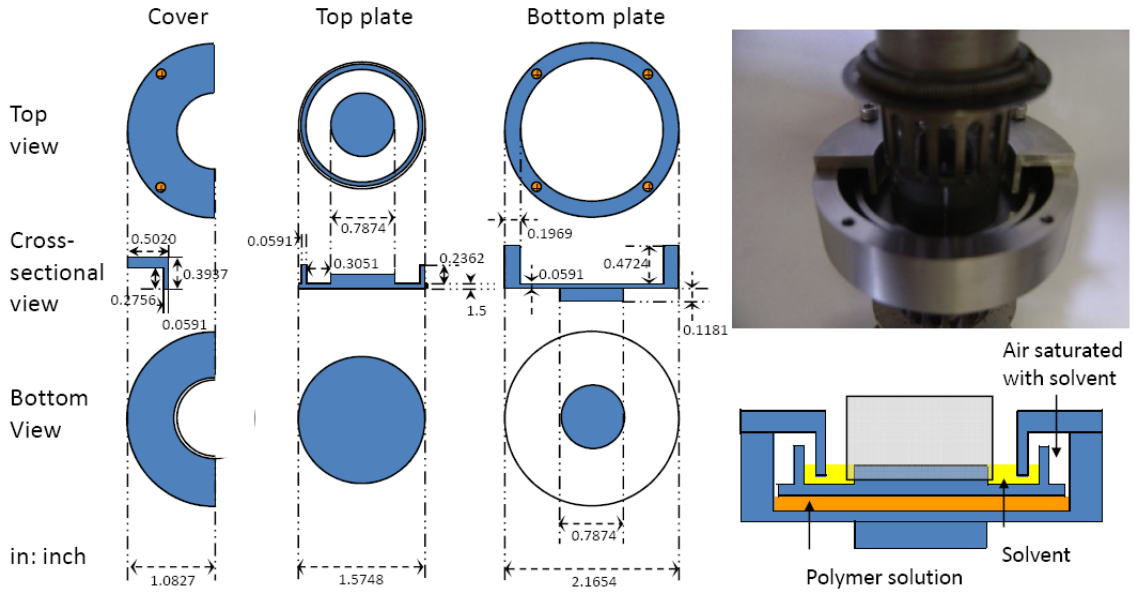


**Figure 5.** Design and schematic of the newly designed modified rheometer plates.

## Improvement of new film casting system

We developed a new film casting system with capability of casting 12" wide films (wet film). As is shown in Fig.1, the system consists of a blade caster, a motor driving device with speed control, a glass substrate, a metal heating panel with temperature controller, and a transparent hood.

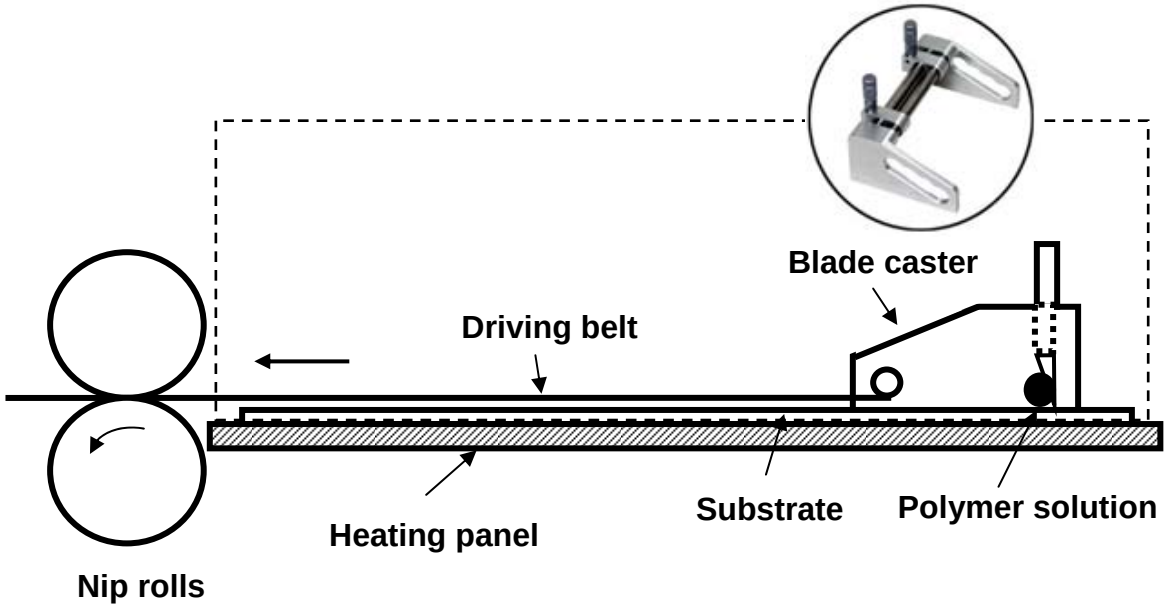


**Figure 1.** Schematic diagram of newer film casting system.

During the trial film casting, however, it was found difficult to generate uniform films with the caster. It is hard to pour the polymer solution uniformly onto the edge part of the blade. It is also difficult to hold the solution there especially when the viscosity of the solution is low. To solve these problems, we developed a new caster with double blade structure (see Figs. 2 and 3). From Fig.2 one can see how it works. We used this caster and generated a number of large films successfully (see Figs. 4 and 5). The films obtained are not only more uniform, but also larger (greater film size/weight of polymer sample) compared to those produced by conventional single blade caster.

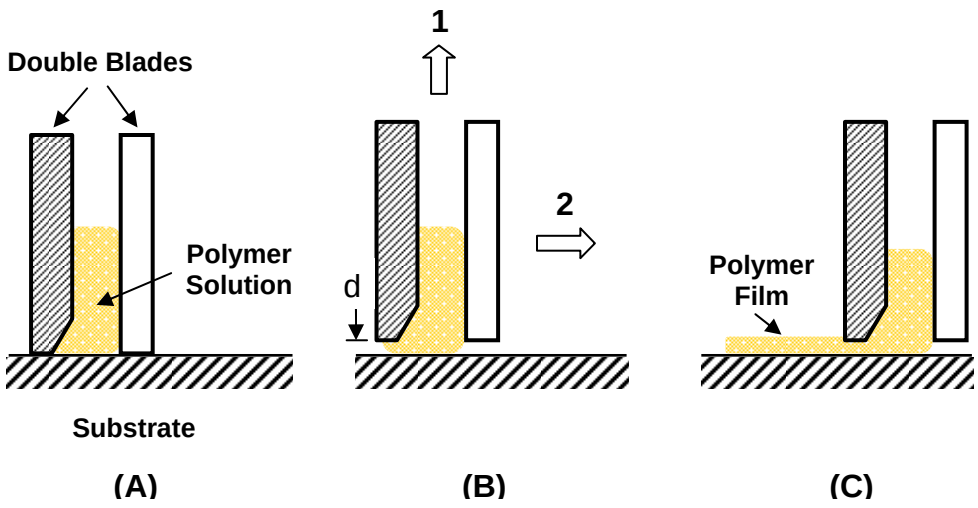


**Figure 7.** Schematic diagram of double blade caster and how it works. (A) Rest the blades on the substrate (glass plate) and pour the polymer solutions in between the blades, (B)Rise the blades to form desired gap between blades and substrate and start to move the blades at constant speed, (C) The wet film with desired thickness and uniformity forms.

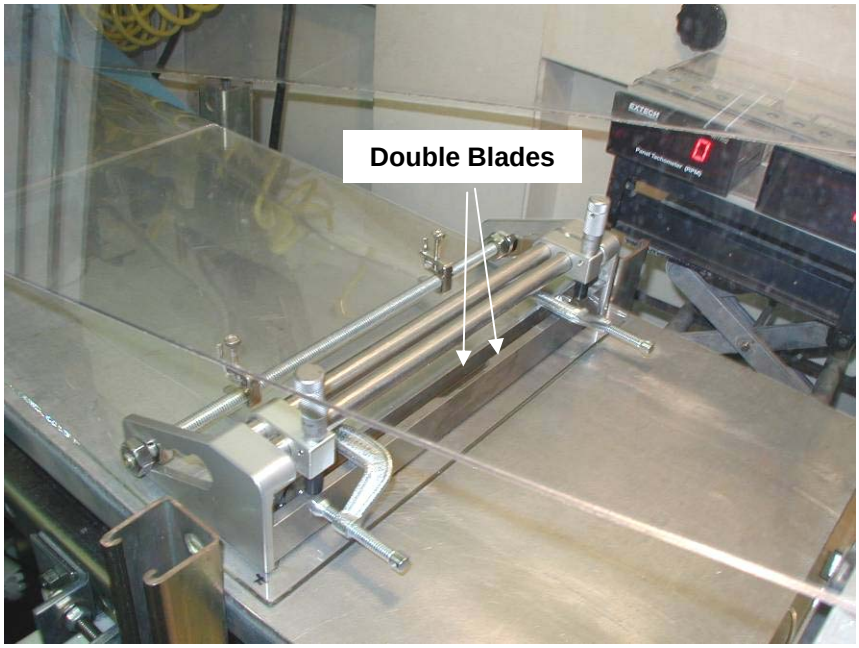


**Figure 8.** Picture showing the double blade caster developed for casting large PEM films.

**Casting of Large Films**

We have run a couple of film castings on this new system successfully (see Fig.4). In Table 1 is presented the conditions used for casting random (BPS35 and 6F40) and block (BPSH-BPS) copolymer films. The pictures of these samples (before acidification) are shown in Fig.5.

**Table 6** Conditions for casting large film samples.

| Polymer | BPS35 | 6F40 | BPSH-BPS |
|---|---|---|---|
| Solvent | NMP | DMAc | NMP |
| Concentration (w/v%) | 20 | 30 | 15 |
| Filter pore size | 5.0 μm | 0.45 μm | 5.0 μm |
| Gap (in) | 0.015 | 0.013 | 0.018 |
| Caster Moving Speed (cm/min) | 427 | 427 | 427 |
| Drying temperature (on plate) | 50°C | 50°C | 65°C |
| Substrate | Glass Plate | Glass Plate | Glass Plate |
| Target dry film thickness | 30 μm | 30 μm | 30 μm |

**Figure 9.** Casting of large films with new caster.


**(A)**


**(B)**

**(C)**

**Figure 10.** Large film samples cast with new film casting system: (A) BPS35, (B) 6F40 and (C) BPSH-BPS.

In an effort to scale-up the film casting and produce more realistic, industrially applicable processing conditions, modification of the reverse-roll coating system are ongoing. Recently, a forced air heater has been installed on the film casting/drying apparatus shown in Figure 6.

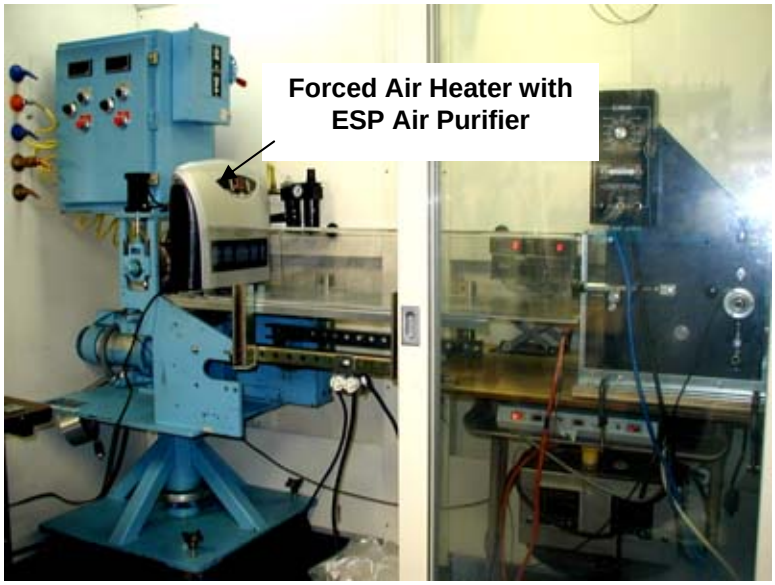


**Figure 6.** Picture showing the film casting system with new forced air heater with ESP air purifier.

The equipment combines a heater and ElectroStatic Precipitator (ESP) air purifier in one unit. The ESP filter captures airborne pollutants and any particles as small as 0.1 micron to ensure the cleanness of the air and the quality of the films. In addition to the conductive heating equipment (heating panel), convection heating to dry the films can be incorporated to allow the films to dry at much higher rate, thereby allowing a wider spectrum of processing conditions to be considered. Similar to the batch-scale system,, the system can be used to study the influence of heating methods/conditions on the morphology and performance of films with the additional advantage of being able to study the effect of scale up. BPS35 films recently cast on the new equipment were analyzed to retrieve information regarding proton conductivity and water uptake.

## REFERENCES

1. Wang, F.; Hickner, M.; Ji, Q.; Harrison, W.; Mecham, J.; Zawodzinski, T.A.; McGrath, J.E. *Macromol. Symp.* **2001,** 175, 387-395.
2. [1] Hickner, M.A.; Ghassemi, H.; Kim, Y.S.; Einsla, B.; McGrath, J.E. *Chem. Rev.* **2004,** 104(10), 4587-4611.
3. [1] Mauritz, K.A.; Moore, R.B. *Chem. Rev.* **2004,** *104*, 4535-4586.
4. [1] Yu, X.; Roy, A.; Dunn, S.; Yang, Y.; McGrath, J.E. *Macromol. Symp.* **2006,** 245–246, 439–449.
5. [1] Yu, Xiang; Roy, Abhishek; Dunn, Stuart; Badami, Anand S.; Yang, Juan; Good, Alec S.; McGrath, James E. Synthesis and Characterization of Sulfonated-Fluorinated, Hydrophilic-

Hydrophobic Multiblock Copolymers for Proton Exchange Membranes. *J. Polym. Sci. Part A: Polym. Chem.*, **2009**, *47*, 1038–1051.

6. [1] Wang, H.; Badami, A.S.; Roy, A.; McGrath, J.E. *J. Polym. Sci. Part A.* **2007**, 45, 284-294.
7. [1] Lee, H.; Roy, A.; Lane, O.; Dunn, S.; McGrath, J.E. *J. Polym. Sci. Part A.* **2007**, 45(21), 4879-4890.
8. [1] Lee, H.-S.; Roy, A.; Lane, O.; Dunn, S.; McGrath, J.E. Hydrophilic-hydrophobic multiblock copolymers based on poly(arylene ether sulfone) via low-temperature coupling reactions for proton exchange membrane fuel cells. *Polymer* **2008**, *49*, 715-723.
9. [1] Roy, A.; Hickner, M.A.; Yu, X.; Li. Y.; Glass, T.E.; McGrath, J.E. *J. Polym. Sci. Part B* **2006**, 44, 2226-2239.
10. [1] Shin, C.K.; Maier, G.; Andreaus, B.; Scherer, G.G. Block copolymer ionomers for ion conductive membranes. *J. Membr. Sci.* **2004**, *245*, 147-161.
11. [1] Zhao, C.; Li, X.; Wang, Z.; Dou, Z.; Zhong, S.; Na, H. Synthesis of block sulfonated poly(ether ether ketone)s (S-PEEKs) materials for proton exchange membrane. *J. Membr. Sci.* **2006**, *280*, 643-650.
12. [1] Zhao, C.; Lin, H.; Shao, K.; Li, X.; Ni, H.; Wang, Z.; Na, H. Block sulfonated poly(ether ether ketone)s (SPEEK) ionomers with high ion-exchange capacities for proton exchange membranes. *J. Power Sources* **2006**, *162*, 1003-1009.
13. [1] Noshay, Allen; McGrath, James E. *Block Copolymers: Overview and Critical Survey*, Academic Press: New York: **1977**.
14. [1] Sankir, M.; Bhanu, V.A.; Harrison, W.L.; Ghassemi, H.; Wiles, K.B.; Glass, T.E.; Brink, A.E.; Brink, M.H.; McGrath, J.E.. *J. Appl. Polym. Sci.*, **2006**, 1004595-4602.
15. [1] Zawodzinski, T. A.; Neeman, M.; Sillerud, L. O.; Gottesfeld, S. *J. Phys. Chem*. **1991**, *95*, 6040.
16. [1] Springer, T. E.; Zawodzinski, T. A.; Wilson, M. S.; Gottesfeld, S. J. *Electrochem. Soc.* **1996**, *143*, 587.
17. Hadjichristidis, N., Pispas, S., and Floudas, G. A., Block Copolymers: Synthetic Strategies, Physical Properties, and Applications, John Wiley & Sons, Inc., New Jersey, 2003.
18. Floudas, G., Pakula, T., Fischer, E. W., Hadjichristidis, N., and Pispas, S., Ordering Kinetics in a Symmetric Diblock Copolymer, Acta Polymer, 45, 176-181, 1994.
19. Avarami, M., Kinetics of Phase Change, 1: General Theory, Journal of Chemical Physics, 7, 1103-1112, 1939.
20. Avarami, M., Kinetics of Phase Change. 2: Transformation-Time Relations for Random Distribution Nuclei, Journal of Chemical Physics, 8, 212-224, 1940.
21. Avarami, M., Granulation, Phase Change, and Microstructure, Journal of Chemical Physics, 9, 177-184, 1941.
22. Hadjichristidis, N., Pispas, S., and Floudas, G. A., Block Copolymers: Synthetic Strategies, Physical Properties, and Applications, John Wiley & Sons, Inc., New Jersey, 2003.
23. Floudas, G., Pakula, T., Fischer, E. W., Hadjichristidis, N., and Pispas, S., Ordering Kinetics in a Symmetric Diblock Copolymer, Acta Polymer, 45, 176-181, 1994.
24. Avarami, M., Kinetics of Phase Change, 1: General Theory, Journal of Chemical Physics, 7, 1103-1112, 1939.
25. Avarami, M., Kinetics of Phase Change. 2: Transformation-Time Relations for Random Distribution Nuclei, Journal of Chemical Physics, 8, 212-224, 1940.

26. Avarami, M., Granulation, Phase Change, and Microstructure, Journal of Chemical Physics, 9, 177-184, 1941.
27. Huang, H., Zhang, F., Hu, Z., Du, B., He, T., Lee, F.K., Wang, Y., and Tsui, O.K.C., Study on the Origin of Inverted Phase in Drying Solution-cast Block Copolymer Films, Macromolecules, 36, 4084-4092, 2003.

**Project Spending and Estimate of Future Spending**

| Quarter | From | To | Estimated Federal Share of Outlays* | Actual Federal Share of Outlays | Estimated Recipient Share of Outlays* | Actual Recipient Share of Outlays | Cumulative |
|---|---|---|---|---|---|---|---|
| 2Q06 | 4/1/2006 | 6/30/2006 | | $14,485.70 | | $0.00 | $14,485.70 |
| 3Q06 | 7/1/2006 | 9/30/2006 | | $75,779.37 | | $0.00 | $90,265.07 |
| 4Q06 | 10/1/2006 | 12/31/2006 | | $50,058.17 | | $42,159.23 | $182,482.47 |
| 1Q07 | 1/1/2007 | 3/31/2007 | | $61,568.73 | | $19,742.80 | $263,794.00 |
| 2Q07 | 4/1/2007 | 6/30/2007 | | $91,408.28 | | $13,087.26 | $368,289.54 |
| 3Q07 | 7/1/2007 | 9/30/2007 | | $156,699.75 | | $11,192.16 | $536,181.45 |
| 4Q07 | 10/1/2007 | 12/31/2007 | | ($61,938.39) | | $14,061.09 | $488,304.15 |
| 1Q08 | 1/1/2008 | 3/31/2008 | | $95,547.90 | | $29,559.00 | $613,411.05 |
| 2Q08 | 4/1/2008 | 6/30/2008 | | $62,839.56 | | $15,134.69 | $691,385.30 |
| 3Q08 | 7/1/2008 | 9/30/2008 | | $123,327.29 | | $18,571.75 | $833,284.34 |
| 4Q08 | 10/1/2008 | 12/31/2008 | | $68,915.81 | | $20,412.06 | $922,612.21 |
| 1Q09 | 1/1/2009 | 3/31/2009 | | $62,466.30 | | $20,412.12 | $1,005,490.63 |
| 2Q09 | 4/1/2009 | 6/30/2009 | | $74,222.24 | | $15,103.61 | $1,094,816.48 |
| 3Q09 | 7/1/2009 | 9/30/2009 | | $28,096.68 | | $30,988.56 | $1,153,901.72 |
| 4Q09 | 10/1/2009 | 12/31/2009 | | $30,995.07 | | ($2,152.04) | $1,182,744.75 |
| 1Q10 | 1/1/2010 | 3/31/2010 | | ($2,233.82) | | ($2,096.50) | $1,178,414.43 |
| **Totals** | | | **$0.00** | **$932,238.64** | **$0.00** | **$246,175.79** | |

**General Notes**: 1) DOE Laboratory partner spending is not included in the above table. 2) The information in this table is consistent with the information provided in the Federal Financial Report (SF 425) submitted on 4/20/2010.